Jimma University

School of Postgraduate Program

Jimma Institute of Technology

Faculty of Electrical and Computer Engineering

Performance Analysis of Microstrip Antenna Array with Semi-elliptical Slotted Rectangular Patch and Ground Structure at 28GHz for Wideband Communication Systems

A Thesis Submitted to Jimma Institute of Technology, School of Graduate Studies in Partial Fulfillment of the Requirements for Master's Degree in Communication Engineering

By:

Ayane Lebeta Goshu

April 21, 2021

Jimma, Ethiopia

Jimma University

School of Postgraduate Program

Jimma Institute of Technology

Faculty of Electrical and Computer Engineering

Performance Analysis of Microstrip Antenna Array with Semi-elliptical Slotted Rectangular Patch and Ground Structure at 28GHz for Wideband Communication Systems

By:

Ayane Lebeta Goshu

Main Advisor: - Kinde Anlay (Assist. Prof., Ph.D.)

Co-Advisor: - Mulugeta Tegegn (M.Sc., Ph.D. Student)

April 21, 2021

Jimma, Ethiopia

I

Declaration

I hereby proclaim that this thesis entitled **"Performance Analysis of Microstrip Antenna Array with Semi-elliptical Slotted Rectangular Patch and Ground Structure at 28GHz for Wideband Communication Systems"** is based on the results found by myself, and all sources of the materials are duly acknowledged. The contents of this document have not been submitted to any other Institute or University for the award of any degree.

Ms. Ayane Lebeta Goshu   _____   _04/05/2021_____

                                             Signature   Date

Advisor

Dr. Kinde Anlay   _____   _30/04/2021_____

                                 Signature   Date

Co-Advisor

Mr. Mulugeta Tegegn   _____   _04/05/2021_____

                                 Signature   Date

Approved by Faculty of Electrical and Computer Engineering Research Proposal Examination Members

1. Dr. Yihenew Wondie   _____   _29/04/2021_____

                                 Signature   Date

2. Engr. Sherwin N. Catolos   _____   _30/04/2021_____
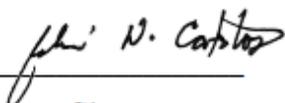
                                 Signature   Date

3. Sofiya Ali   _____   _05/03/2021_____

                                 Signature   Date

Abstract

The fifth-generation (5G) of cellular communication networks is desired to operate at the mm-wave frequency band, which has different propagation constraints like relatively high path losses and atmospheric absorption. To mitigate these effects, it is crucial to construct a low-cost and low-profile antenna array which maintains high performance over a broad frequency spectrum. In this respect, microstrip patch antenna (MPA) arrays are considered as a candidate antenna type. But, the gain of MPA is low, the bandwidth is too narrow and the integration of a large of elements in the array leads to increased sidelobe level, which decreases radiation efficiency and directivity of the antenna. Besides, the substrate thickness deteriorates the antenna's bandwidth and radiation efficiency by increasing the surface wave and spurious feed radiation. Various design techniques of MPA were reported to alleviate these limitations and improve its performance for 5G communication systems. These include using the slotted patch, defected ground plane, increasing the array elements, changing substrate material, and feeding techniques. But, obtained performance is low for 5G communications. The existing studies' main emphasis was on single element and linear rectangular MPA arrays. A few studies have been carried out to explore the extensive design of planar MPA arrays to improve the bandwidth, gain, and scanning capability of a one-dimensional rectangular MPA array. Thus, to address these challenges, in this study, the performance analysis of a single element, planar 2x2, 4x4, and 8x8 rectangular MPA arrays are presented by introducing a semi-elliptical slot structure on a radiating patch and ground plane, and tuning key dimensions of the antenna. All the proposed MPA arrays are simulated using CST-MW studio and found that the return loss, bandwidth, and gain of the a semi-elliptical slotted single element MPA are -37.784dB, 1.132GHz, 7.128dBi, respectively. The gain, bandwidth, and total efficiency of the studied 2x2, 4x4, and 8x8 MPA array are about 13.24dBi, 16.54dBi, 21.45dBi; 1.33GHz, 1.461GHz, 1.561GHz; 97.03%, 81.72%, 69%, respectively. Likewise, their return loss and VSWR are -43.321dB, -40.665dB, -22.678dB; 1.014, 1.019, 1.159, respectively. The simulation results show that the introduced semi-elliptical slot on the patch and ground plane significantly influences the structure's current distribution. As a result, the radiation efficiency is increased and thereby the bandwidth of the antenna. Moreover, tuning the antenna's key dimensions and etched portion affects the bandwidth, gain, directivity, radiation efficiency, and amount of the antenna's power loss. In general, all the proposed planar rectangular MPA arrays satisfy the requirements of a 5G antenna. As compared to other similar works therefore, the studied antenna provides a highly competitive and improved performance.

Acknowledgment

First of all, I would like to express my heartfelt gratefulness to the Almighty God for his eternal support throughout my life and his kind assistance in writing this research paper. Secondly, I would like to express my deepest gratitude to my main Advisor, Kinde Anlay (Assistant Professor, Ph.D.) and Co-advisor, Mulugeta Tegegn (M.Sc., Ph.D. Student) for their unlimited support through guidance and the provision of appropriate information during advising time to carry out this research. Finally, I would like to thank everyone who has an essential role in the successful completion of this thesis and express my apology that I could not list all their names here.

Table of Contents

List of Figures

List of Tables

List of Acronymys

2D	Two Dimensional
3D	Three Dimensional
3GPP	Third-generation Partnership Project
4G	Fourth-generation
5G	Fifth-generation
AF	Array Factor
BW	Bandwidth
CST	Computer Simulation Technology
dB	Decibel
DGS	Defect Ground Structure
DMPA	Defected Microstrip Patch Antenna
FCC	Federal Communication Commission
FP	Feed Point
Gbps	Gigabit-per-second
GHz	Giga-hertz
GPL	Ground Plane Length
GPW	Ground Plane Width
IL	Inset Length
IoT	Internet of Things
IS	Inter-element Space
IW	Inset Width
MHz	Mega-hertz
mm	Millimeter
M2M	Machine to Machine
MPA	Microstrip Patch Antenna
MW	Micro-wave
PDA	Power Divider Arm
PL	Patch Length
PW	Patch Width

RF   Resonant Frequency

RL   Return Loss

ST   Substrate Thickness

VSWR   Voltage Standing Wave Ratio

ZMTL   Microstrip Transmission Line Impedance

Z_0 Characteristic Impedance

Z_{pe} Patch Edge Impedance

Z_{QT} Quarter-wavelength Transformer Impedance

ε_r Substrate Dielectric Constant

η_{rad} Radiation Efficiency

λ_{SM} Wavelength of Substrate Material

Chapter One

Introduction

1.1. Background of the Study

Wireless communication technology is universal technology that has influenced people's daily lives than any other technologies and has improved the way cellular and wireless communication networks are used drastically [1]. Nowadays, many mobile devices are getting connected to the existing cellular networks, which are causing a continuous increase in data traffic and device connections, resulting in the need for huge capacity in the upcoming years [2], [3]. However, the allowable frequency ranges of the fourth-generation mobile network technology capacity are insufficient to support and address current rapid growth network traffic. To alleviate these issues, the use of currently unused mm-wave frequency band is highly encouraged, and the fifth-generation of wireless technology is launched in some parts of developed countries [4].

Therefore, in 5G communication systems, the mm-wave frequency band, which can provide unauthorized bandwidth of up to 1GHz and low latency is considered as a key factor to resolve exponential data traffic increment. Thus, by taking advantage of using the mm-wave frequency band, the 5G system supports three major service classes. These are enhanced high-speed movable and fixed broadband, and low latency communications, and M2M communications [5]. The first class is the key characteristic of this platform, particularly in the early stage of its deployment. Thus, the productivity and efficiency of device connectivity in society will be improved by this superiority of the 5G infrastructure over existing cellular networks.

The second one offers a minimal delay, in which several end users within the range of the same base station can use a 1Gbps internet connection for critical applications and unrestricted call rates. In the last class, a vast amount of links from low-power machines can be assisted by 5G technology. In this technology, the supported data rate will reach a limit of one hundred times the bandwidth of the 4G networks. Thus, for instantaneous connectivity, 5G frameworks and advancements migrate to advanced mobile networks, allow large machine-type interactions, and encourage network applications that demand ultra-high reliability and minimal latency [6], [7].

To recognize the anticipated performances of the 5G wireless communication systems, the working frequency is selected from low, medium, and high-frequency bands. Nevertheless, the selection of band relies on its characteristics, and specifically, the capacity of spectrum resources

is an issue applied in 5G systems. Accordingly, under 3GPP release 15, two new frequency band have been defined for 5G communication systems. These are frequency band one (450MHz - 6GHZ, in which the upper limit can be extended up to 7.125GHz) and frequency band two (24.25GHz - 52.6GHz). Recently, the initial deployment of 5G communication systems has been launched in China, South Korea, and Japan by using the first frequency band as the working frequency. However, in order to meet the demands for extra frequency band, primarily for fixed/mobile 5G applications that need significant bandwidth to support higher speeds >1Gbps with lower latency, the FCC approved the appointment of wide bandwidths of more than one GHz at 28, 37, and 39GHz [6], [8].

Thus, for the next phase deployment of indoor broadband access point applications, to introduce fixed point-to-point and point-to-multipoint high-speed backhaul connectivity at home and other applications, and mid-sized cell outdoor applications, the 28GHz frequency band has got high research interest from scientific research community. Because, this frequency band contains huge volume and the opportunity of assigning bulky spectrum resources. In addition, the size of the antenna at this frequency band is very compact, thereby, the antenna designer can integrate large number of array elements to construct massive antenna arrays, which can mitigate the effects of using high frequency band as the working frequency. Moreover, the 28GHz band could be made available by reallocating the local multipoint block distribution service, which is suitable for a variety of applications. Mobile applications, which are currently a core aspect of 5G deployment endorsed by national carriers and other organizations, may use the 28GHz band [9], [10].

In another perspective, the complete deployment of a 5G scheme needs antenna infrastructure planning and the introduction of new technological resolutions, which can be more reliable to build inside the public service buildings such as train stations, stadiums, and shopping malls. To achieve high data speeds, antennas for 5G wireless technology at a higher frequency are expected to be wideband so that many devices can be able to retrieve [11]. To mitigate the radio wave impediments, they should have a high gain; among many others, human beings are likely barriers of the mm-wave system, which are causing greater transmission loss due to high operating frequency [12]. These create fresh hindrances for antenna manufacturers to fulfill the system's specifications. In general, wireless technology advancements require less weight, low profile antennas, low cost, easy and mass manufacture, compatible with planar and non-planar surfaces, and mechanically stable while mounted on rigid surfaces [13].

For wireless devices, microstrip patch antennas are the proposed solutions and reflect a perfect option in this regard. They are ideal for installing spacecraft, satellites, aircraft, vehicles, and lightweight, portable communication equipment on the outside. The MPA plays a key role in the fastest-growing field of wireless communication [14], [15]. Despite to this, compared to traditional microwave antennas, MPA has some restrictions like the thickness of the dielectric substrate deteriorating the antenna bandwidth and radiation efficiency by increasing surface wave and spurious feed radiation and the feeding line. Consequently, undesired cross-polarized radiation is led by feed radiation effects. Also, the MPA experiences losses like a dielectric, conductor, and radiation, resulting in bandwidth reduction and gain reduction. This poses a design challenge for the MPA designers to meet the broadband and high gain requirement of 5G millimeter-wave communication systems [16-19].

Hence, to overwhelm the drawbacks mentioned above of a single element MPA and enhance the performance for 5G systems, several research studies have been carried out. These works have been performed by using various approaches, including a U-slotted patch [4], adding extra structure on radiating patch [12], modifying the feeding techniques [20], [21], the defected ground structure and Y-shaped patch [22], X-shape slotted [23], introducing multiple slots [24], [25], etched patch [26], various substrate material types [27], a substrate integrated waveguide patch, multi-patch designs, multi-layer by employing diverse impedance matching techniques [28]. Nonetheless, by using the aforementioned techniques, the achieved simulation results of the single element MPA reported in recent scientific literature reveal that the bandwidth is narrow, the radiation pattern is relatively wide, and thereby gain and directivity of the radiation pattern are low to be used in the 5G wireless communication systems. Thus, attempting to improve the performance of a single element MPA, different linear rectangular MPA arrays have been reported in [19], [20], [29-33].

From the simulation results, it has been realized that the proposed linear rectangular MPA arrays improved the performance of a single element rectangular MPA. Conversely, some of the achieved performance metrics are low compared to the necessities for 5G communication systems. Likewise, linear antenna arrays can scan only a one-dimensional plane, i.e., either the elevation plane or the azimuth plane. In general, it can be inferred that the linear MPA array's main constraints are unable to scan the radiation beam in more than one direction, and the magnitude of the sidelobe level is another major issue in the radiation pattern.

3

Subsequently, to mitigate the performance limitations of the linear array and, in general, to boost a patch antenna performance, very few studies of planar MPA array designs [16], [19], [33-36] have been carried out. The reported planar arrays alleviated the performance limitations of the linear MPA array in the aspect of scanning capability. However, the achieved bandwidth, gain, and directivity are still low for 5G communication systems. For that reason, the scientific research community has continued the struggle to boost the performance of MPA in terms of all performance metrics. Thus, from the reported literature, it can be observed that different techniques have been used to enhance the performance of the rectangular MPA. However, as far as the information of the current researcher, the study did not explore the performance enhancement of planar MPA arrays by introducing the defect structure on both the radiating element and ground plane simultaneously to boost the bandwidth, gain, directivity, and also, to minimalize the magnitude of a return loss of MPA.

Therefore, the main objective of this study is to enhance the performance of MPA array for 5G communication systems. To achieve this objective, the semi-elliptical slotted rectangular patch and ground plane have been used. In addition, the antenna key physical dimensions tuning technique is utilized. In general, in this study, the design and then enhancing the performance of the single element MPA and planar 2x2, 4x4, and 8x8 rectangular MPA arrays have been explicitly presented.

1.2. Statement of the Problem

The current 4G wireless technology failed to cope with cellular users' rapid growth, causing high network traffic and large capacity. Afterward, nowadays, 5G wireless technologies are launched in some parts of industrialized countries like China and America. The new 5G communication systems are desired to have low latency, better reliability, network scalability, and better system efficiency to support large numbers of integrated services and advanced applications for a huge number of end-users by providing high data rate for each by utilizing mm-wave frequency bands as a working frequency. Thus, higher frequencies are a potential candidate for future applications and accommodate uninterrupted services over the broader spectrum allocations.

On the other hand, as moving towards using higher frequency bands, they come up with different propagation constraints like relatively high path loss, foliage loss, penetration loss, and much low diffraction. Moreover, in this spectrum band, all the communication signals between the transmitter and receiver should be in line-of-sight forms, which is very difficult to achieve in crowded environments due to the blockage of various obstacles and then limit the movement of end mobile users. To mitigate these problems, the mobile devices desired to be used along with 5G mm-wave communication systems require high-performance antenna arrays having a low profile, compact size that is conformable and mechanically stable to planar and non-planar surfaces, which can function over a wide frequency band.

Regarding to this, microstrip patch antennas are more prominent and selected over other antenna types. Inspite, the microstrip patch antenna's bandwidth is incredibly narrow, gain and directivity are low for 5G communication systems. Also, poor impedance matching in the structure cause numerous power losses, which result in the deterioration of the radiation efficiency and, at the same time, the bandwidth of the antenna. For this reason, to alleviate these drawbacks, different single element MPA designs are demonstrated. To advance a single MPA performances, different linear and few planar MPA arrays are simulated and presented in the recent literature with acceptable simulation results. Yet, in general, the directivity, bandwidth, and gain of all proposed designs are low. Thus, currently, extensions of scientific research investigations are highly required to enhance the rectangular MPA performance for 5G communication systems.

1.3. Objectives of the Study

1.3.1. General Objective

The general objective of this thesis work is to analyze the performance of microstrip antenna array with a semi-elliptical slotted rectangular patch and ground plane to improve its performance for 5G communication systems.

1.3.2. Specific Objectives

The specific objectives of this study are:

- ❖ To enhance the rectangular microstrip patch antenna arrays bandwidth and radiation efficiency for 5G communication systems.
- ❖ To increase the rectangular microstrip patch antenna arrays gain and radiation pattern directivity for 5G communication systems.
- ❖ To minimize different types of power losses caused due to the impedance mismatch and incompatibility issue of rectangular MPA array for 5G communication systems.

1.4. Research Questions

To achieve the above objectives, this thesis seeks to answer the following questions:

- ❖ How does the defect structure on the patch and ground plane can improve the radiation efficiency and bandwidth of the rectangular MPA array?
- ❖ How does the arrangement of array elements, tuning key design parameters of the antenna, and introduce defect structure on patch and ground plane affect the gain, directivity, bandwidth, and rectangular radiation efficiency MPA array?
- ❖ How do the impedance mismatches within the rectangular MPA array's feeding network structure affect the amount of the power losses and radiation efficiency, and how the selected size dimensions cause incompatibility issues in the 5G communication systems?

1.5. Significance of the Study

The 5G communication systems are estimated to operate in extremely high-frequency bands. In this mm-wave frequency band, the communication signals are easily blocked by the obstacle, thereby increasing the path losses. In general, the efficient communication requires the transmitter and the corresponding receiver to be in the line-of-sight range. The surrounding buildings and trees can, in such circumstances, have a major impact on the performance of 5G mm-wave wireless networks, especially for individual users of mobile devices. Accordingly, to mitigate these problems, an antenna array with compact size, wide bandwidth, and high gain is highly required.

In this study, the semi-elliptical slot structure has been introduced on the radiating microstrip patch and ground plane, which significantly affects the current distribution of both structure and then increases the magnitude of the fringing field producing radiation of the antenna. The performance trade-off design parameters are seriously analyzed, afterward the important physical dimensions of the antenna structure has been tuned. So, the effect of the impedance mismatch in the feeding network structure is reduced. Consequently, in general, high power losses due to poor impedance matching is minimized, which dimish the radiation efficiency of the antennas. Moreover, the narrow bandwidth of MPA has been significantly improved. The proposed antenna array can provide different high data rate services for huge number of users in public services area like stadiums, train stations, and shopping malls.

On the other hand, in addition to aforementioned techniques, by increasing the array's radiating element numbers, the directivity and gain of the MPA array are profoundly increased. The proposed planar MPA can mitigate the effects of high propagation constraints caused due to a high working frequency. Furthermore, the proposed planar rectangular MPA array in this study minimizes the magnitude of the sidelobe level in which the interference at the receiver side will be easily handled. Also, since the planar patch antenna array's scanning plane is in both directions, it is feasible for any users in any direction, the interruption of users' communication due to the communication beam misalignments is alleviated. In general, the finding of the proposed MPA array in this study contributes a lot in different prespectives for the emerging 5G communication systems.

1.6. Scope of the Study

To implement the rectangular MPA array for 5G mm-wave applications, basic adjustments are required to meet the necessities. So that, the key concepts that have been addressed in this thesis work are presented as follows.

The first concept that has been addressed in this study is the designing, modeling, performance analysis, and enhancement of the single element MPA. Then, the semi-elliptical slot structure has been introduced to the radiating patch and ground plane to affect the current distribution and improve the antenna's performance. Next, the designed modified single element patch antenna is used as a building block to design planar 2x2, 4x4, and 8x8 rectangular MPA arrays. For all of the proposed designs, by introducing defect on both the radiating element and ground plane, tuning the values of the design parameters, simulating repeatedly, and mitigating the impedance mismatches within the feeding networks, which causes the different forms of power losses, the performance of antenna has been analyzed.

Moreover, the achieved simulation results have been compared with designs presented in the literature in terms of return loss, radiation efficiency, gain, VSWR, and bandwidth. Generally, in this thesis work, all of the studied antennas are successfully simulated using CST software. However, to validate whether achieved simulation results are attainable in real-world implementation, their hardware is not manufactured and tested in the antenna laboratory.

1.7. Limitation of the Study

While conducting this study, the following limitations were encountered. The researcher faced shortage of super computer to simulate all the proposed design. Since antenna design and analysis at high frequency, introduction of defected structure on both the radiating element and ground plane poses computational complexity. The performance of the proposed MPA meets standard settings and can be used for 5G communication systems as it can be inferred from the simulation results obtained in CST MW software. But, due to the lack of antenna laboratory, the proposed antenna is not yet fabricated to see wether the simulation result is also achievable in real world.

1.8. Organization of the Paper

The overall document of this paper is organized into five chapters. The chapter first consists of the background of the study, statement of the problem, objectives of the study, and research questions. It also discusses the significance, scope, and limitation of the study. In the second chapter, the theoretical background of MPA, a description of the rectangular MPA design parameters, and governing equations are presented. Finally, literature reviews of proposed designs of single element and array of rectangular MPA have been discussed. The third chapter presents the design procedures and design calculations of single element and planar rectangular MPA arrays. The fourth chapter is about the simulation results and discussions of the proposed typical, modified single element, and rectangular MPA arrays. Lastly, the fifth chapter of the study is the conclusion and recommendation of future works.

Chapter Two

Theoretical Background and Literature Review

The overall content of this chapter is ordered into three major sections. In section one, the general overviews of; the theoretical background, modeling of a patch antenna, the detailed description of design parameters, and the governing equations used in the design of a single element rectangular MPA are presented. The second section presents the theoretical overview and governing equations of the planar rectangular MPA array and also the performance metrics of the patch antenna. In the third section, literature reviews of the microstrip patch antenna are presented, which consists detailed review of the single element, linear, and planar rectangular MPA array. Lastly, the conceptual framework of the study is briefly described.

2.1. Basic Theory and Working Principle of Single Element Rectangular MPA

As shown in Figure 2.1, MPA is a single-layer design comprising mainly four parts, i.e., substrate, patch, feeding portion, and a ground plane. The basic antenna element is a strip conductor of thickness t, length PL, and width PW on a dielectric substrate with a thickness of ST supported by a ground plane. The radiating patch may have any shape, but it is usually elliptical, rectangular, triangular, circular, and square to facilitate the analysis and simply performance predictions. Whereas the rectangular patch antenna is widely used from all types of patch antennas [18], [38].
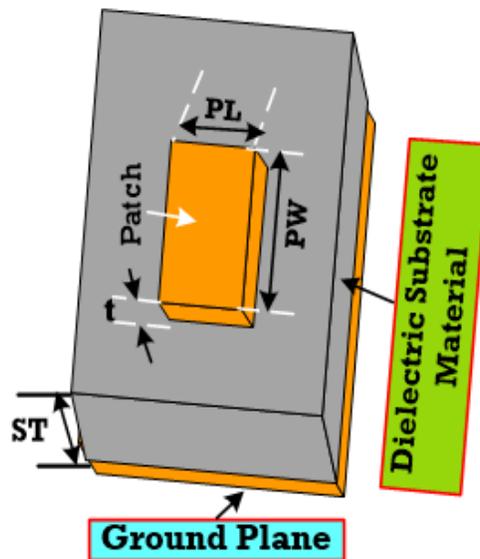
Figure 2.1. Rectangular Patch Antenna Physical Structure [18].

As it provides mechanical support and affects the electrical efficiency of the antenna, the substrate material is an important parameter. Therefore, the selection of dielectric substrate materials with their thickness and dielectric constant needs accuracy. A thicker substrate through a low dielectric constant is chosen for a higher frequency communication to minimize losses, enhance bandwidth and increase radiation efficiency, but it causes the surface waves to propagate and spurious coupling [20], [37-39].

To describe how the MPA operates, the voltage, current, and impedance distribution of the patch indicated in Figure 2.2 are important factors. Ideally, at the end of the patch, the current is zero; the voltage and impedance are maximum, which is 300Ω. Also, at the patch center, the current is maximum, the voltage is minimum, and the impedance is minimum. For a particular design, the impedance of 50Ω point is located and used for feed position [18], [39], [40].
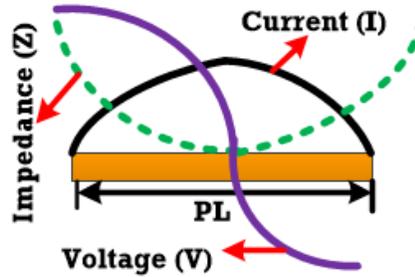
Figure 2.2. The Patch Antenna Impedance, Voltage, and Current Distribution [39].

The equations of current I and impedance Z are given by equations 2.1 and 2.2 [18].

$$I = \int JdS \tag{2.1}$$

$$Z = \frac{0.5 P_{tot}}{I^2} \tag{2.2}$$

Where J is current density, Z is impedance, P_{tot} is total power received, and I is current.

As a given patch antenna is excited, the fringing E-fields produced among the ground plane and patch edges add up in phase due to voltage distribution and then generate the radiation. With regard to the ground structure, the electric fields at the edges can be split into normal components along the width in opposite directions in which they offset each other, and the in-phase tangential components are added together to provide maximum radiation fields, which are normal to the surface of the patch as indicated in Figure 2.3 [18], [40], [41].

11
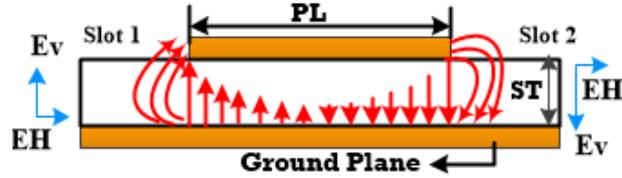
Figure 2.3. Decomposition of the Field at the Patch Edge [18], [40].

Owing to fringing field effects, the rectangular patch of the antenna appears electrically greater than its actual size. The patch dimension along its length is extended by a distance of ΔPL on each end, as shown in Figure 2.4 [18].
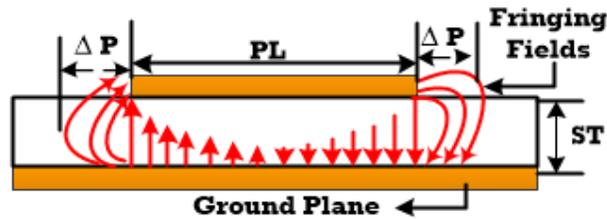
Figure 2.4. Length Extension Due to Fringing Effects [18].

2.2. Modeling of Patch Antenna as a Transmission Line

The MPA is represented in the transmission line model by two radiating slots of PW width and ST thickness, separated by a transmission line of PL length, as shown in Figure 2.5. It is easy to use the transmission line model and gives good physical insight. Again, it is useful to predict the input characteristic of the patch due to its accuracy, numerical efficiency, and it also plays an important role in modeling antenna arrays. Nonentheless, all types of configurations cannot be analyzed using a transmission line model in which only the input characteristic of fundamental resonance can be predicted [18], [38].
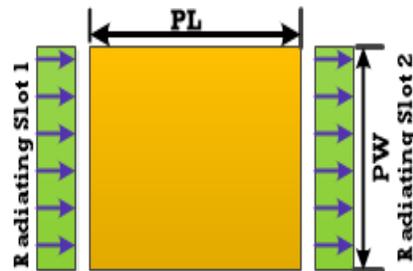
Figure 2.5. Side View of the Transmission Line Model [38].

The rectangular MPA can be slots exhibited using parallel RC circuits, which can be seen in Figure 2.6. Each of them is expressed as an equivalent electrical circuit that denotes the antenna in the

form of two radiating slots is symbolized by a parallel equivalent admittance (Y) with susceptance (B) and conductance (G) [18].

(a)   (b)
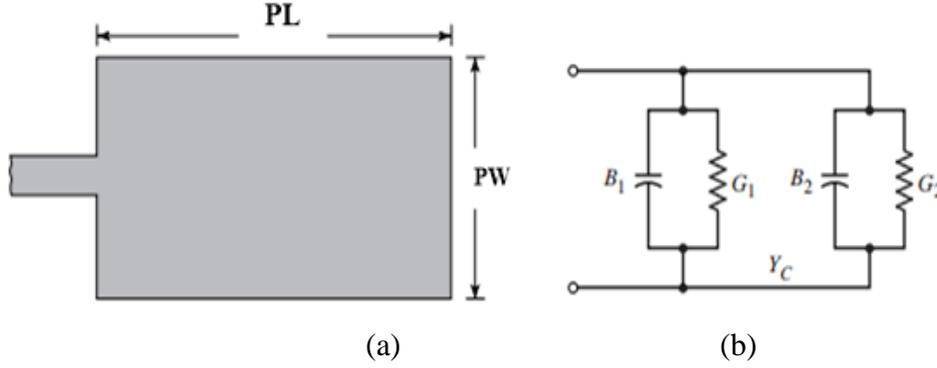
Figure 2.6. Rectangular MPA (a) With Equivalent Circuit Diagram (b) [18].

By considering an infinitely wide and uniform slot, the equivalent admittance of slot one can be written as [18]:

$$Y_1 = G_1 + jB_1 \tag{2.3}$$

Also, for a slot of finite width PW, conductance G and susceptance B are given by [18]:

$$G_1 = \frac{PW}{120\,\lambda_0}[1 - \frac{1}{24}(KoST)^2], \frac{ST}{\lambda_0} < \frac{1}{10} \tag{2.4}$$

$$B_1 = \frac{PW}{120\,\lambda_0}[1 - 0.636\ln(KoST)], \frac{ST}{\lambda_0} < \frac{1}{10} \tag{2.5}$$

Where K_0 is the constant, ST is the thickness of the substrate, λ_0 is a free-space wavelength, PW is patch width, B_1 and G_1 are susceptance and conductance of slot one, respectively.

The overall admittance generated at one radiating slot is calculated by using the transformation formulas of the transmission line to transform the admittance at the other radiating slot. Theoretically, $0.5\lambda_{SM}$ separates the two slots. Where λ_{SM} is the dielectric substrate material wavelength. Due to fringing effects, the length patch is electrically longer than the actual length. Hence, the separation of the two slots is less than $0.5\lambda_{SM}$. But, if the length is properly chosen in the range of $0.47\lambda_{SM} < PL < 0.49\lambda_{SM}$, the transformed admittance of slot two can be written as [18]:

$$\tilde{Y_2} = \tilde{G_2} + j\,\tilde{B_2} = G_1 - jB_1 \tag{2.6}$$

$$\tilde{G_2} = G_1 \tag{2.7}$$

13

$$B_{\tilde{2}} = -B_1 \tag{2.8}$$

In order to transfer maximum power from the port to the feed line that is connected to it, perfect impedance matching is necessary for the feeding network. The input impedance plays a crucial part in deciding the amount of power provided to the feed line. The total input admittance and the impedance of resonant input is real and is given by [18]:

$$Y_{in} = Y_1 + Y_{\tilde{2}} = B_1 + G_1 - B_1 + G_1 = 2G_1 \tag{2.9}$$

$$Z_{in} = \frac{1}{Y_{in}} = R_{in} = \frac{1}{2G1} \tag{2.10}$$

By increasing the width of the patch, the input resistance can be reduced. Because the aperture performance of a single patch continues to decline, this is permissible as long as the PW/PL ratio does not exceed 2. When slot one is considered as a reference slot, the input resistance is calculated using equation 2.10, in which the mutual effect between the slots is not considered. While the mutual effect is considered between the slots, the RF resistance is given by [18]:

$$Z_{in} = \left[\frac{1}{G_1 \pm G_{12}} \right] \tag{2.11}$$

For modes with odd (anti-symmetric) resonant voltage distribution, the plus sign in the denominator is used in the above equation, while the minus sign is used for modes with even (symmetric) resonant voltage distribution. Also, a recessed IL distance from slot one is used, as shown in Figure 2.7, to adjust the resonant input resistance of an inset feed. Using a microstrip-line feed whose characteristic impedance is given by equation 2.12, this technique can be used effectively to match the patch antenna [18].

$$ZMTL = \frac{120\pi \sqrt{\varepsilon_{reff}}}{\frac{WMTL}{ST} + 1.393 + 0.667\ln\left(\frac{WMTL}{ST} + 1.44 \right)}, \frac{WMTL}{ST} > 1 \tag{2.12}$$

Where ST is the thickness of the substrate, WMTL is the width microstrip transmission line, and ε_{reff} is effective dielectric constant.

In terms of the far-zone fields, mutual conductance is described as:

$$G12 = \frac{1}{|V0|^2} Re \iint_S E1 * H_{\tilde{2}}^* .ds \tag{2.13}$$

Where the electric field radiated by slot one is E_1, H_2^* is the magnetic field radiated by slot two, the voltage across the slot is V_0, and the integration is carried out over a large radius sphere.
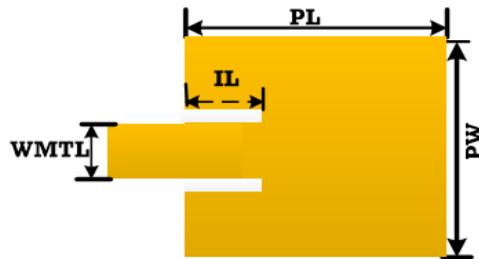
Figure 2.7. Microstrip-Line Feed Recessed [18].

2.3. Microstrip-Line Feed

The feeding system of the antenna affects the antenna's input impedance and features. In microstrip feeding techniques, the microstrip-line, which is a conducting strip with a much smaller width compared to the patch, provides antenna excitation. So, by adjusting the inset location, this technique is easy to produce, model, and easy to match. However, as the thickness of the substrate increases, the surface waves and spurious feed radiation also increase, which restricts the bandwidth to 2-5 percent for practical designs and contributes to an increase in the cross-polar level [18].
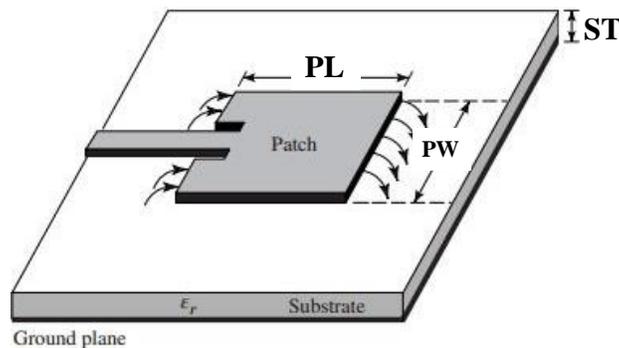
Figure 2.8. Patch Antenna With Microstrip Feed-Line [18].

2.4. Fundamental Design Parameters of Single Rectangular MPA

The antenna performance characteristics are mainly specified by the geometry shape, the physical structure dimensions, and the material properties from which it is produced. The very primary step to begin the designing of the rectangular MPA is carefully choosing the initial design parameters like resonant frequency at which the given antenna operates. Also, the dielectric constant (ε_r) is another important factor, which is used as an insulator. This increases the fringing fields that

15

account for radiation and usually selected in the $2.2 \leq \varepsilon_r \leq 12$ range [18]. Afterward, to design a rectangular MPA, the following parameters have to be calculated with immense attention. These include the length and width of the patch and feeder line, the place of the feed point, the substrate thickness, the patch's effective length, the patch's extension length, the ground plane dimensions, and other essential parameters.

2.4.1. Substrate Thickness

Dielectric substrate thickness is typically in the range of $0.003\lambda_0 \leq ST \leq 0.05\lambda_0$. The limitation on the thickness of the substrate for a given material and RF is governed by [43]:

$$ST \leq 0.06 \frac{C}{2\pi RF\sqrt{\varepsilon_r}}$$ (2.14)

If the thickness of the substrate of the MPA is very small, there is a reflection of waves at the edge of the patch that is generated in the dielectric substrate. As a result, a very small amount of energy is radiated. The field variations along the height are unchanged when the substrate's thickness is very minimal ($ST \ll \lambda_{SM}$). Hence, the substrate thickness can be calculated using the equation [44]:

$$ST = \frac{0.3C}{2\pi RF\sqrt{\varepsilon_r}}$$ (2.15)

Where ST is the thickness of the substrate, C is light speed, ε_r is dielectric constant, and RF is the resonant frequency.

2.4.2. Patch Width

The width of the patch has less influence on the radiation pattern and resonant frequency. But, it greatly affects the antenna radiation efficiency, bandwidth, and cross-polarization characteristics. The radiation efficiency of the patch antenna increases as the width goes up to half the wavelength. The patch antenna width is calculated using equation [37]:

$$PW = \frac{C}{2RF\sqrt{\frac{\varepsilon_r+1}{2}}}$$ (2.16)

Where PW denotes patch width, C is the speed of light, RF denotes resonant frequency, and ε_r is a dielectric constant.

2.4.3. Effective Dielectric Constant

The effective dielectric constant is specific to the framework of a fixed dielectric transmission line, and it offers a useful correlation between the impedance and velocity of different wavelengths. Its range is between $1 < \varepsilon_{reff} < \varepsilon_r$, so that the fields are not completely limited to the substrate but even to the fringe and disperse in the air. After the patch width and substrate thickness are known, the effective dielectric constant can be calculated using equation 2.17 [42].

$$\varepsilon_{reff} = \frac{(\varepsilon_r + 1)}{2} + \frac{(\varepsilon_r - 1)}{2}\left(1 + 12\left(\frac{ST}{PW}\right)\right)^{-0.5} \tag{2.17}$$

Where ε_{reff} denotes effective dielectric constant, ε_r is the substrate dielectric constant, PW is the patch width, and ST is the substrate thickness.

2.4.4. Effective Patch Length

The effective length of the patch is a sum of actual length and twice of extended length, or it can be calculated using equation 2.18. Effective length is used to calculate the original length of the patch and mathematically given by [37]:

$$PL_{eff} = \frac{C}{2RF\sqrt{\varepsilon_{reff}}} \tag{2.18}$$

Where PL_{eff} represents the effective length of the patch, C denotes the speed of light, ε_{reff} is an effective dielectric constant, and RF is a resonant frequency.

2.4.5. Patch Length Extension

Electrically, MPA seems greater than its actual dimensions due to fringing field effects. Because of this, both sides of the patch extend the length of the antenna, as indicated in Figure 2.4. This phenomenon is represented by ΔPL and calculated using the equation given by [38]:

$$\Delta PL = (0.412ST)\frac{(\varepsilon_{reff} + 0.3)\left(\frac{PW}{ST} + 0.264\right)}{(\varepsilon_{reff} - 0.258)\left(\frac{PW}{ST} + 0.8\right)} \tag{2.19}$$

Where ΔPL is the patch length extension, ε_{reff} is the effective dielectric constant, ST and PW are the substrate thickness and width patch, respectively.

17

2.4.6. Patch Length

The actual length of the patch is a crucial parameter in patch antenna design since it determines the resonant frequency. The patch length is typically about $0.3333\lambda_0 < PL < 0.5\lambda_0$ [42] for a rectangular microstrip antenna, where λ_0 is the wavelength of free-space. The actual length of the patch, mathematically described by [37]:

$$PL = PL_{eff} - 2\Delta PL \tag{2.20}$$

Where PL_{eff} is the effective length, ΔPL is the patch length extension, and PL is patch length.

2.4.7. Ground Plane Dimensions

In fact, the fields are not only limited to the patch, i.e., a fraction of the fields lies outside the physical dimensions of the patch because the dimensions are finite. The overall dimension of the substrate is designed to completely encapsulate the patch and the feed line. It means that the ground plane dimensions have to be large enough to support fringing fields and calculated using equations given by [37]:

$$GPL = PL + 6ST \tag{2.21}$$

$$GPW = PW + 6ST \tag{2.22}$$

Where GPL is ground plane length, GPW is the ground plane width, PL is patch length, PW is patch width, and ST is substrate thickness.

2.4.8. Location of the Feed point

The position of the feed point to the patch antenna is in X-Y coordinates, as X_f and Y_f, respectively, in order to balance the impedance mismatch between the edge of the patch and the feeder. The formula used to calculate the feed point locations is given by [20]:

$$Xf = \frac{PL}{2\sqrt{\varepsilon_{reff}}} \tag{2.23}$$

$$Yf = \frac{PW}{2} \tag{2.24}$$

Where X_f and Y_f are X-Y coordinates, PW and PL are the patch width and length, respectively.

2.4.9. Impedance Matching

As the electromagnetic radiation propagates to various parts of the antenna, each interface experiences different impedances. It allows some of the electromagnetic waves to bounce back to the source if there is an impedance mismatch at either of the interfaces. Effective matching increases the antenna's performance, thus increasing the antenna's bandwidth and reducing signal loss due to reflection. The efficient coupling matching network is used to attempt to match the impedance characteristics of the two elements over the selected frequency range [37]. The matching coupling network is shown in Figure 2.9 and is used to link the patch to the transmission line.
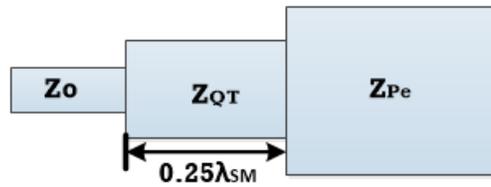
Figure 2.9. Coupling Matching Network [37].

Theoretically, the impedance is around 300Ω at the patch edge. However, it can be matched to Z_0 = 50Ω transmission lines using different matching networks. To adjust the impedance between the transmission line and the edge of the patch, the quarter-wavelength impedance transformer is widely used. By calculating the impedance at the edge of the patch using the mathematical equations provided by equation 2.25, the quarter-wavelength transformer impedance can be designed [37].

$$Z_{Pe} = 90\frac{(\varepsilon_r)^2}{(\varepsilon_r - 1)}\left(\frac{PL}{PW}\right)^2 \qquad (2.25)$$

$$Z_{QT} = \sqrt{Z_0 * Z_{pe}} \qquad (2.26)$$

Where Z_{pe} is impedance at the edge of the patch, Z_0, and Z_{QT} are characteristic and quarter-wavelength transformer impedance, respectively.

2.4.10. Width and Length of Microstrip Transmission Line

Between the source and the edge of the patch antenna, a microstrip transmission line is aligned. The interface exists along the width of the feeder line between the antenna and the feed line. Furthermore, for a given feed line width, the impedance is almost independent of the length

variation. The impedance varies with the width rather than its length. The length of the transmission line of the microstrip is calculated using [37]:

$$\text{LMTL} = \frac{\lambda_{SM}}{4} = \frac{\lambda_0}{4\sqrt{\varepsilon_r}}$$

(2.27)

Free-space wavelength is calculated by the equation given by:

$$\lambda_0 = \frac{C}{RF}$$

(2.28)

Where C is light speed, RF is the resonant frequency, λ_0 is the wavelength in free-space, whereas λ_{SM} is the wavelength in the substrate, and ε_r is a dielectric constant of the substrate.

The width of the microstrip transmission line is given by the equation [37]:

$$\text{WMTL} = \frac{5.98ST \dfrac{1}{\exp\left(\dfrac{Z_0\sqrt{\varepsilon_r + 1.41}}{87}\right)} - t}{0.8}$$

(2.29)

Where ST is substrate thickness, Z_0 is the characteristic impedance of the microstrip transmission line, t is the thickness of the patch, and ε_r is a dielectric constant of the substrate.

2.4.11. Inset Dimension

Inset Length: If the inset location is pushed from the edge of the patch towards the middle, impedance drops easily. Inset feed depth (IL) is used to provide impedance matching with a 50Ω connector. Mathematically, the inset length is given by the equation [45]:

$$\text{IL} = \left(\frac{PL}{\pi}\right)\text{Cos}^{-1}\sqrt{\frac{Z_0}{Z_{QT}}}$$

(2.30)

Where PL is the patch length, Z_0 and Z_{QT} are the characteristic and quarter-wavelength transformer impedance, respectively.

Inset Width (IW): The patch antenna's resonant frequency depends on the notch gap or the width of the inset. The expression that refers to the width of the inset and resonant frequency is given by [8]:

$$IW = \frac{4.65 * 10^{-12} * C}{RF \,(\text{in GHz}) \sqrt{2 * \varepsilon_{reff}}} \qquad (2.31)$$

Where C is the speed of light, RF is the resonant frequency, and ε_{reff} is the effective dielectric constant of the substrate.

2.4.12. Feed Point Width and Length

The width of the feed point can be obtained by using the equation given by [46]:

$$WFP = \frac{2ST}{\pi} \left[\left((B-1) - \ln(2B-1) \right) + \left(\frac{\varepsilon_r - 1}{\varepsilon_r} \left(\ln(B-1) + 0.39 - \frac{0.6}{\varepsilon_r} \right) \right) \right] \qquad (2.32)$$

Where ST is the substrate thickness, ε_r is a dielectric constant, and B is a constant.

Before calculating the width of the feed point, B and ZMTL must be calculated. ZMTL is calculated by using equation 2.12 and B can be obtained using the equation below [40].

$$B = \frac{60\pi^2}{ZMTL \sqrt{\varepsilon_r}} \qquad (2.33)$$

The length of the feed point is calculated by using the equation given below [18].

$$LFP = \frac{\lambda_{eff}}{4} \qquad (2.34)$$

The effective wavelength λ_{eff} is given by:

$$\lambda_{eff} = \frac{\lambda_0}{\sqrt{\varepsilon_{reff}}} \qquad (2.35)$$

Where λ_0 is the free-space wavelength, C is the speed of light, λ_{eff} is the effective wavelength, RF is the resonant frequency, and ε_{reff} is the substrate effective dielectric constant.

2.5. Planar Rectangular Microstrip Patch Antenna Array

In many applications, because of its minimized size, a single antenna is typically good to use. But in terms of gain, bandwidth, directivity, and other metrics, single antenna's performance is greatly degraded. Therefore, the use of an array in the antenna design is needed to minimize these drawbacks. An array is the design of two or more elements of the antenna that are included to

improve the performance of the antenna, particularly in terms of overall gain, radiated power, directivity, and various losses of power [3], [18], [40].

In the antenna array, antenna elements can be placed in either linear or planar geometry. In a linear antenna, these elements are arranged along the X or Y axis only. By using a linear array, better performance over a single antenna in terms of radiation pattern directivity, gain, and maximized signal strength can be provided. The beam scanning ability of the linear array is only limited to a single direction and the overall efficiency is reduced [18].

The planar array antenna in which array elements are placed in both X and Y plane is essential. The planar array antenna provides 2D beam scanning, minimized sidelobe level, null steering to the interference direction, and main beam placement directed to the desired signal. In addition, when a planar array has a separable excitation, an analysis can be done simply by considering each sub-array row (column) as a single element and then taking all rows (columns) into account to form a linear array row (column) [41], [47].
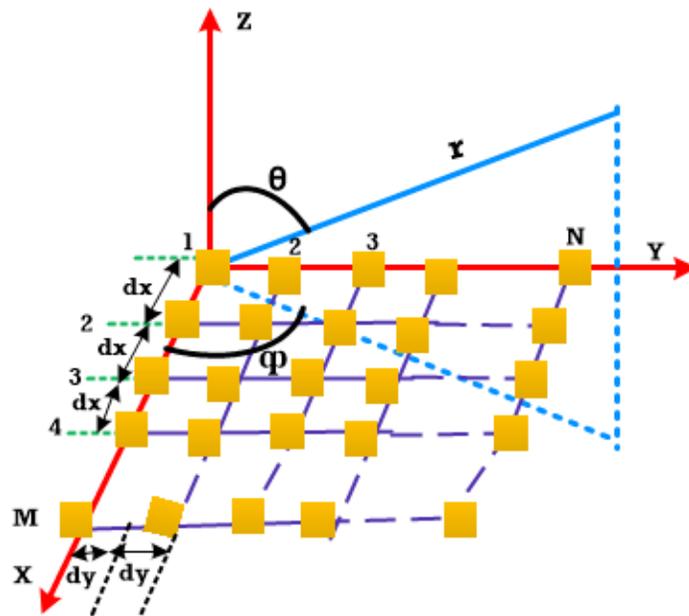
Figure 2.10. The Structure of MxN Antenna Array [41], [47].

The planar array's array factor is expressed as the multiplication of two linear arrays factors, i.e. one along the X-axis and one along the Y-axis. Let us assume that the space between all elements is equal to the d_x interval and the β_x progressive shift for the element of the mth row and the first column of the array matrix. The excitation amplitude of the element at the point with coordinates

22

$x = (m\text{-}1)\, d_x$, $y = 0$, is denoted by I_{m1}. Then, the linear array's array factor with M elements along the X-axis can be given as [18]:

$$AF_{x1} = \sum_{m=1}^{M} I_{m1} e^{j(m-1)(kd_x \sin\theta\cos\phi + \beta_x)} \tag{2.36}$$

Where $sin\theta cos\phi = cos\gamma_x$ is with respect to the X-axis directional cosine.

Similarly, if N of these arrays are positioned in the Y-direction next to one another, a rectangular array is created. Again, by considering that at a distance of d_y they are equally spaced and there is a progressive phase shift along each row of β_y and assuming that the distribution of the normalized current along each of the X-directed array is the same but that the absolute values correspond to a factor of I_{1n} (n = 1, 2. . . N), the array factor of a linear array of elements along the Y-axis is written as [18]:

$$AF_{1Y} = \sum_{n=1}^{N} I_{1n} e^{j(n-1)(kd_y \sin\theta\cos\phi + \beta_y)} \tag{2.37}$$

The pattern of a rectangular array, together with the X and Y directions, is the product of the array factors of the linear arrays. The array factor of the whole planar array is can be written as [18]:

$$AF = \sum_{n=1}^{N} I_{1n} \left[\sum_{m=1}^{M} I_{m1} e^{j(m-1)(kd_x \sin\theta\cos\phi + \beta_x)} \right] e^{j(n-1)(kd_y \sin\theta\cos\phi + \beta_y)} \tag{2.38}$$

All of the m and n components have the same excitation amplitudes in a uniform planar array. So, it is possible to treat I_{m1} and I_{1n} as I_0. The array factor of the planar array as a whole can then be written as:

$$AF = I_0 \sum_{m=1}^{M} I_{m1} e^{j(m-1)(kd_x \sin\theta\cos\phi + \beta_x)} \sum_{n=1}^{N} I_{1n} e^{j(n-1)(kd_y \sin\theta\cos\phi + \beta_y)} \tag{2.39}$$

The normalized array factor can be found as:

$$AF_n(\theta, \phi) = \left[\frac{\sin\left(\frac{M\psi_x}{2}\right)}{M\sin\left(\frac{\psi_x}{2}\right)} \right] \left[\frac{\sin\left(\frac{N\psi_y}{2}\right)}{N\sin\left(\frac{\psi_y}{2}\right)} \right] \tag{2.40}$$

Where $\psi_x = kd_x\, Sin\theta cos\phi + \beta_x$ and $\psi_y = kd_x\, Sin\theta cos\phi + \beta_y$.

2.6. Performance Metrics of the Antenna

The description of different parameters is required to define the antenna's performance. Some of the parameters are interrelated and, for a full explanation of the antenna performance, not all of them need to be defined. So, the parameters that are used to analyze the output of the patch antenna are presented in this section. Return loss (RL) is a very important parameter in the communication system and is defined as the loss of signal power due to a reflection in a transmission line at a discontinuity. The discontinuity can be caused by a discontinuity between the feed line and the port, or by a device inserted into the line.

Likewise, the VSWR is a measure of the efficiency of the transmission of radio frequency power across a transmission line. VSWR is one with the entire sum of input power being transmitted without any reflection for the optimum transmission line, and in realistic situations, any value less than two is also considered acceptable. The loss of return is expressed in dB and is given by [18], [28], [40]:

$$RL\ (dB) = -20log\ |\Gamma| \qquad (2.41)$$

The reflection coefficient (Γ) can be written as:

$$|\ \Gamma\ | = \frac{V_{0\,-}}{V_{0\,+}} = \frac{Z_{QT} - Z_0}{Z_{QT} + Z_0} \qquad (2.42)$$

Where v_{0^+} is the incident wave, v_{0^-} is the reflected wave, Z_{QT} and Z_0 are the quarter-wavelength transformer impedance and characteristic impedance, respectively.

As a function of the angular orientation and radial distance from the antenna, the radiation pattern is a graphical representation of the properties of antenna radiation. Properties of radiation include the density of field strength, power flux, intensity of radiation, directivity, and phase or polarization. In the far-field area, the radiation pattern is calculated and is depicted as a function of the directional coordinates. As seen in the figure below, the radiation pattern consists of the main lobe, sidelobe, and back lobe [18], [28], [40].
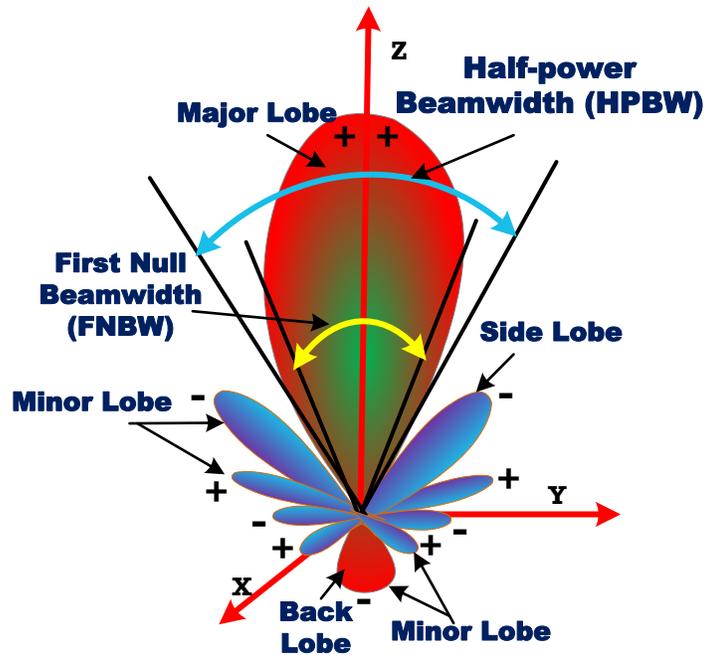
Figure 2.11. Directional Antenna's Radiation Pattern [18], [28].

While the amount of power packed in the beam is due to the antenna gain, the shape of the radiation beam depends on the directivity. The antenna gain is used to imply the antenna's ability to concentrate energy in a given direction. A given antenna's directivity and gain can be determined using the following equations [18].

$$D = \frac{4\lambda U}{\mathrm{Pr}\, ad} \tag{2.43}$$

$$G = D \text{ x } \eta_{rad} \tag{2.44}$$

Where D denotes directivity, P_{rad} is total radiated power, G is gain, U represents radiation intensity, and η_{rad} is radiation efficiency.

Furthermore, an antenna's bandwidth defines the frequency range over which the signal can be sent or received by the antenna. The use of the -10dB frequency in the return loss plot is a realistic way of obtaining the antenna's bandwidth [18].

2.7. Literature Reviews of Microstrip Patch Antenna

2.7.1. Reviews of Single Microstrip Patch Antenna

In recent years, improving communication networks involves the development of low-cost, low-weight, and low-profile antennas capable of sustaining high performance over a large frequency spectrum. Though the MPA is a very prospective candidate for 5G wireless applications, it faces different performance limitations. Hence, to improve and overcome the drawbacks of this antenna, several designs of single element patch antenna have been proposed and reviewed as follows.

Accordingly, broadband MPA for 5G wireless systems operating at 28GHz has been proposed in [6]. The antenna has a central operating frequency of 28GHz and can be used in the LMDS frequency band. With dimensions of 6.2mm x 8.4mm x 1.57mm, the antenna has a compact structure. As a substrate for the antenna construction, which has a dielectric coefficient of 2.2 and a thickness of 1.57mm, the Rogers RT Duroid 5880 material was used. Using the simulation, a low reflection coefficient of -22.51dB, a high energy gain value of 3.6dBi, a large operating band of 5.57GHz, and high energy efficiency were achieved by the antenna. As can it be seen from simulated observations, broad bandwidth is achieved. The achieved gain is yet very low, the magnitude of the return loss is high, and the substrate thickness is too large to be used for mobile 5G applications. Further, any shape changes are not included in the paper to improve main performance metrics.

In other similar work, in [21], inset feed compact mm-wave MPA at 28GHz is demonstrated for future 5G applications. The suggested antenna consists of a Rogers substrate with an εr of 2.2 and a thickness of 0.254mm and is excited by inset feeding technique. This antenna achieved a return loss of -34.05dB, VSWR of 1.75, bandwidth of 582MHz, and gain of 8dB. This result reveals that the proposed antenna has better performance regarding to return loss and bandwidth. However, the achieved magnitude of VSWR is large, which shows that there is much impedance mismatch and more energy has been reflected to the source.

Likewise, by using the same substrate material type and feeding technique, the design of a rectangular MPA is presented in [10], [48]. The proposed antenna in [10] obtained the return loss, VSWR, bandwidth, gain, radiation efficiency, and sidelobe level of 13.48dB, 1.5376, 847MHz, 6.63dB, -1.538dB, and -15.3dB, respectively. From this attained result, even though the performance in terms of bandwidth and magnitude of sidelobe level is good, still improvement in

gain, directivity, and radiation efficiency is required. The simulated similar work reported in [48] shows the return loss of -22.2dB, VSWR of 1.34, and gain of 6.85dB, respectively. The antenna provides the minimum return loss and VSWR, which gives better impedance matching and improved radiation efficiency. But, the achieved gain is low and the performance in the aspect of bandwidth is not analyzed for the proposed MPA.

Moreover, by varying dimensions of the patch and the substrate, the work reported in [12] presents the design and analysis of mm-wave MPA for 5G applications. To design this antenna, Rogers substrate is selected with a dielectric constant of 1.9 and a thickness of 0.3mm, and the patch is excited using an inset feeding approach. Keeping other parameters constant and varying length of the patch from 3.3mm to 3.7mm, the authors concluded that, there is no significant variation in the gain, radiation efficiency, and directivity of the antenna at a lower length. It is shown that the bandwidth and return loss are 0.5GHz and -12dB, respectively, in which the bandwidth is slightly increased whenever the length of the patch is above 3.6mm and changing the width of the patch from 4.4mm to 4.8mm, there is no acceptable value for bandwidth, radiation efficiency, and resonant frequency. Lastly, it is concluded that with lower values of substrate thickness, both gain and directivity are enhanced. The acquired result indicates that the proposed patch has a VSWR of 1.01, radiation efficiency of -0.6892dB, directivity of 8.333dBi, and sidelobe level of -18.3dB.

In designing the patch antenna, the selection of substrate material is an essential system requirement. Using a variety of substrate material types with distinct dielectric constant has an impact on the antenna performance. Relating to this, for the 5G network, a compact multiband microstrip patch antenna with a high gain was investigated in [27]. In this design, the width and length of the plane are modified to optimize the antenna performance and the substrate material is varied with various thicknesses to enhance the bandwidth. After analyzing different substrate types such as FR4, RT5880, RT3003, and RT6010 in the paper, it is concluded that RT6010 outperforms. Hence, the authors selected RT6010 substrate with ε_r of 10.2, a thickness of 1.6mm, and a tangent loss of 0.0023. Its overall dimension is 16.4mm x 15.5mm x 1.6mm and the inset feeding approach is incorporated to excite the patch.

By simulating the structure of the antenna, this antenna acquired return loss, VSWR, gain, and radiation efficiency of -17.8338dB, 1.2994, 12.013dB, and 92.655%, respectively. The bandwidth of the antenna is improved with 0.44GHz, 1.2GHz, 4.52GHz, 1.62GHz, 2.97GHz, and 0.3GHz at

a center frequency of 28.075GHz, 29.57GHz, 33.47GHz, 35.72GHz, 38.2GHz, and 39.85GHz, respectively. Even though good performance for this antenna is achieved in terms of return loss, gain, and VSWR, the selected patch size, dielectric constant, and thickness of the substrate are large which can cause the incompatibility issue in small handheld devices.

Likewise, another substrate type is used for the design and simulation of a rectangular MPA at 28GHz in [49] for 5G technology. The selected substrate material is Taconic TLY-5 with ε_r of 2.2, a thickness of 0.12mm, and a loss tangent of 0.0009. The overall dimension of the patch antenna is 7.14mm x 8.52mm x 0.12mm and excited by the microstrip inset feed technique. After analyzing the effect of different gap widths on the patch, the return loss equal to -27.7dB, VSWR of 1.22, bandwidth of 463MHz, gain of 6.72dB, the radiation efficiency of -1.199dB, and beam width of 74.4° have been obtained.

In general, the performance of the designs reported in [12], [20], [21], [27] shows good performance in the aspect of gain and directivity. Nevertheless, the antenna VSWR shown in [21] is large compared to [10], [12], [27] and return loss of antennas cited in [6], [10], [12], [21], [27] is large seen with that of the antenna presented in [20]. Also, the achieved radiation efficiency in [27] outperforms work reported in [10], [12]. Attempt to improve the bandwidth of MPA, design reported in [6], [10] outperforms design cited in [20], [21], [27], [49] but in terms of return loss and VSWR, the antenna design in [10] underperforms the designs revealed in [20], [21], [27], [48], [49].

From the comparison, it can be inferred that the reported designs have performance limitations in order to meet 5G necessities and still their enhancement is required. In another way, the improvement in the performance of a single element antenna has been achieved by changing and modifying the geometry of the MPA. These techniques are applied to overcome the drawbacks of conventional MPA that are inherent to narrow bandwidth and poor efficiency. So, proper enactment of slots with different shapes and defective ground surface techniques are used in uplifting the bandwidth capacity in compact size MPA. In this regard, the following works of the proposed patch antenna with these methods have been reviewed and presented.

In [4], a multiband U-shaped slotted MPA for 5G wireless communication is proposed. In this paper, the patch antenna is considered using Rogers RT 5880 substrate with ε_r of 2.2 and a height of 0.254mm at a resonance frequency of 28GHz and 38GHz. The resonant frequency of 38GHz is

achieved by inserting two U-shaped slots and using a microstrip inset feed-line of 50Ω to excite the patch. Additionally, the effects of parameters of the antenna like; length, width, and the distance between slots are analyzed. From this analysis, better return loss is achieved at patch length, width, and slot distance of 3.27mm, 4.09mm, and 0.2mm, respectively. The simulation result shows that the return loss of -32dB and -40dB; gain of 6.7dB and 7.92dB at 28GHz and 38GHz, respectively. Even though the insertion of slots improved the magnitude of the return loss of the designed antenna, other performance metrics need more improvement and also, performance in terms of bandwidth is not investigated in the proposed antenna.

Similarly, bandwidth enhanced mm-wave antenna with E-slotted for 5G wireless applications is demonstrated in [24]. The patch is designed using substrate FR-4 with ε_r of 4.4, a thickness of 1.6mm, and a loss tangent of 0.0025. An inset feeding approach is incorporated to excite it and the whole dimension of this antenna is 4.35mm x 5.5mm x 1.6mm. From the simulation result, it is found that the return loss, bandwidth, and gain are -48.25dB, 4.07GHz, and 5.61dBi, respectively. Whereas, the measured result shows that the return loss of -39.7dB, the bandwidth of 4.1GHz, and a gain of 5.32dBi. This reveals that the proposed antenna has better performance with regard to return loss and bandwidth. However, the path loss that comes across the communication system cannot be alleviated because of the low gain attained. Additionally, the effect of the chosen substrate thickness will cause a reduction in radiation efficiency because of the large amount of input power dissipated in the resistor.

In [51], a 28GHz broadband MPA for 5G wireless applications is demonstrated. The Rogers RT/Duroid5880 substrate material, with a dielectric constant of 2.2, the thickness of 0.3451mm, and loss tangent of 0.0009 were utilized for the examined antenna to function at 28GHz. The simulation results reveal that, the antenna has a low return loss of -54.49dB, a bandwidth of 1.062GHz, a gain of 7.554dBi. In addition, 98% and -18.4dB are the radiation efficiency and sidelobe level of the proposed MPA, respectively. The proposed rectangular MPA has got better performance in the aspect of RL, gain, bandwidth, and radiation efficiency. Though, the obtained bandwidth and gain is poor for 5G wireless applications.

Likewise, [52] presented design and analysis of a 28GHz MPA for 5G communication systems. In the paper, FR-4 substrate material with dielectric constant of 4.4 and thickness of 0.244mm is used. The attained result shows that the return loss, VSWR, bandwidth, directivity, gain, and

radiation efficiency are -38.86dB, 1.023, 1.046GHz, 7.509dBi, 7.587dBi, and 98.214% respectively. The key inference of this result is that the obtained results are good in terms of bandwidth, VSWR, radiation efficiency, and gain. However, using FR-4 for higher frequency applications gives raise to low performance.

Moreover, integrating both slotted shape and defective ground structure, the designs of the MPA for 5G application are reported in [22], [23]. In [22], a compact size Y-slotted patch antenna has been made using Rogers/RT Duroid 6002 substrate with thickness equal to 0.762mm, ε_r of 2.94, and tangent loss equal to 0.0012. Using the simulation, the achieved RL, VSWR, bandwidth, gain, directivity, and radiation efficiency are -56.95dB, 1.002, 1.38GHz, 7.6dB, 7.67dB, and 98% respectively. This result shows that better performance is achieved in terms of return loss, VSWR, gain, and bandwidth. But, the radiation efficiency of the antenna has deteriorated and the selected height of the substrate imposes an impact on the compatibility.

Likewise, the X-shape slotted patch antenna studied in [23] demonstrates a printed wideband antenna designed using Rogers substrate with ε_r of 2.2, a thickness of 0.254mm, and tangent loss of 0.0009 and excited by coaxial feeding technique. The attained result indicates that the return loss, VSWR, bandwidth, gain, and radiation efficiency are -20.03dB, 1.22, 2.11GHz, 5.23dB, and -0.8181dB, respectively. The key implication of this result is that the performance is good in terms of bandwidth, return loss, and VSWR, but low gain is obtained that cannot mitigate high path loss encountered and which in turn creates a less directive beam. Above and beyond, the use of a coaxial feeding approach is not appropriate for applications like cellular devices.

Furthermore, a slotted MPA working at 28GHz for 5G communication networks is designed and analyzed in [26]. It aimed to develop a single-element directional antenna using the FR4 substrate with ε_r of 4.4, height of 0.8mm, and a tangent loss of 0.02. To excite and match the impedance between the feeder and the edge of the patch, an inset feeding technique is incorporated. The antenna provides the return loss, VSWR, bandwidth, gain, and efficiency are -39.37dB, 1.022, 2.48GHz, 6.37dB, and 86.73%, respectively. The mm-wave-based circular slot MPA in [25] is suggested for 5G communication. The designed antenna is desired to operate at 32GHz and is developed using Rogers substrate with ε_r of 2.2, a thickness of 0.5mm, and a tangent loss of 0.0009. The overall physical structure of the antenna is 6mm x 6mm x 0.5mm and it is excited by the inset feeding technique. The simulation result of this antenna establishes that the return loss, VSWR,

bandwidth, gain, radiation efficiency, and directivity of the antenna are -28.47dB, 1.078, 1.9GHz, 7.63dB, -1.707dB, and 7.632dB, respectively. Even though the authors recommended the proposed MPA as a viable choice for metal-rimmed cell phone devices, the resonance frequency of 32GHz is not allotted by FCC yet.

Generally, by modifying and inserting different shapes of slots in a single MPA, the designs reported in [23], [24], [26], [51], [52] attempted to improve the bandwidth. Nevertheless, low gain is achieved in [23], [24] and large magnitude of return loss are observed in [23]. So, to enhance the gain, directivity, and VSWR, works demonstrated in [4], [22], [25], [51], [52] achieved better performance. The obtained results in [22] outperform [4], [23-25], [51], [52] in terms of RL. Inspite, the radiation efficiency of the antenna cited in [25] is lower than the antenna reported in [22], [51], [52]. From this review, it can be inferred that all these designs have drawbacks and need to be enhanced for modern antenna communication in 5G technology. Hence, here reviews of the proposed linear and planar configuration of the MPA arrays are presented in the following section.

2.7.2. Reviews of Microstrip Patch Antenna Arrays

A summary of the numerous detailed studies of a single element of MPA is provided in the above section. Still, the results obtained by these designed antennas do need enhancement in performance to be used in 5G communication networks. This is because, at a higher frequency, there is the air ingestion of electromagnetic waves and path losses which affect the overall performance of the antenna. As a result, several small antenna elements are combined in array form to improve some of the performance metrics like gain and directivity.

Hence, the need for designing an antenna array to get better performance and mitigate the problem of attenuation at a higher frequency band which is selected as the operating frequency is highly increased. In this repect, numerous authors studied and analyzed the performance of an MPA array by using distinct configurations along with different sizes of array elements. Thus, the studies of the proposed MPA arrays for further enhancement in future wireless applications are reviewed and presented as follows.

Attempting to improve the performance of a single MPA, the design and analysis of a 28GHz mm-wave antenna array for 5G communication systems is discussed in [30], [32]. To design both antennas Rogers substrate with ε_r of 2.2 has been used. More specifically, the antenna studied in [30] used a quarter-wave transformer feeding technique whereas the antenna cited in [32] used the

31

inset feeding technique for excitation. In paper [30], with various types of substrate and with differing thicknesses, it is found that the resonant frequency of single patch, 2x1, and 4x1 antenna array are 27.87GHz, 27.91GHz, and 27.59GHz, respectively. For optimized 2x1 and 4x1 array, the return loss of -20.31dB and -17.6dB, the gain of 10.07dB and 13.55dB, and bandwidth of 526MHz and 540.8MHz are observed, respectively.

On the other hand, the work in [32] attained a return loss of -18.64dB at 29.09GHz and a gain of 10.14dB. Additionally, between the operating frequency ranges of 24.81GHz - 33GHz, the bandwidth of 26% with VSWR ≤ 1.85 is achieved. Even though the performance is optimized in terms of some performance metrics in both papers, from the simulation, it can be inferred that the working frequency of the anticipated antenna is not accurate at 28GHz.

Microstrip antenna arrays can be arranged in different styles of feeding networks including series, corporate, and combination of both feeding networks. The series feed is simple to design but the power is not spread evenly among all the array antenna elements. While using the corporate feed, a large transmission line and thick substrate are required in designing the large size antenna array, which results in the introduction of much more transmission losses. So, to handle this problem, a hybrid feed structure is used in many designs [50].

From this point of view, in [29], a four-element MPA array with a corporate-series feed network for 5G communication is studied. This paper uses a Taconic RF-45 substrate with εr 4.5, a thickness of 1.6mm and a tangent loss of 0.0037 to design the antenna. In addition, the Yagi elements with two reflector elements and three director elements are loaded into the design to increase the total bandwidth and antenna gain. The achieved result of this antenna indicates that the return loss, bandwidth, and gain of the 4x1 array antenna are -48.6dB, 5.72GHz, and 9.49dB, respectively. Although better performance is obtained in terms of return loss, bandwidth, and gain, performance is not considered in terms of other metrics.

For cellular communications, the steerable directional antenna system is preferable since it has a good beam tracking ability. Accordingly, for 5G cellular communication, the design and simulation of directive high gain MPA array is studied in [20]. The proposed antenna consists of a Rogers substrate with a thickness of 0.254mm and ε_r of 2.2. The transmission line phase shifter is used to steer the antenna in the desired direction and the inset feed technique is being used for the matching between the patch and the feeder line. At 28GHz, the simulated results of single

patch, 2x1, 4x1, and 8x1 MPA array show that, the return loss of -59.369dB, -16.65dB, -37.57dB, and -50.99dB; the gain of 8.5dBi, 12.43dBi, 16.48dBi, and 21.04dBi; the directivity of 8.41dBi, 12.44dBi, 16.45dBi, and 20.94dBi, respectively. The bandwidth of a single patch and 8x1 array is 430MHz and 520MHz, respectively.

Even though better performance is attained for the return loss and gain, the magnitude of VSWR and the efficiency of the proposed antenna are not analyzed. Also, due to the dimension of the phase shifter structure incorporated at the feeding network to steer the antenna radiation beam, it creates incompatibility issues. Furthermore, in [31], a broadband microstrip antenna design with 16 array elements was proposed for the 5G applications. The antenna is designed using Rogers substrate with ε_r, tangent loss, and the thickness of 2.2, 0.0009, and 0.254mm, respectively. To excite the patch antenna, the quarter-wave transformer feeding technique is used. Using the simulation, at a operating frequency, the designed antenna provides return loss, bandwidth, gain, and sidelobe level of -37.254dB, 1.3851GHz, 18.5dB, and -2.6dB, respectively. The key implication of the attained result is that in terms of return loss, bandwidth, VSWR, and gain, the designed antenna has better performance. But, a large magnitude of sidelobe level is formed which leads to interference at the receiver side.

In an antenna array, arranging elements in a planar configuration provides high antenna efficiency and better gain in the communication systems. It also reduces the sidelobe level which in turn minimizes the amount of interference at the receiver side. In effect of this, a 28GHz planar MPA for future 5G wireless networks and applications is presented in [16]. To design the antenna, Rogers substrate is used with dielectric constant, thickness, and tangent loss of 2.9, 2.9mm, and 0.0025, respectively. The overall physical size of the antenna is 26.51mm x 20.37mm x 2.9mm and excited by the inset feeding technique. The performed simulation of the 2x2 array indicates that the VSWR, bandwidth, gain, directivity, return loss, and efficiency is 1.232, 400MHz, 8.393dBi, 10.130dBi, -19.66dB, and 82.85%, respectively. The key implication of the achieved result is that good performance is achieved in the aspect of return loss and VSWR. However, some other parameters are needed to be improved, and the selection of substrate thickness provides size incompatibility.

In another similar work cited in [35], the design of a 2x2 MPA array at 28GHz for mm-wave communication is demonstrated. This patch antenna is designed using a substrate foam with ε_r of

1 and a height of 1.5mm and an inset feeding technique is incorporated for excitation. The simulated result shows that the return loss, VSWR, bandwidth, gain, radiation efficiency, and sidelobe level are -74dB, 1.01, 4GHz, 23.8dB, 99%, and -5dB, respectively. The proposed antenna has achieved better results in most of its performance metrics by using the substrate called foam with a dielectric constant of 1 which in turn reduces the size of the antenna exceedingly. Nonentheless, using a thicker foam substrate that has a dielectric constant out of the acceptable range i.e., between 2.2 and 12, is very costly in which the antenna becomes fragile and not durable which leads to difficulty in real-time applications.

Likewise, in [32], a 4x4 U-slot patch array antenna at 28GHz is proposed for 5G communication. The antenna is designed by using a Taconic TLY substrate material with thickness, ε_r, and tangent loss of 0.508mm, 2.2, and 0.0009, respectively. The power divider is used to supply the elements of the array and a quarter-wavelength transformer is used to balance the patch's impedance line. The simulation result indicates that the return loss of -10dB is attained along with a bandwidth of the single antenna is 3.77GHz and that of an array is 4.91GHz. The maximum gain of the antenna is 16.48dBi and 17.01dBi in the X-Z and Y-Z planes, respectively. Although wide bandwidth and high gain are achieved, there are sidelobe s formed which cause the beam radiation in undesired directions. Not only this, the large amount of return loss means that the antenna and the driving transmission line have a high impedance mismatch.

In [33], the design and comparative performance assessment of different size of linear and planar rectangular MPA array configurations have been proposed. The simulation results show that directivity of the proposed single element, 2x1, 4x1, 2x2, 4x4, and 8x8 rectangular MPA arrays are 7.41dBi, 9.451dBi, 11.2dBi, 11.12dBi, 15.80dBi, 19.31dBi; the return losses are -20.24dB, -19.88dB, -27.42dB, -32.688dB, - 33.15dB, -17.75dB. As well, the radiation efficiency is more than 94.95% for one dimension MPA arrays and 79% for 2D MPA arrays. In the paper, it has been found that tuning the width of the patch, microstrip feeder line, ground plane, and inset gap affect the input impedance, directivity, bandwidth, and radiation efficiency of the antenna. However, achieved bandwidth is very narrow, which disagrees with the requirements of 5G antenna, the gain is very low, and the magnitude of return loss the antenna arrays is largely due to poor impedance matching made in the feeding networks. The substrate material used was FR-4, which provides low performance for higher frequency applications.

The work in [36] presents an ultra-wideband microstrip array antenna for 5G mm-wave applications. The antenna is designed using Rogers RT/5880 substrate with a thickness of 0.787mm, and a proximity coupling approach is incorporated to excite it. To advance the performance of the antenna, a combination of stepped line cut and U-slot has been used. It is observed from the simulation results that the antenna's return loss, bandwidth, and gain are -20.52dB, 4.47GHz, and 8.71dB, respectively. Although the proposed antenna's bandwidth is largely improved by using the proximity coupling feed technique, since perfect alignment is required, it is tough to manufacture. The gain of the antenna has deteriorated for the array, and the design did not analyze the performance to minimize the magnitude of VSWR and sidelobe level.

Similarly, a 28GHz printed antenna with improved gain using an array for 5G communication is presented in [19]. In the paper, both the linear and planar array is designed using substrate FR-4 with a height of 1.6mm, and a quarter-wave impedance transformer line feeding approach is incorporated for the excitation. From the simulation result, it can be noticed the return loss of a single patch, 2x1, and 2x2 are -14.15dB, -14.8dB, and -20dB; the gain of 6dBi, 6.15dBi, and 7.2dBi; the bandwidth of 0.8GHz, 0.77GHz, and 0.95GHz, respectively. Furthermore, the design and analysis of a novel patch antenna array are reported in [5] for 5G mm-wave applications. It presented multiband antennas designed with the Rogers substrate, which contains ε_r of 2.2, a thickness of 0.508mm, and a tangent loss of 0.0013. The techniques used to excite the antenna are tapered line feeding, and the overall sizes of the 2x1 and 2x2 array are 30mm $\times$ 7mm x 0.508mm and 24mm x 20mm x 0.508mm, respectively.

The output of the simulation shows that using a linear array at 44.8GHz and 67.8GHz, the achieved maximum and minimum gain is 14.22dB and 9.9dB, respectively. The authors then concluded that a linear antenna array has a higher gain than a planar array, while a planar array's bandwidth and return loss are better than that of linear. From this, it can be seen that, even though the radiation efficiency for both proposed antennas is in the range of 90%, the performance is not improved in terms of most of performance metrics simultaneously. Moreover, the analysis of antenna held under different frequencies reveals that better results are achieved as resonant frequency is increasing. But these operating frequencies are not approved by FCC yet.

In the above sections, reviews of single elements and arrays of MPA at 28GHz have been presented. So, to design and attempting to improve the performance of a single element MPA for

5G communication systems, several research studies have been carried out as reported in [4], [10], [12], [21-26], [48], [49], [51], [52]. From briefly reviewed papers in the above sections, it can be observed that the antenna designs presented in [12], [20], [21], [27], [33], [49] achieved narrow bandwidth. Whereas the attained bandwidth in [6], [22-26], [51], [52] is very wide, which is very suited for 5G communication systems. However, because of the less efficient impedance matching used, the return loss of a single element MPA reported in [10], [12], [23], [27], [33] is large. Similarly, works demonstrated in [20], [21], [25], [27], [52] achieved high gain, although, the magnitude of VSWR of [10], [21], [48] is large, which are deteriorating the antenna radiation efficiency.

Furthermore, antennas studied in [6], [23], [24], [26] have low gain. The radiation efficiency of the antennas cited in [10], [25], [49] is low, which needs to be improved. Trying to diminish these limitations, the single element MPA with significantly better radiation efficiency was proposed in [12], [26], [27], [33], [51], [52]. But, more generally, a single antenna's radiation pattern is comparatively broad with less value of gain along with larger physical dimensions. Most of the reviewed simulation results of single-element MPA mentioned in the current scientific literature are within the acceptable range, and the performance is enhanced in terms of very few performance metrics.

Thus, the above overall study of patch antenna shows that there is no single antenna with good performance in terms of all key performance metrics. Consequently, to enhance the performance of a single element MPA, different sizes of the linear MPA array designs are reported in [19], [20], [29-33]. In particular, attempting to increase the performance of the antenna in the aspect of directivity, return loss, and gain, numerous designs have been reported in [20], [29-31], [33] by increasing the number of array elements, using proper impedance matching technique, and varying the substrate thickness. The proposed rectangular MPA reported in [19], [20], [30], [33] show narrow bandwidth and also large return loss due to poor impedance matching. Whereas the proposed rectangular MPA array presented in [29], [31], [32] achieved significantly wide bandwidth and low magnitude of return loss.

Trying to mitigate the propagation effects at a higher frequency band, linear MPA arrays characterized by high gain were proposed in [20], [30], [31], [33]. Conversely, the gain of the patch arrays reported in [19], [29], [32] is low. In the above-mentioned papers, it can be seen that

the studied linear MPA boosted the performance of a single antenna in terms of only limited parameters. Also, there is a high magnitude of sidelobe level produced in the design, which creates high interference at the receiver side. As well, there is an incompatibility issue because of substrate thickness and they only scan in a single direction, which is failed to satisfy one of the requirements to be used in modern antenna systems, more specifically, for 5G mm-wave communication systems.

Hence, to overcome the performance constraints of linear MPA arrays with different sizes, planar MPA array designs are reported in [16], [19], [34-36]. The simulated structures reveal that the bandwidth of the MPA arrays presented in [16], [19] is narrow, which is against the requirements of 5G communication systems. Whereas the MPA array designs reported in [34-36] achieved profoundly wide bandwidth. In the same manner, the patch antenna arrays cited in [34], [35] have improved gain and radiation efficiency. While the gain of the MPA arrays reported in [16], [19], [36] is low, and the return loss is large.

Generally, the proposed planar patch antenna arrays improved the performance of both single element and linear MPA array in terms of scanning plane and some performance metrics. However, in most of the reported literature, the design consideration was to boost the performance of the antenna with only a limited number of performance metrics, which is inefficient for 5G wireless technologies. It can be deduced that the studies did not explore more effective planar MPA array designs by incorporating different etched structures on the patch and the ground plane structure to enhance the bandwidth, gain, and radiation efficiency for 5G communication systems. Therefore, further research investigations are highly required to improve their performance for 5G mm-wave communication systems. In this repect, in this study, the design and then performance enhancement of planar MPA arrays by introducing defect structure on both the patch and the ground plane structure is explicitly presented.

Chapter Three

Design of Single Element and Planar Rectangular MPA Array

Two key sections organize the overall content of this chapter. Firstly, the design methodology and numerical design calculations for the dimensions of the rectangular single element MPA were presented. The second section presents the design methodology and design calculations of different sizes of planar rectangular MPA arrays.

3.1. Design Methodology of a Single Element Rectangular MPA

To accomplish any design goals, clearly stated methodology and procedures are very mandatory. On this point, the overall procedure that has been used in this thesis work is shown in Figure 3.1. To begin with the patch antenna design, the very basic procedures start by selecting the resonant frequency and substrate material type along with its thickness and dielectric constant. Next, by substituting the selected initial design parameters in the governing equation given in chapter two, all physical dimensions of the antenna such as width and length of the patch, ground plane, microstrip feeder line, and feed point of the antenna are going to be calculated.

Subsequently, the structural modeling and performance analysis of a typical single patch antenna will be simulated by the CST simulator. Then, its performance will be checked whether it is acceptable or not as seen with standard settings of 5G antennas. According to 3GPP, these standards are as follows: return loss should be less than -10dB, gain is between 6dBi and 9dBi, directivity lies between 7dBi and 10dBi, VSWR between 1 and 2. If the achieved simulation result is not acceptable compared to these standards, it goes back and re-simulated by tuning the dimensions of the antenna. If an acceptable result is obtained, then simulation outputs of the designed antenna will be compared to that of similar designs reported in the literature.

Then, if the attained result is less than the similar works, again re-simulating along with antenna dimensions tuning will be held. Attempting to enhance the performance of a typical single antenna designed in the above section in terms of directivity, bandwidth, and gain, the modified single rectangular MPA is going to be designed by introducing the defect on both radiating patch and ground plane structure. Afterward, the structural modeling and performance analysis of the modified single patch antenna will be done by the simulation. Then, the performance of the designed antenna is checked whether it is acceptable or not. If the achieved result is not acceptable, it goes back and re-simulated by tuning the dimensions of the antenna structure.

If an acceptable result, the designed antenna will be compared with the typical single rectangular MPA and with the simulation results reported in the scientific literature. Then, if the attained result is less than the existing similar works, re-simulating will continue. However, if the modified single MPA outperforms both the typical single MPA and most of the reported design in recent literature, the achieved simulation result is documented, and the modified patch antenna is then used as the building block to begin the design of the planar KxK rectangular MPA array.
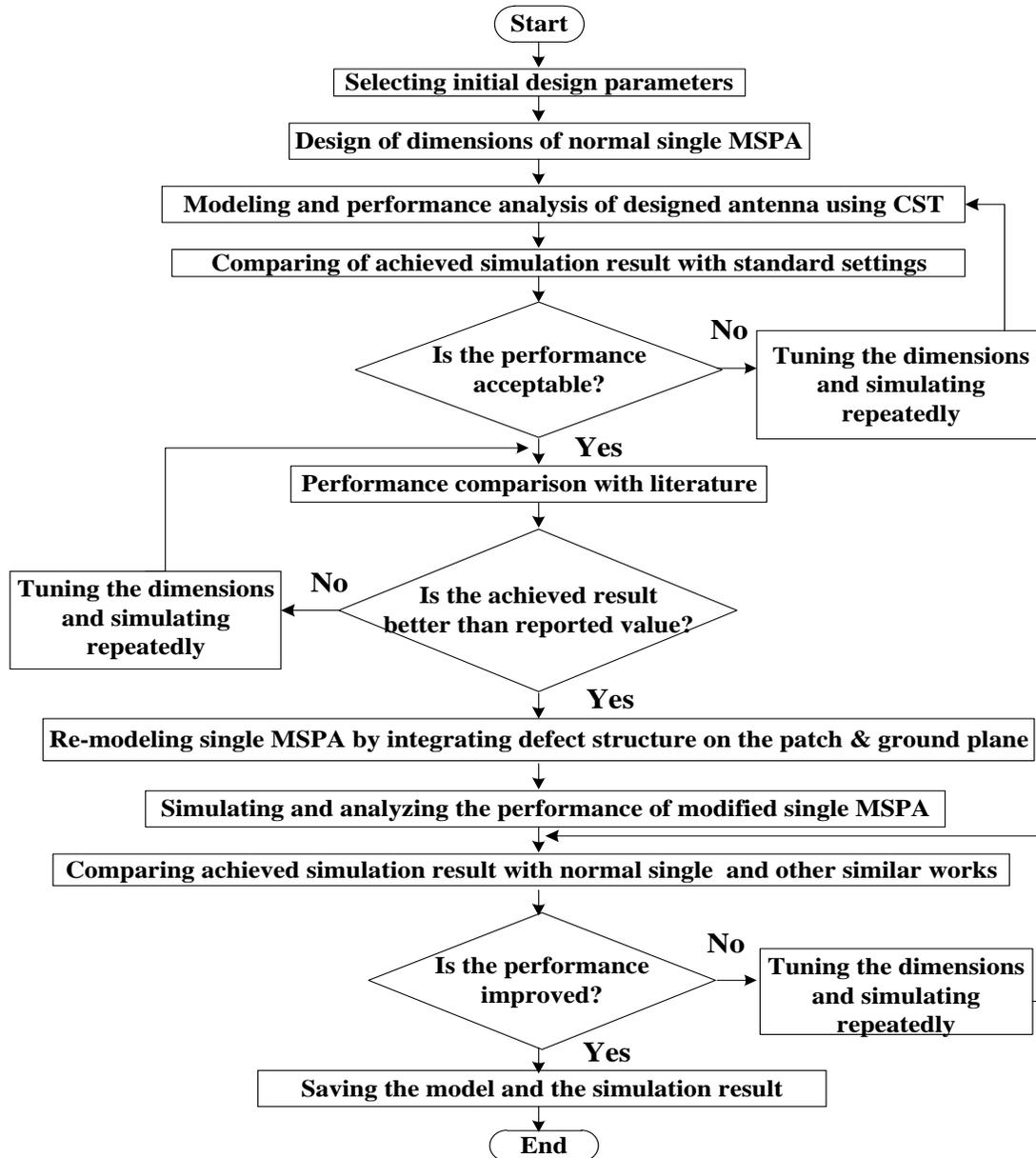
Figure 3.1. Design Methodology of Single Element MPA.

3.2. Design Calculations of Typical Single Element Rectangular MPA

As stated in the above section, to start the design of the patch antenna, first, the initial design parameters are selected. Accordingly, in this study, the substrate material of Rogers RT 5880 with a dielectric constant of 2.2 and a thickness of 0.34490mm is used, and 28GHz frequency has been selected as a resonant frequency. By using these initial design parameters, all physical dimensions of substrate thickness, length, and width of the radiating patch, feeder-line, and ground plane, inset length, inset width, and feed point location are calculated as follows by using the governing equations given in chapter two.

Substrate Thickness (ST): The substrate material's thickness is calculated by substituting the values of; C, ε_r, and RF in equation 2.15, which are $3 * 10^8$ m/sec, 2.2, and 28GHz, respectively.

$$ST = \frac{0.3C}{2\pi RF\sqrt{\varepsilon_r}} = \frac{0.3 * 3 * 10^8 \text{ m/sec}}{56\pi * 10^9 /\text{sec} * \sqrt{2.2}} = \frac{0.9}{260.94516} * 10^{-1} = 0.34490 \text{mm}$$

Patch Width (PW): The patch width is calculated by substituting $C = 3 * 10^8$ m/sec, $\varepsilon_r = 2.2$, and RF = 28GHz in equation 2.16.

$$PW = \frac{C}{2RF\sqrt{\frac{\varepsilon_{r+1}}{2}}} = \frac{3 * 10^8 \text{ m/sec}}{56 * 10^9 * \sqrt{1.6} * \frac{1}{\text{sec}}} = \frac{3}{70.835019} * 10^{-1} \text{m} = 4.23519 \text{mm}$$

Effective Dielectric Constant (ε_{reff}) and Effective Length of the Patch (PL$_{eff}$): After the values of PW and ST are calculated, the effective dielectric constant is obtained by substituting; $C = 3 * 10^8$ m/sec, $\varepsilon_r = 2.2$, PW = 4.23519mm, ST = 0.34490mm, and RF = 28GHz in equation 2.17.

$$\varepsilon_{reff} = \frac{(\varepsilon_{r+1})}{2} + \frac{(\varepsilon_{r-1})}{2}\left(1 + 12\left(\frac{ST}{PW}\right)\right)^{-0.5} = 1.6 + \frac{1.2}{2}\left(1 + 12(0.08144)\right)^{-0.5} = 2.02669$$

Next, by substituting $C = 3 * 10^8$ m/sec, $\varepsilon_{reff} = 2.02669$, and RF = 28GHz in equation 2.18, the patch antenna's effective length is calculated as follows.

$$PLeff = \frac{C}{2RF\sqrt{\varepsilon_{reff}}} = \frac{3 * 10^8 \text{ m/sec}}{56 * 10^9 * 1.42362 * \frac{1}{\text{sec}}} = \frac{3}{79.72264} * 10^{-1} \text{m} = 3.76305 \text{mm}$$

Patch Length Extension (ΔPL) and Patch Length (PL): The patch length extension is calculated by replacing the values of; PW, ST, and ε_{reff} in equation 2.19, which are 4.23519mm, 0.34490mm, and 2.02669, respectively.

$$\Delta PL = (0.412 ST)\frac{(\varepsilon reff + 0.3)\left(\dfrac{PW}{ST} + 0.264\right)}{(\varepsilon reff - 0.258)\left(\dfrac{PW}{ST} + 0.8\right)} = (0.14209mm)*\frac{29.18477}{23.13353} = 0.17927mm$$

Next, the value of patch length is found by substituting the values of PL_{eff} and ΔPL in equation 2.20, which are 3.76305mm and 0.17927mm, respectively.

$$PL = PL_{eff} - 2\Delta PL = 3.76305mm - 2(0.17927mm) = 3.40451mm$$

Ground Plane Length and Width (GPL and GPW): The dimension of the ground plane should be strong enough to direct the radiated energy to the desired direction. Hence, the ground plane's length and width are calculated by substituting PL = 3.40451mm, PW = 4.23519, and ST = 0.34490mm in equations 2.21 and 2.22, respectively.

$$GPL = PL + 6ST = 3.40451mm + 6(0.34490mm) = 5.47391mm$$

$$GPW = PW + 6ST = 4.23519mm + 6(0.34490mm) = 6.30459mm$$

Feed Point Location: The feed point location of the patch antenna can be found by substituting; PL = 3.40451mm, PW = 4.23519mm, and ε_{reff} = 2.02669 in equations 2.23 and 2.24. Therefore, the location of the feed point along the X-axis (X_f) and Y-axis (Y_f) is calculated as:

$$Xf = \frac{PL}{2\sqrt{\varepsilon reff}} = \frac{3.40451mm}{2\sqrt{2.02669}} = \frac{3.40451mm}{2.84727} = 1.19572mm$$

$$Yf = \frac{PW}{2} = \frac{4.23519mm}{2} = 2.11759mm$$

The performance characteristic of the patch antenna is highly dependent on impedance matching status in the feeding network. The impedance at patch's edge can be calculated by substituting PW = 4.23519mm, PL = 3.40451mm, and ε_r = 2.2 in equation 2.25.

$$ZPe = 90\frac{(\varepsilon r)^2}{(\varepsilon r - 1)}\left(\frac{PL}{PW}\right)^2 = 90\frac{(2.2)^2}{(1.2)}\left(\frac{3.40451mm}{4.23519mm}\right)^2 = 234.56869\Omega$$

After Z_{pe} is calculated, the quarter-wavelength transformer impedance can be calculated by substituting Z_{pe} and $Z_0 = 50\Omega$ values in equation 2.26.

$$Z_{QT} = \sqrt{Z_0 * Z_{pe}} = \sqrt{50 * 234.5686} = 108.29789\,\Omega$$

Width and Length of the Microstrip Transmission Line (WMTL and LMTL): The width of microstrip transmission line can be calculated using equation 2.29 and substituting ST = 0.34490mm, ZMTL = 50Ω, ε_r = 2.2, and t = 0.035mm (standard thickness for copper metal). The width of the microstrip transmission line becomes:

$$\text{WMTL} = \dfrac{5.98ST\dfrac{1}{\exp\left(\dfrac{Z0\sqrt{\varepsilon r}+1.41}{87}\right)} - t}{0.8} = \dfrac{\left(\dfrac{2.062502\text{mm}}{\exp(1.09195)} - 0.035\text{mm}\right)}{0.8} = \dfrac{(0.6571\text{mm})}{0.8} = 0.82137\text{mm}$$

The microstrip transmission line impedance is strongly dependent on the microstrip transmission line width. The length should also be considered since it can create compatibility issues. Hence, by replacing the values of; λ_0 = 10.7143mm, ε_r = 2.2, and ε_{reff} = 2.02669 in equation 2.27, the length of the microstrip transmission line is:

$$\text{LMTL} = \dfrac{\lambda_{SM}}{4} = \dfrac{\lambda_0}{4\sqrt{\varepsilon_r}} = \dfrac{\lambda_0}{4\sqrt{2.2}} = \dfrac{10.7143 \text{ mm}}{5.93296} = 1.80589 \text{ mm}$$

Length and Width of Inset Feed (IL and IW): The inset length and width are calculated by substituting PL = 3.40451mm, Z_0 = 50Ω, and Z_{QT} = 108.29789Ω in equation 2.30 and also, substituting C = 3*10^8m/sec, ε_{reff} = 2.02669, and RF = 28GHz in equation 2.31, respectively.

$$\text{IL} = \left(\dfrac{PL}{\pi}\right)Cos^{-1}\sqrt{\dfrac{Z_0}{Z_{QT}}} = \left(\dfrac{3.40451\text{mm}}{3.14}\right)Cos^{-1}\left(\sqrt{\dfrac{50}{10829789}}\right) = 0.89268\text{mm}$$

$$\text{IW} = \dfrac{4.65*10^{-12}*C}{RF\,(\text{in GHz})\sqrt{2*\varepsilon reff}} = \dfrac{3*4.65*10^{-4}}{28\sqrt{2*2.0669}} = \dfrac{13.95*10^{-4}}{56.37242}\text{m} = 0.02475\text{mm}$$

Width and Length of the Feed Point (WFP and LFP): The width and length for the feed point can be calculated by substituting; ST = 0.34490mm, B = 7.98490, ε_r = 2.2 in equation 2.32 and λ_0 = 10.7143mm and ε_{reff} = 2.02669 in equation 2.34, respectively.

$$\text{WFP} = \frac{2\text{ST}}{\pi}\left[((B-1)-\ln(2B-1))+\left(\frac{\epsilon r - 1}{\epsilon r}\left(\ln(B-1)+0.39-\frac{0.6}{\epsilon r}\right)\right)\right] = 5.40305 * 0.21957 \text{ mm} = 1.18635 \text{ mm}$$

$$\text{LFP} = \frac{\lambda_0}{4\sqrt{\epsilon_{\text{reff}}}} = \frac{7.52609 \text{ mm}}{4} = 1.88152 \text{ mm}$$

To enhance the performance of the rectangular MPA, different shapes of defect structures can be incorporated in the radiating patch or/and the ground plane. Regarding to this, in this study, after optimizing the rectangular MPA, a semi-elliptical slot is introduced to both the radiating element and group plane of rectangular MPA. This half-ellipse part on both the radiating element portion and the ground plane has been etched out to boost the performance characteristics, as indicated in Figure 3.2.
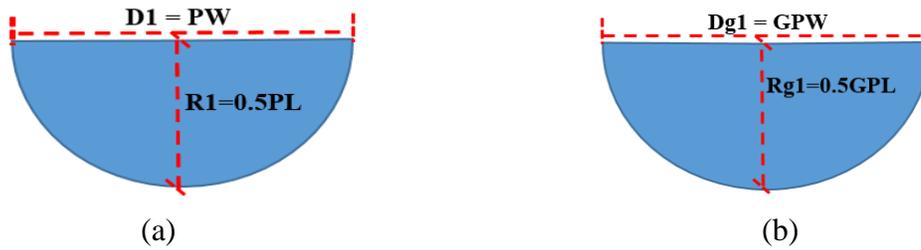
Figure 3.2. The Semi-elliptical Slot Structure on the Patch (a) and Ground Plane (b).

Therefore, to analyze its performances, above semi-elliptical slot is introduced on the radiating patch with different dimension as shown in the Figure 3.3. By considering the rigorous mathematical representation of ellipse, in the first case, the diameter of the ellipse is the same as width of the patch width along the major axis and half of the patch length along minor axis. In the second case, the diameter of the ellipse is half of the patch width and length along the major axis and minor axis respectively. In the last case, the diameter of the ellipse is two third of the radiating patch width along major axis and along minor axis it is still half of the patch length. Generally, in all cases the dimension of minor axis is kept constant as half patch length and that of major axis is varied in logical manner of calculating the dimension of the ellipse on the basis of radiating element width.
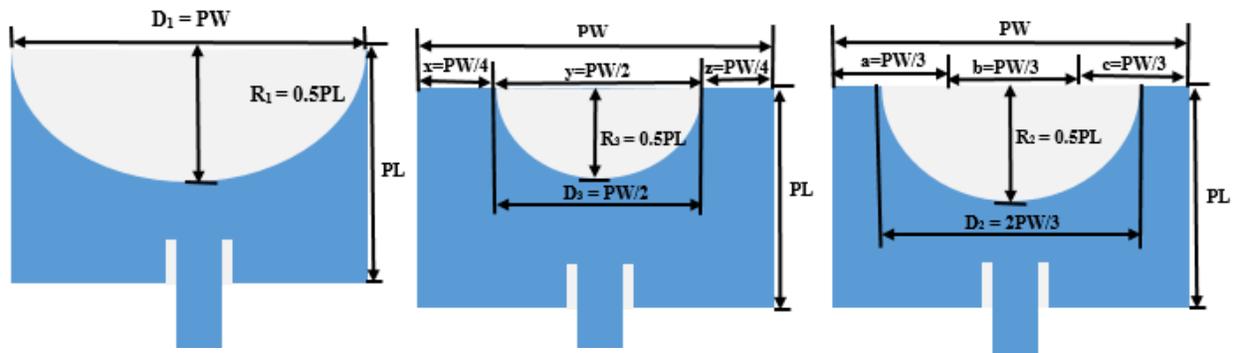
Figure 3.3. Semi-elliptical Slotted Radiating Patch with Different Dimension.

After setting the dimensions of the slot, CST Microwave Studio simulator is used to determine the optimal dimensions of the slots. The optimal performance of the antenna is obtained when the diameter of the major axis of the slot is 3.15mm for radiating element and 4.67mm for the ground plane structure; and when the diameter of minor axis of the slot is 1.22mm for the radiating element and 2.33mm for the ground plane structure. Inset-fed structure is used to improve the reflection coefficient of the antenna.

The explicitly calculated dimensions for single element rectangular MPA are tabulated in Table 3.1 and the complete physical structures of the proposed typical and modified semi-elliptical slotted MPA are shown in Figure 3.4.

(a)   (b)
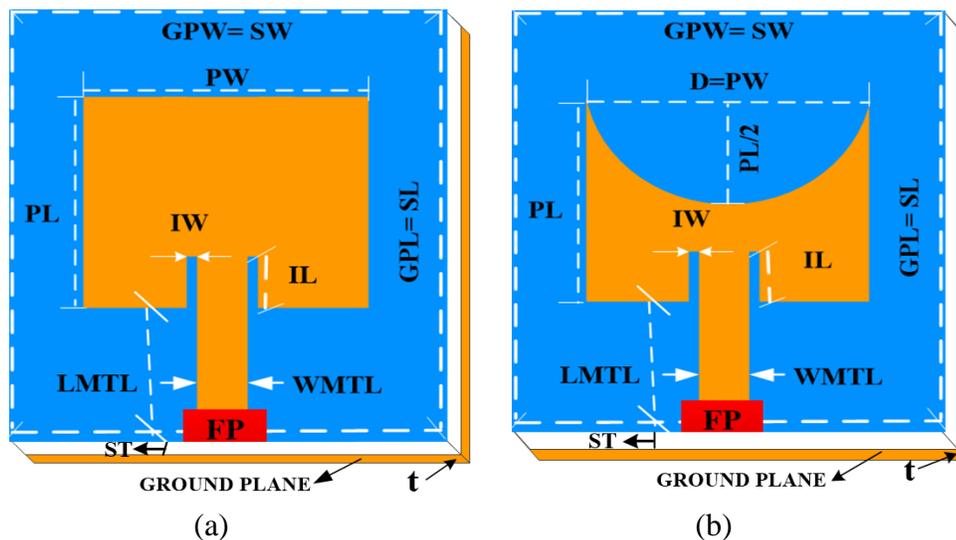
Figure 3.4. (a) Typical and (b) Semi-elliptical Slotted MPA.

44

Table 3.1. Designed Parameters for Single Element Rectangular MPA.

Designed Antenna Parameters	Symbols	Values (mm)
Substrate Thickness	ST	0.34490
Patch Width	PW	4.23519
Effective Dielectric Constant	ε_{reff}	2.02669
Effective Length of the Patch	PL_{eff}	3.76305
Patch Length Extension	ΔPL	0.17927
Patch Length	PL	3.40451
Location of the feed point along the X-axis	X_f	1.19572
Location of the feed point along the Y-axis	Y_f	2.11759
Length Microstrip Transmission Line	LMTL	1.80589
Width Microstrip Transmission Line	WMTL	0.82137
Length of Inset Feed	IL	0.89268
Width of Inset Feed	IW	0.02475
Ground Plane Width	GPW	6.30459
Ground Plane Length	GPL	5.47391
Length of the Feed Point	LFP	1.88152
Width of the Feed Point	WFP	1.18635

3.3. Design Methodology of a Planar KxK Rectangular MPA Array

The design methodology that has been used to design different sizes of planar MPA array is indicated in Figure 3.4. Thus, the planar 2x2 patch antenna array has been designed to continue designing the different sizes of the MPA array using the modified single element MPA designed in section 3.2 as the building block, and then its structure is modeled, and the performance is analyzed using software simulation.

In the same manner, as a typical and modified single patch antenna, its performance is checked if it lies within standard settings of the antenna and then antenna for 5G mm-wave communication systems or not. This will be performed with the standards given for the performance metrics antenna for 5G mm-wave systems. If it is not acceptable, tuning the dimensions of the design and re-simulating the structure will continue.

If obtained simulation results are acceptable, the performance comparison with similar designs reported in the recent literature will take place, and if the performance is low, the planar 2x2 patch antenna will be redesigned by optimizing the design parameters. When the designed antenna reveals better performance, the achieved simulation result is documented, and then the designed structure is used as the building block to design planar 4x4 MPA array, and the same process continues for its designing and performance analysis. Afterward, the designed and improved planar 4x4 MPA is then used as a building block for the design of an 8x8 MPA array.

This process will continue in the same way until the achieved and increased performance simulation results of the designed planar MPA array is applicable for 5G mm-wave communication systems. In this overall progression, there will be some techniques used while analyzing and increasing the performance of the planar MPA array. For instance, the choice of proper feeding methods, the introduction of the defected structure as required, and adjusting the physical dimensions will be made.

```
                          ┌─────────┐
                          │  Start  │
                          └─────────┘
                               │
                               ▼
              ┌──────────────────────────────────────┐
              │   Selecting initial design parameters │
              └──────────────────────────────────────┘
                               │
                               ▼
              ┌──────────────────────────────────────┐
              │  Design of dimensions of normal single MSPA │
              └──────────────────────────────────────┘
                               │
                               ▼
      ┌─────────────────────────────────────────────────────────────┐
   ┌─▶│ Modeling, simulating and performance analysis of designed antenna using CST │
   │  └─────────────────────────────────────────────────────────────┘
   │                           │
   │                           ▼
   │  ┌─────────────────────────────────────────────────────────────┐
   │  │ Comparing of achieved simulation result with standard settings & literature │
   │  └─────────────────────────────────────────────────────────────┘
   │                           │
   │           No              ▼
 ┌────────┐◀───────────◇ Is the performance ◇
 │Tuning the│           ◇   acceptable?     ◇
 │dimensions│           ◇                   ◇
 │repeatedly│                    │ Yes
 └────────┘                      ▼
   ▲          No        ◇ Is the achieved result ◇
   └──────────────◀─────◇ better than reported value? ◇
                               │ Yes
                               ▼
    ┌──────────────────────────────────────────────────────────────┐
    │ Re-modeling single MSPA by integrating defect structure on the patch & ground plane │
    └──────────────────────────────────────────────────────────────┘
                               │
                               ▼
        ┌──────────────────────────────────────────────────┐
        │ Simulating and analyzing the performance of modified single MSPA │
        └──────────────────────────────────────────────────┘
                               │
                               ▼
    ┌──────────────────────────────────────────────────────────┐
    │ Comparing achieved simulation result with normal single and other similar works │
    └──────────────────────────────────────────────────────────┘
                               │
                               ▼           No      ┌──────────┐
                    ◇ Is the performance ◇────────▶│Tuning the│
                    ◇   improved?        ◇         │dimensions│
                               │ Yes              └──────────┘
                               ▼
  ┌──────────────────────────────────────────────────────────────┐
  │ Design of K x K MSPA array using modified single element as a building block │◀──┐
  └──────────────────────────────────────────────────────────────┘                   │
                               │                                                      │
                               ▼                                                      │
      ┌──────────────────────────────────────────────────┐                          │
      │ Simulating the modeled MSPA and analyzing its performance │                  │
      └──────────────────────────────────────────────────┘                          │
                               │                                                      │
                               ▼                                                      │
      ┌──────────────────────────────────────────────────┐                          │
      │ Comparing achieved simulation result with recent literature │                │
      └──────────────────────────────────────────────────┘                          │
                               │              No      ┌──────────┐                   │
                    ◇ Is the performance ◇───────────▶│Tuning the│                   │
                    ◇   improved?        ◇            │dimensions│                   │
                               │ Yes                 └──────────┘                   │
                               ▼                                                      │
      ┌──────────────────────────────────────────────────┐                          │
      │ Saving the simulation result and design next planar array │──────────────────┘
      └──────────────────────────────────────────────────┘
                               │
                               ▼
      ┌──────────────────────────────────────────────────┐
      │ Document all saved simulation results of all designed MSPA │
      └──────────────────────────────────────────────────┘
                               │
                               ▼
                          ┌─────────┐
                          │   End   │
                          └─────────┘
```

Figure 3.6. Design Methodology of Planar KxK Rectangular MPA Array.

3.4. Design Calculations of Planar 2x2 Rectangular MPA Array

The single element MPA antenna's radiation pattern is broad, and its gain is low. Even though some linear MPA array has been designed to improve these drawbacks, the beam scanning direction is limited to a single direction, either the azimuth plane or elevation plane. Hence, in this section, the planar 2x2 rectangular MPA array is proposed to mitigate these limitations and enrich modern communication systems with two-dimensional beam scanning.

To design a planar 2x2 rectangular MPA array, four modified single rectangular MPA elements are used as a building block. The elements are grouped into one pair of 2x1 linear configurations. Therefore, the Planar 2x2 MPA array can be designed by connecting a pair of 2x1 rectangular MPA arrays using a 100Ω feeder line. A quarter-wave impedance transformer is used to decrease the antenna return loss. This improves the matching quality of the radiating element and the feeder line. The design parameters of a single element antenna are used to design a 2x2 rectangular MPA array, and the remaining design parameters of a 2x2 rectangular MPA array are calculated as follows:

Inter-element Space: The mutual coupling between the array's elements decreases the radiation efficiency of the antenna by increasing the sidelobe. To minimize this effect, the inter-element space (IS) has to be greater than half of the free-space wavelength (IS $\geq 0.5\lambda_0$). Also, to avoid grating lobe, separation distance should be less than the free-space wavelength (IS $\leq \lambda_0$), i.e., the selection should be between $0.5\lambda_0 \leq$ IS $\leq \lambda_0$. In this design, an inter-element space of 5.35mm has been selected.

Length and Width of 1:2 Power Divider: The width of 1:2 power divider (WPD) is the sum of; IS, PW, and WMTL. The width is calculated by adding their values, i.e., 4.23519mm, 5.35mm, and 0.82137mm.

$$WPD = 5.35mm + 4.23519mm + 0.82137mm = 10.40656mm$$

With the design parameters of RF = 28GHz, ST = 0.34490mm, ε_r = 2.2, and Z_0 = 50Ω, the microstrip transmission line width is 0.82137mm. The length of 1:2 power divider (LPD) is a microstrip transmission line with 100Ω. The LPD is half of the width of 0.82137mm, which is 0.41069mm.

Length and Width of Power Divider Arm: The length of the power divider arm (LPDA) is the same as the LMTL, which is 1.80589mm. Similarly, the width of the power divider arm (WPDA) is equivalent to the WMTL, which is 0.82137mm. The WPDA is 0.82137mm.
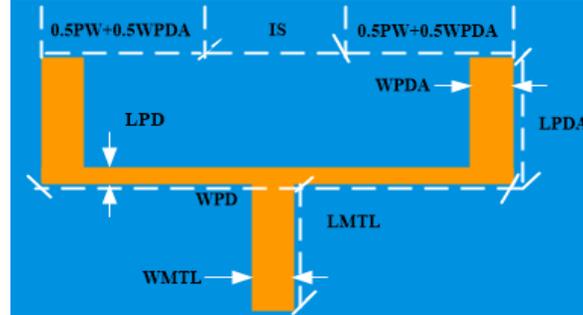

Figure 3.7. 1:2 Power Divider.

Length and Width of Microstrip Transmission Line Connecting two 2x1 MPA arrays: The length of the microstrip transmission line connecting two 2x1 MPA arrays ((LMTLC) $_{2x1}$) is the sum of the values of; IS, PL, and LMTL. Hence, by adding these dimensions together i.e., IS = 5.35mm, PL = 3.40451mm, and LMTL = 1.80589mm, the (LMTLC) $_{2x1}$ is equal to 10.56040mm. The width of the microstrip transmission line connecting two 2x1 MPA arrays ((WMTLC) $_{2x1}$) is the same as the WMTL. Thus, the (WMTLC) $_{2x1}$ is 0.82137mm.

Length and Width of First, Second, and Third-Quarter impedance transformer: The length of the first-quarter transform (LQ1) is $0.25\lambda_{SM}$. Since λ_{SM} is 7.22358mm, which is obtained by substituting the values of λ_0 = 10.7143mm and ε_r = 2.2 in equation $\lambda_{SM} = \lambda_0 / \sqrt{\varepsilon_r}$, LQ1 becomes 1.80589mm. Similarly, the width of the first-quarter transform (WQ1) is half of WMTL. Hence, WQ1 is 0.41069mm. The width of the second-quarter transform (WQ2) is the same as the length of the third-quarter transform (LQ3), which again identical to the value of WMTL. So, their values become WQ2 = LQ3 = WMTL = 0.82137mm. The length of the second-quarter transform (LQ2) is the same as the width of the third-quarter transform (WQ3), i.e., LQ2 = WQ3 = 0.90295mm.
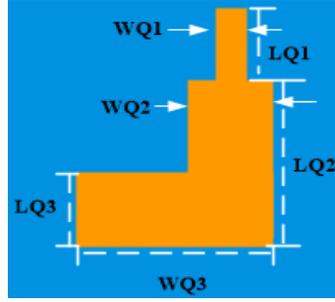
Figure 3.8. Quarter Impedance Transformer.

Length and Width of connected 2x2 MPA array: The length of connected 2x2 MPA array ($(PL)_{2x2}$) is calculated by using $(PL)_{2x2} = 2PL + IS + 2LMTL$. Thus, by adding the values of $PL = 3.40451mm$, $IS = 5.35mm$, and $LMTL = 1.80589mm$ together, the $(PL)_{2x2}$ becomes:

$$(PL)_{2x2} = 6.80902mm + 5.35mm + 3.61178mm = 15.77080mm$$

The width of connected 2x2 MPA array ($(PW)_{2x2}$) is given by $(PW)_{2x2} = 2PW + IS$. Hence, by adding the values of $PW = 4.23519mm$ and $IS = 5.35mm$, then the $(PW)_{2x2}$ calculated as:

$$(PW)_{2x2} = 8.47038mm + 5.35mm = 13.82038mm$$

Ground Plane Length and Width of 2x2 MPA array: The length and width of ground plane ($(GPL)_{2x2}$ and $(GPW)_{2x2}$) are calculated by using the $(PL)_{2x2} = 15.77080mm$, $(PW)_{2x2} = 13.82038mm$, and $ST = 0.34490mm$ as follows.

$$(GPL)_{2x2} = (PL)_{2x2} + 6(ST) = 15.77080mm + 2.0694mm = 17.84020mm$$
$$(GPW)_{2x2} = (PW)_{2x2} + 6(ST) = 13.82038mm + 2.0694mm = 15.88978mm$$

Length and Width of Last Microstrip Transmission Line of planar 2x2 MPA array: The length of the last microstrip feeder line of planar 2x2 MPA array ($(LLMTL)_{2x2}$) is half of the WMTL, which is 0.82137mm. Hence, $(LLMTL)_{2x2}$ is equal to 0.41069mm. Next, the width of the last microstrip transmission line of planar 2x2 rectangular MPA array ($(WLMTL)_{2x2}$) is obtained by using the equation given by; $0.5(GPW)_{2x2} - (WQ3 - WQ2) - 0.25WQ2 - 0.5(WMTLC)_{2x1}$. By substituting the values of $(GPW)_{2x2}$, WQ3, WQ2, and $(WMTLC)_{2x1}$, which are 15.88978mm, 0.90295mm, 0.82137mm, and 0.82137mm, respectively, $(WLMTL)_{2x2}$ becomes 7.24683mm.

Width and Length of the Feed Point: The width of the feed point (WFP) for the microstrip transmission line of 0.82137mm is calculated above, which is equal to 1.18635mm. Therefore, for microstrip transmission line width of 0.41069mm, it is half of 0.82137mm, which becomes

50

0.59318mm. Since the impedance is less dependent on the transmission line length, the length of the feed point (LFP) is 1.88152mm. In general, the above calculated physical dimensions of the planar 2x2 rectangular MPA array are arranged in Table 3.2 and the physical structure of this antenna array is indicated in Figure 3.7.

Table 3.2. Designed Parameters for Planar 2x2 Rectangular MPA Array.

| Designed Antenna Parameters	Symbol	Values (mm)
Substrate Thickness	ST	0.34490
Patch Width	PW	4.23519
Patch Length	PL	3.40451
Length of Inset Feed	IL	0.89268
Width of Inset Feed	IW	0.02475
Length of Microstrip Transmission Line	LMTL	1.80589
Width of Microstrip Transmission Line	WMTL	0.82137
Length of 1:2 Power Divider	LPD	0.41069
Width of 1:2 Power Divider	WPD	10.40656
Length of Power Divider Arm	LPDA	1.80589
Width of Power Divider Arm	WPDA	0.82137
Width of the First-Quarter transformer	WQ1	0.41069
Length of the First-Quarter transformer	LQ1	7.22358
Width of Second-Quarter transformer	WQ2	0.82137
Length of Second-Quarter transformer	LQ2	0.90295
Width of Third-Quarter transformer	WQ3	0.90295
Length of Third-Quarter transformer	LQ3	0.82137
Ground Plane Width of 2x2 MPA	$(GPW)_{2x2}$	15.88978
Ground Plane Length of 2x2 MPA	$(GPL)_{2x2}$	17.84020
Length of Last Microstrip Transmission Line of 2x2 MPA	$(LLMTL)_{2x2}$	0.41069
Width of Last Microstrip Transmission Line of 2x2 MPA	$(WLMTL)_{2x2}$	7.24683
Length of the Feed Point	LFP	1.88152
Width of the Feed Point	WFP	0.59318
Inter-element Space	IS	5.35
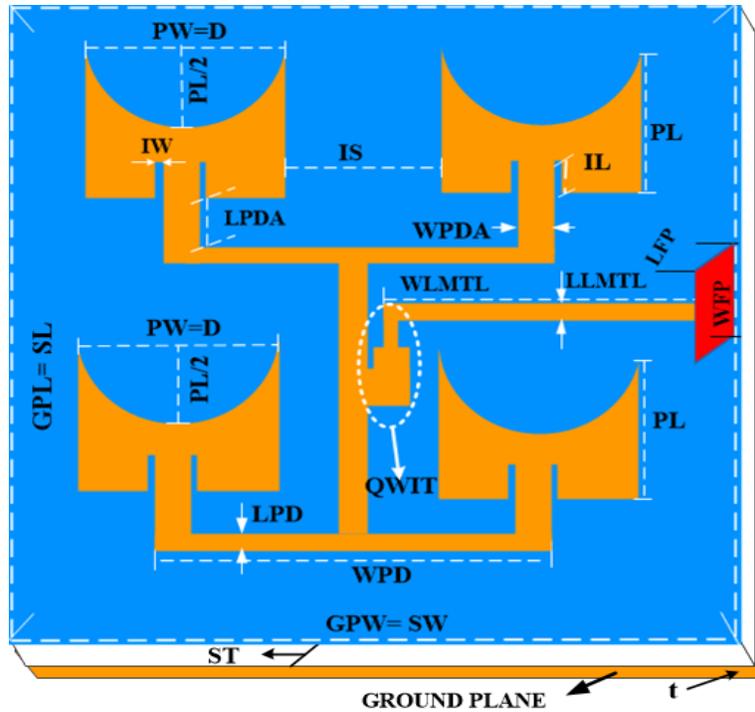
Figure 3.9. Planar 2x2 Rectangular MPA Array.

3.5. Design Calculations of Planar 4x4 Rectangular MPA Array

The planar 2x2 rectangular MPA array improved the antenna's performance in terms of the gain and beam-scanning ability in two directions. In order to attain the optimal performance, in this section, a 4x4 MPA array is proposed, which enhances the performance obtained in a single and 2x2 MPA array. To design a planar 4x4 rectangular MPA array, four 2x2 rectangular MPA arrays are used. The elements are grouped into two pairs of 2x2 planar configurations, and then each group of 2x2 planar configurations is placed over each quadrant of the X-Y coordinate axis. Therefore, the design parameters of single and planar 2x2 rectangular MPA are directly used, and the remaining design parameters are calculated as follows.

Length and Width of Microstrip Transmission Line Connecting two 2x2 MPA arrays: The gap between the quarter transformer and edge along the patch length (G (gap)) can be calculated using the mathematical equation given as; G (gap) = 0.5WPD – (WMTL + WQ3 + 0.5PW). By substituting WMTL = 0.82137mm, WQ3 = 0.90295mm, PW = 4.23519mm, and WPD = 10.40656mm, then the gap between the quarter transformer and left edge of the patch can be calculated as follow.

52

G (gap) = 0.5WPD – (WMTL + WQ3 + 0.5PW) = 5.20328mm – 3.84192mm = 1.36136mm

After the gap is calculated next, the width of the microstrip transmission line connecting two 2x2 MPA ((WMTLC) $_{2x2}$) is obtained by using the equation given below.

$$(WMTLC)_{2x2} = 2PW + 2G (gap) + 0.5WQ2 + 4WQ1 + IS$$

Hence, by substituting PW = 4.23519mm, WQ2 = 0.82137mm, WQ1 = 0.41069mm, and IS = 5.35mm in above equation, the (WMTLC) $_{2x2}$ can be calculated as below.

$$(WMTLC)_{2x2} = 8.47038mm + 2.72272mm + 7.403445mm = 18.59655mm$$

The length of the microstrip transmission line connecting two 2x2 MPA ((LMTLC) $_{2x2}$) is half of the WMTL, i.e., 0.82137mm. Therefore, the value of (LMTLC) $_{2x2}$ is 0.41069mm.

Length and Width of Center transmission Line Connecting two 2x4 MPA arrays: The length of center microstrip transmission line connecting two 2x4 MPA arrays ((LCMTLC) $_{2x4}$) is calculated by substituting the dimensions of IS = 5.35mm, PL = 3.40451mm, and LMTL = 1.80589mm in equation (LCMTLC) $_{2x4}$ = IS + 2PL + 2LMTL. Hence, (LCMTLC) $_{2x4}$ is 15.7708mm, and also, the width of the center microstrip transmission line connecting two 2x4 MPA arrays ((WCMTLC) $_{2x4}$) is half of the previously calculated value of WMTL. Henceforward, the (WCMTLC) $_{2x4}$ is equal to 0.41069mm.

Length and Width of connected 4x4 MPA array: The length of connected 4x4 MPA array ((PL) $_{4x4}$) is calculated using equation given by; (PL) $_{4x4}$ = 4PL + 3IS. So, by substituting PL = 3.40451mm and IS = 5.35mm, the (PL) $_{4x4}$ is equal to 29.66804mm. The width of connected 4x4 MPA array ((PW) $_{4x4}$) is calculated using equation (PW) $_{4x4}$ = 4PW + 3IS. Hereafter, by substituting PW = 4.23519mm and IS = 5.35mm, the (PW) $_{4x4}$ is 32.99076mm.

Ground Plane Length and Width of 4x4 MPA array: The ground plane length and ground plane width ((GPL) $_{4x4}$ and (GPW) $_{4x4}$) are calculated by using the value of (PL) $_{4x4}$ and (PW) $_{4x4}$ calculated in the above section and substrate thickness, which is 0.34490mm. The (GPL) $_{4x4}$ and (GPW) $_{4x4}$ are calculated as shown below.

$$(GPL)_{4x4} = (PL)_{4x4} + 6(ST) = 29.66804mm + 2.0694mm = 31.73744mm$$
$$(GPW)_{4x4} = (PW)_{4x4} + 6(ST) = 32.99076mm + 2.0694mm = 35.06016mm$$

Length and Width of Last Microstrip Transmission Line of 4x4 MPA array: The length of the last microstrip transmission line of 4x4 MPA array ((LLMTL) $_{4x4}$) is half of the value of the

WMTL. But, the WMTL is 0.82137mm. Hence, the $(LLMTL)_{4x4}$ is equal to 0.41069mm. Similarly, the width of the last microstrip transmission line of 4x4 MPA array $((WLMTL)_{4x4})$ is calculated using the equation given by; $0.5(GPW)_{4x4} - 0.5(WCMTLC)_{2x4}$. By substituting $(WCMTLC)_{2x4} = 0.41069mm$ and $(GPW)_{4x4} = 35.06016mm$, then $(WLMTL)_{4x4}$ is obtained as follows.

$$(WLMTL)_{4x4} = 0.5(GPW)_{4x4} - 0.5(WCMTLC)_{2x4}$$
$$(WLMTL)_{4x4} = 17.53008mm - 0.205345mm = 17.32474mm$$

The overall physical dimensions of the planar 4x4 rectangular MPA array calculated in the above section are tabulated in Table 3.3 and the corresponding physical structure is shown in Figure 3.8.

Table 3.3. Designed Parameters for Planar 4x4 Rectangular MPA Array.

| Designed Antenna Parameters	Symbol	Values (mm)
Substrate Thickness	ST	0.34490
Patch Width	PW	4.23519
Patch Length	PL	3.40451
Length of Inset Feed	IL	0.89268
Width of Inset Feed	IW	0.02475
Length of Microstrip Transmission Line	LMTL	1.80589
Width of Microstrip Transmission Line	WMTL	0.82137
Length of 1:2 Power Divider	LPD	0.41069
Width of 1:2 Power Divider	WPD	10.40656
Length of Power Divider Arm	LPDA	1.80589
Width of Power Divider Arm	WPDA	0.82137
Width of the First-Quarter transformer	WQ1	0.41069
Length of the First-Quarter transformer	LQ1	7.22358
Width of Second-Quarter transformer	WQ2	0.82137
Length of Second-Quarter transformer	LQ2	0.90295
Width of Third-Quarter transformer	WQ3	0.90295
Length of Third-Quarter transformer	LQ3	0.82137
Ground Plane Width of 4x4 MPA	$(GPW)_{4x4}$	35.06016
Ground Plane Length of 4x4 MPA	$(GPL)_{4x4}$	31.73744
Length of Last Microstrip Transmission line of 4x4 MPA	$(LLMTL)_{4x4}$	0.41069
Width of Last Microstrip Transmission line of 4x4 MPA	$(WLMTL)_{4x4}$	17.32474
Length of the Feed Point	LFP	1.88152
Width of the Feed Point	WFP	0.59318
Inter-element Space	IS	5.35
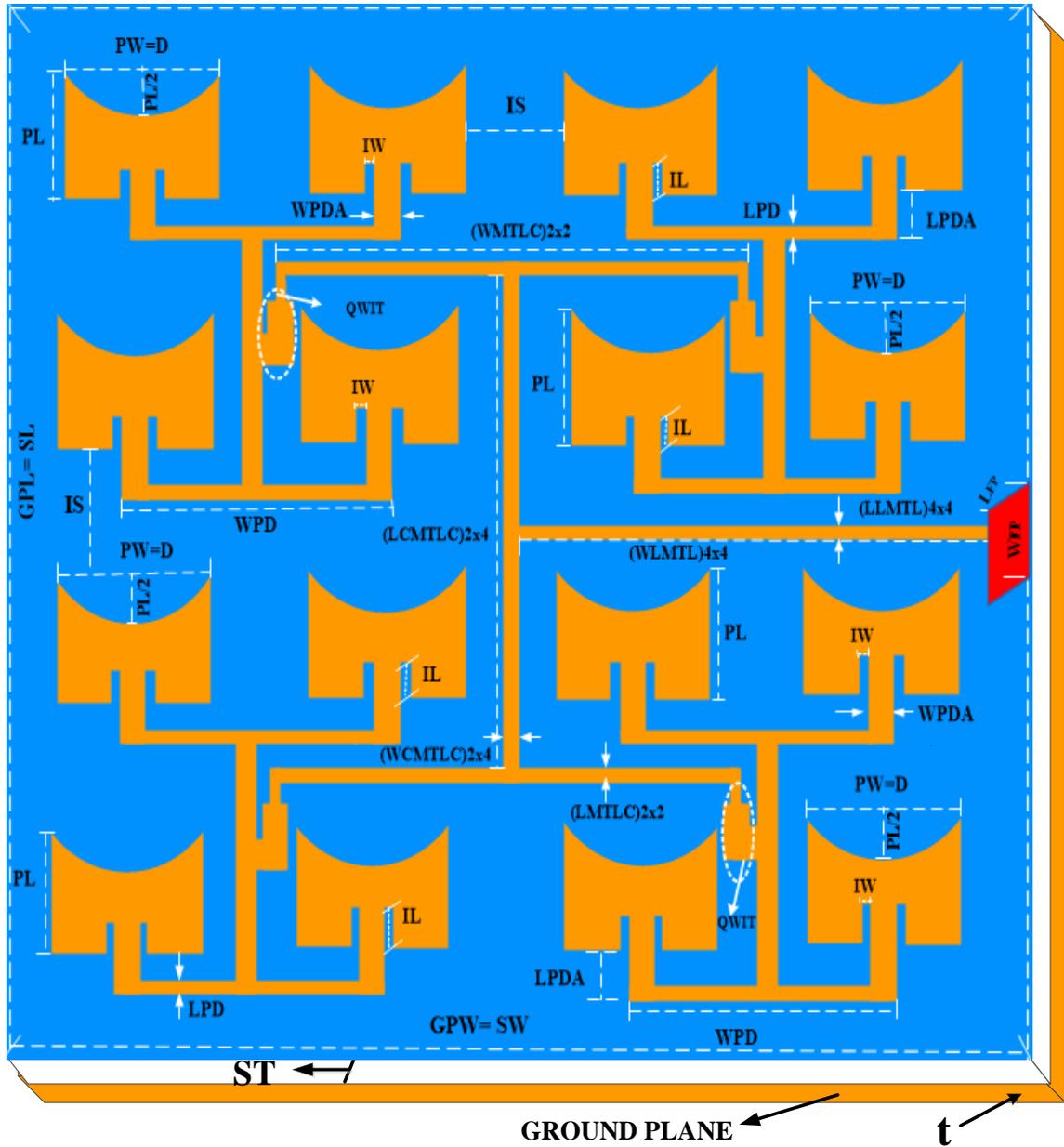
Figure 3.10. Planar 4x4 Rectangular MPA Array.

3.6. Design Calculations of Planar 8x8 Rectangular MPA Array

In this section, the design of the rectangular 8x8 MPA array is proposed to enhance the performance achieved in the 2x2 and 4x4 rectangular MPA array. To design an 8x8 MPA array, 64 antenna elements are required. So, the designed parameters for 2x2 and 4x4 MPA array in the above sections are used as they are, and the remaining parameters are calculated as follows.

Length and Width of Microstrip Transmission Line Connecting two 4x4 MPA arrays: The width of the microstrip transmission line connecting two 4x4 MPA arrays ($(WMTLC)_{4x4}$) is obtained by using the equation given below.

$$(WMTLC)_{4x4} = 2((0.5IS - 0.25WMTL) + 2PW + IS)$$

So, by replacing IS = 5.35mm, WMTL = 0.82137mm, and PW = 4.23519mm in above equation, the $(WMTLC)_{4x4}$ is equal to 32.58008mm. The length of the microstrip transmission line connecting two 4x4 MPA arrays ($(LMTLC)_{4x4}$) is half of WMTL, i.e., 0.82137mm. Therefore, the $(LMTLC)_{4x4}$ is 0.41069mm.

Length and Width of Center Microstrip Transmission Line Connecting two 4x8 MPA arrays: By using the following equation, the length of the center microstrip transmission line connecting two 4x8 MPA arrays ($(LCMTLC)_{4x8}$) is determined.

$$(LCMTLC)_{4x8} = 2(0.5IS - 0.25WMTL) + 4IS + 4PL + 4LMTL$$

So, by replacing the values of IS = 5.35mm, WMTL = 0.82137mm, PL = 3.40451mm, and LMTL = 1.80589mm in the above equation, the $(LCMTLC)_{4x8}$ becomes 47.18092mm. Also, the width of the center microstrip transmission line connecting two 4x8 MPA arrays ($(WCMTLC)_{4x8}$) is half of the previously calculated value of WMTL. Hence, the dimension of $(WCMTLC)_{4x8}$ is equal to 0.41069mm.

Length and Width of connected 8x8 MPA array: The length of connected 8x8 MPA array ($(PL)_{8x8}$) is calculated using equation given by; $(PL)_{8x8} = 8PL + 7IS$. Then, by replacing PL = 3.40451mm and IS = 5.35mm, the $(PL)_{8x8}$ becomes 64.68608mm. The width of connected 4x4 MPA array ($(PW)_{8x8}$) is calculated by using equation given by; $(PW)_{8x8} = 8PW + 7IS$. Hereafter, by substituting PW = 4.23519mm and IS = 5.35mm, the $(PW)_{8x8}$ is 71.33152mm.

Ground Plane Length and Width of 8x8 MPA array: The dimensions of the ground plane length and width ($(GPL)_{8x8}$ and $(GPW)_{8x8}$) are calculated using the above-calculated dimensions of $(PL)_{8x8}$ and $(PW)_{8x8}$ and the thickness of the substrate, i.e., 0.34490mm. The $(GPL)_{8x8}$ and $(GPW)_{8x8}$ dimensions are calculated as follows.

$$(GPL)_{8x8} = (PL)_{8x8} + 6(ST) = 64.68608mm + 2.0694mm = 66.75547mm$$

$$(GPW)_{8x8} = (PW)_{8x8} + 6(ST) = 71.33152mm + 2.0694mm = 73.40092mm$$

Length and Width of Last Microstrip Transmission Line of 8x8 MPA array: The length of the last microstrip transmission line of 8x8 MPA array ($(LLMTL)_{8x8}$) is half of the WMTL, where

WMTL is 0.82137mm. Hence, the dimension of (LLMTL) $_{8x8}$ is the same as 0.41069mm. Similarly, the width of the last microstrip transmission line of 8x8 MPA array ((WLMTL) $_{8x8}$) is calculated by substituting (WCMTLC) $_{8x8}$ = 0.41069mm and (GPW) $_{8x8}$ = 73.40092mm in the following equation.

$$(WLMTL)_{8x8} = 0.5(GPW)_{8x8} - 0.5(WCMTLC)_{8x8}$$

$$(WLMTL)_{8x8} = 36.70046mm - 0.205345mm = 36.49512mm$$

The calculated physical dimensions of the planar 8x8 rectangular MPA array are tabulated in Table 3.4 and the corresponding physical structure is indicated in Figure 3.9.

Table 3.4. Designed Parameters for Planar 8x8 Rectangular MPA Array.

| Design Parameters	Symbol	Values (mm)
Substrate Thickness	ST	0.34490
Patch Width	PW	4.23519
Patch Length	PL	3.40451
Length of Inset Feed	IL	0.89268
Width of Inset Feed	IW	0.02475
Length of Microstrip Transmission Line	LMTL	1.80589
Width of Microstrip Transmission Line	WMTL	0.82137
Length of 1:2 Power Divider	LPD	0.41069
Width of 1:2 Power Divider	WPD	10.40656
Length of Power Divider Arm	LPDA	1.80589
Width of Power Divider Arm	WPDA	0.82137
Width of the First-Quarter transformer	WQ1	0.41069
Length of the First-Quarter transformer	LQ1	7.22358
Width of Second-Quarter transformer	WQ2	0.82137
Length of Second-Quarter transformer	LQ2	0.90295
Width of Third-Quarter transformer	WQ3	0.90295
Length of Third-Quarter transformer	LQ3	0.82137
Ground Plane Width of 8x8 MPA	(GPW) $_{8x8}$	73.40092
Ground Plane Length of 8x8 MPA	(GPL) $_{8x8}$	66.75547
Length of Last Microstrip Transmission line of 8x8 MPA	(LLMTL) $_{8x8}$	0.410685
Width of Last Microstrip Transmission line of 8x8 MPA	(WLMTL) $_{8x8}$	36.49512
Length of the Feed Point	LFP	1.88152
Width of the Feed Point	WFP	0.59347
Inter-element Space	IS	5.35
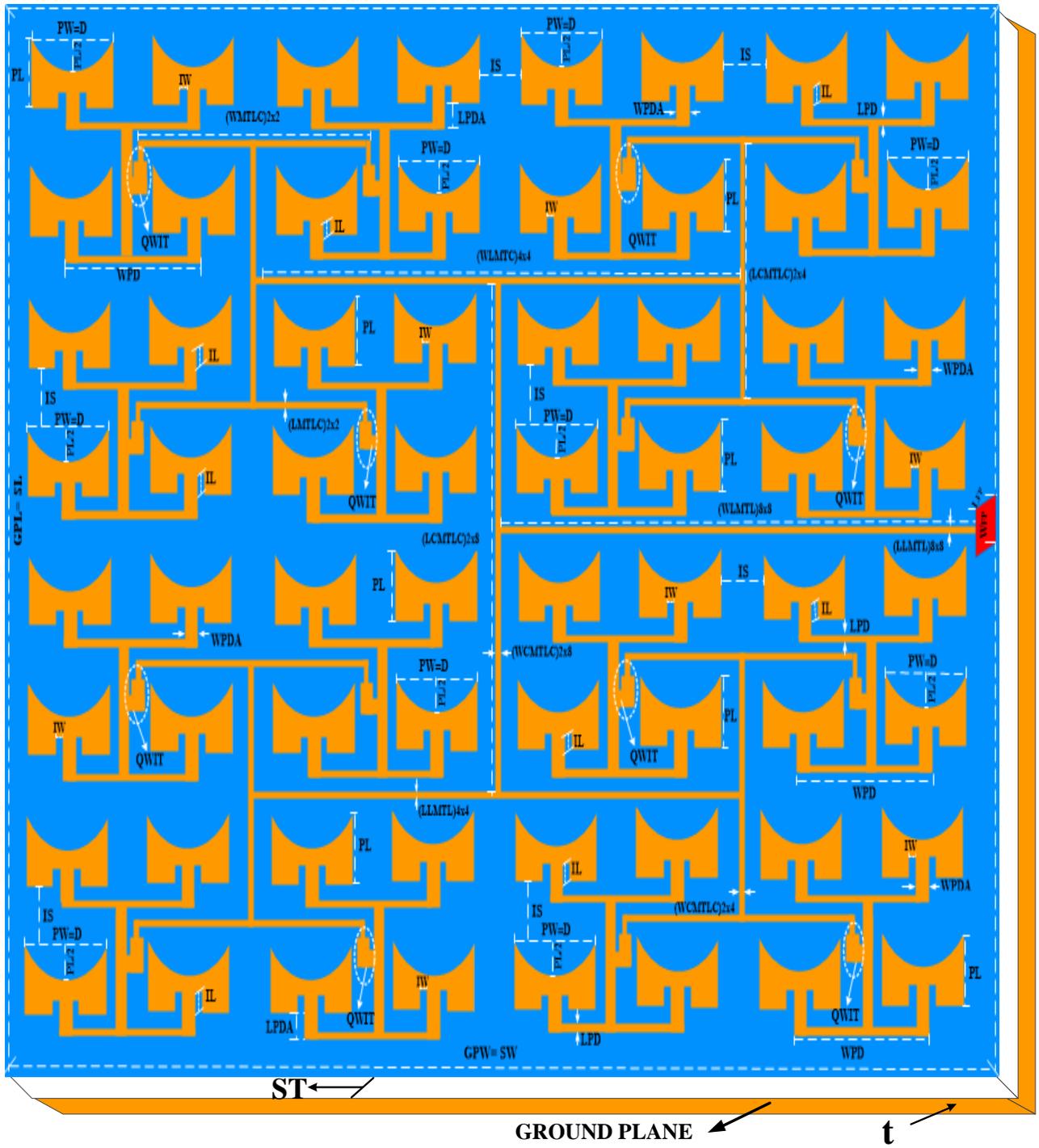
Figure 3.11. Planar 8x8 Rectangular MPA Array.

Chapter Four

Simulation Results and Discussions

This chapter discusses simulation results and discussions of various single element MPA structures and planar rectangular MPA arrays for 5G communication systems. To validate and analyze the performance of the designed antenna, CST-MW Studio is used. It offers the choice of multiple powerful solver modules, i.e., the frequency-domain and transient-solver, which are general-purpose 3D Electromagnetic of CST simulator. In this study, the frequency-domain analysis has been selected to analyze the performance of the designed rectangular MPA array in terms of VSWR, return loss, bandwidth, radiation efficiency, gain, and directivity of the radiation pattern. Generally, this chapter is arranged under two sections. In the first, the simulation results of different single rectangular MPA structures have been discussed. In the second section, the simulation results and discussions of planar 2x2, 4x4, and 8x8 rectangular MPA arrays are presented.

4.1. Performance Analysis of Various Single Element MPA

In this section, simulation-based performance analysis of MPA with a different configuration for 5G communication systems is discussed. The numerically calculated dimensions for a single element rectangular MPA have been explicitly presented in chapter three and tabulated in Table 3.1. The tuned physical dimensions of the structures, which have been used in the simulation process, are listed in Appendix One. Therefore, all of the graphs displayed in this section are obtained using the physical dimensions given in the appendix.

The design of the proposed antenna started with typical rectangular MPA with an inset-feed structure, as shown in Figure 4.1a. A semi-elliptical slot is introduced in the ground plane in Figure 4.1b. Likewise, a semi-elliptical structure is introduced in the radiating patch of the antenna, as shown in Figure 4.1c. In a similar pattern, semi-elliptical slots of different sizes have been introduced in the patch, as shown in Figure 4.1 (d-f).

The impact of introducing different structures in MPA is studied, and comparative analysis is performed. Figure 4.1 (a-c) shows the effect of introducing defect structures on the performance of the MPA. The simulated reflection coefficients of the three structures are shown in Figure 4.2. Among the three structures, the structure without defect (Figure 4.1a) has achieved the lowest reflection coefficient, bandwidth, directivity, gain, and radiation efficiency.

Introducing a semi-elliptical slot on the ground structure (Figure 4.1b) improves the bandwidth, gain and directivity of the antenna. The semi-elliptical slot on the radiating patch of the antenna (Figure 4.1c) improves the bandwidth and radiation efficiency, as indicated in Table 4.1. Further study was conducted to analyze the effect of the size of the slot on the performance of the MPA. The size of the semi-elliptical slot is varied as shown in Figure 4.1 (d-f) and its effect is analyzed as depicted in Figure 4.3. The performance of the optimized antenna structure (Figure 4.1e) achieves the best performance among all the other structure as depicted in Figure 4.3. Making the slot size above or below the optimal dimension of the antenna, deteriorates the performance of the antenna.
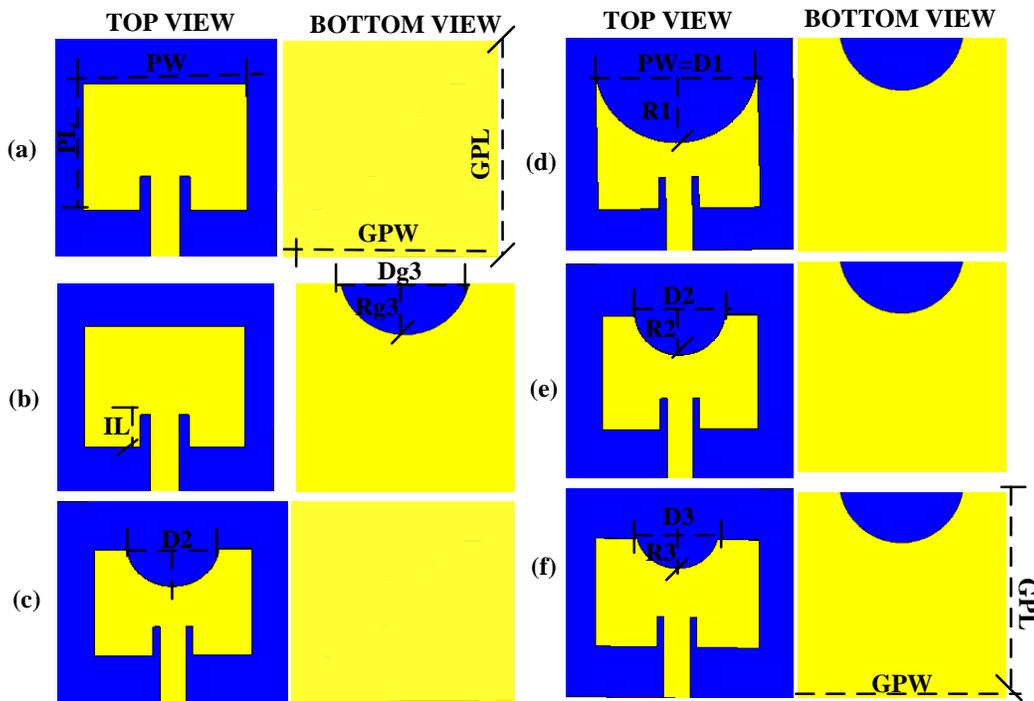
Figure 4.1. Physical Structure of Examined MPA: (a) Typical MPA, (b) Typical MPA With DGS, (c) DMPA With Typical Ground Plane, and (d, e, f) Varied Patch Defect With DGS.

Where the dimension of D1=PW, R1=0.5PL, D2=2*PW/3, R2=PL/3, D3=PW/2, R3=PL/4, and Rg3=GPL/3, Dg3=2*GPW/3 and DMPA denotes defected microstrip patch antenna.
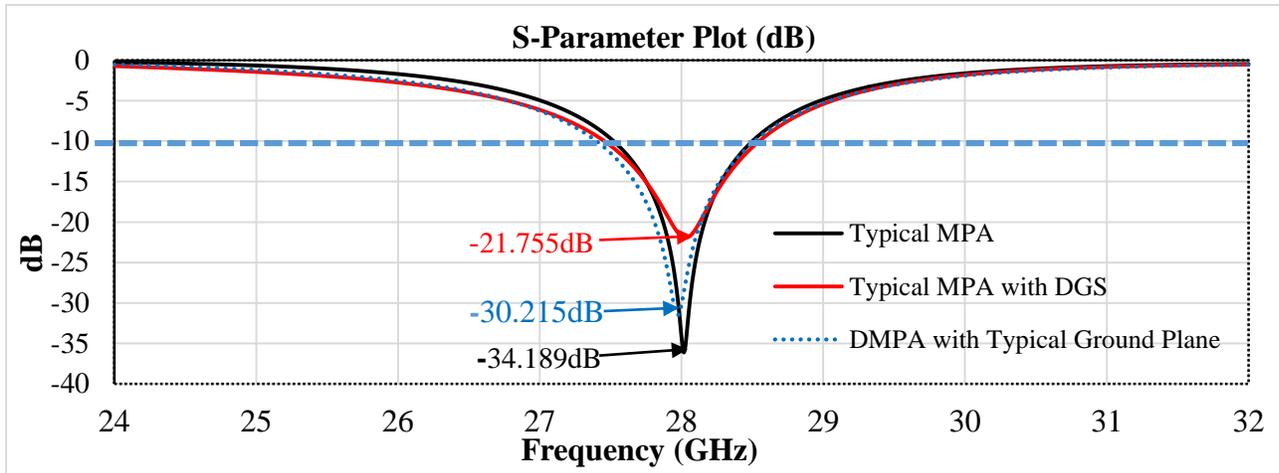
Figure 4.2. The Return Loss of the Antenna Structures Shown in Figure 4.1 (a-c).
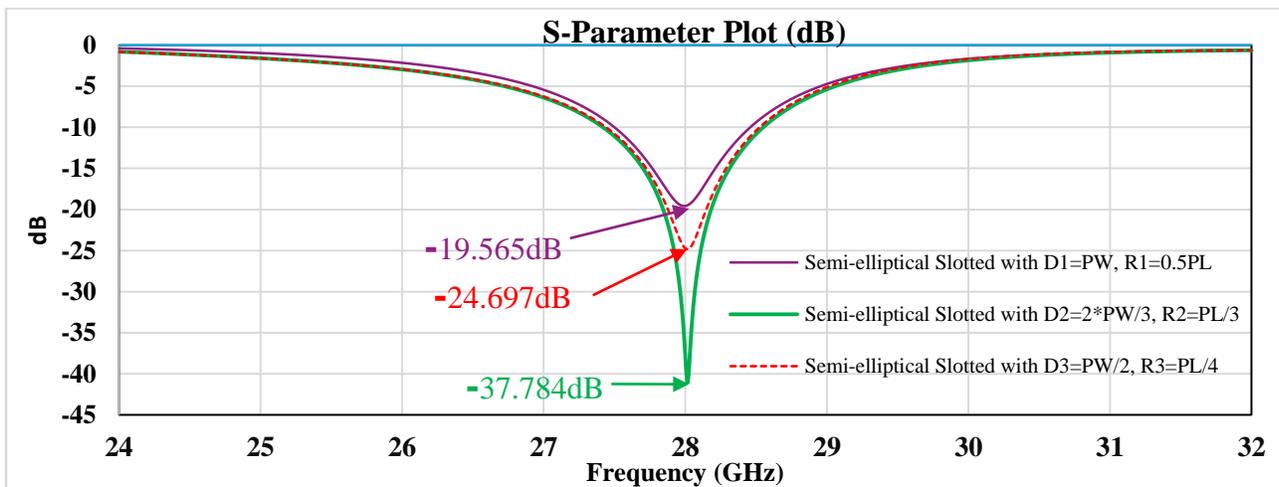
Figure 4.3. The Return Loss of the Antenna Structures Shown in Figure 4.1 (d-f).

Table 4.1. Designed Comparison of the Performance of Different MPA Structures.

Antenna Structures (Figure 4.1)	Performance Metrics					
	S_{11} (dB)	BW (GHz)	G (dBi)	D (dBi)	VSWR	η_{tot} (%)
(a)	-34.189	0.978	6.667	6.689	1.039	98.22
(b)	-21.755	1.092	7.038	7.121	1.178	98.37
(c)	-30.215	1.117	6.931	6.942	1.064	99.66
(d)	-19.565	0.959	7.112	7.174	1.235	97.49
(e)	-37.784	1.132	7.128	7.183	1.026	98.74
(f)	-24.697	1.085	7.094	7.132	1.124	98.79

Where S_{11} denotes return loss, BW denotes bandwidth, G is gain, D represents directivity, VSWR denotes voltage standing wave ratio, and η_{tot} denotes total efficiency.

61

The simulated results reveal that the analyzed typical and semi-elliptical slotted MPA's return loss is less than -10dB between 27.522GHz and 28.5GHz, as shown in Figure 4.4a and between 27.419GHz and 28.551GHz as shown in Figure 4.4b, respectively. At the resonant frequency (28GHz), the return losses are -34.189dB and -37.784dB, respectively. Therefore, as it can be seen from these results, the optimized semi-elliptical slotted MPA achieved minimum return loss compared to the typical and other MPA structures.

In addition, from Table 4.2, it is evident that its return loss is minimum as compared to simulation results achieved in [4], [6], [12], [19], [21], [23], [25], [27], [33], [48], [49]. However, it is large as compared to the results of antenna design reported in [10], [24], [26], [51], [52]. Furthermore, the -10dB bandwidth of the proposed antenna is 1.132GHz (4.043%) as shown in Table 4.1. The obtained bandwidth of modified antenna is wide as compared to the previous similar works reported in [10], [12], [19-21], [27], [33], [49], [51], [52] as listed in Table 4.2. Conversely, achieved bandwidth is narrow compared to designs demonstrated in [6], [23-26].
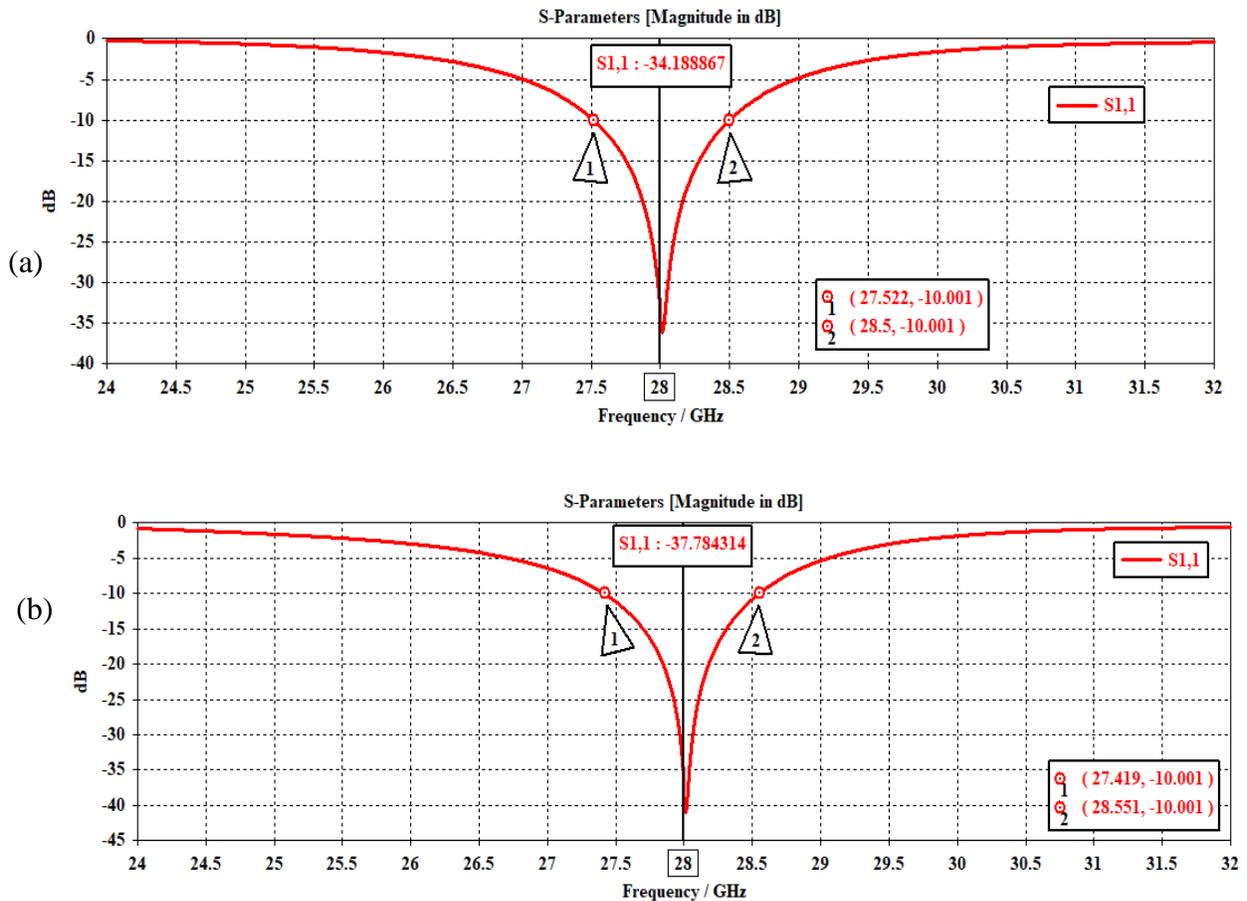
Figure 4.4. Return Loss Plot of (a) Typical and (b) Semi-elliptical Slotted Single MPA.

62

Generally, the minimum return loss and wide bandwidth have been attained since poor impedance matching at the feeder point, and patch edge has been minimized using the inset-feed impedance matching technique and tuning the design parameters. Besides, by creating the defect on both the patch antenna and ground plane along with the fringing patch width, which is used to change the current distribution of both structures, the high input impedance at the resonant frequency is minimized. Accordingly, considerable input power is transferred to the transmission line, and small input power is returned as a return loss. Thereby, the antenna's radiation efficiency is increased, which leads to enhanced bandwidth.

Furthermore the VSWR plot of the proposed typical and modified single rectangular MPA is shown in Figure 4.5. As observed from the plot, at the resonant frequency, the VSWR of the proposed normal and modified single rectangular MPA are 1.039 and 1.026, respectively. In a rigorous way of description, as the feeder-line is moved to the patch's center, the impedance mismatch between the patch's transmission line and the edge will be reduce reduced [18]. In this study, the patch and ground plane's introduced defect highly influences input impedance at the resonant frequency.
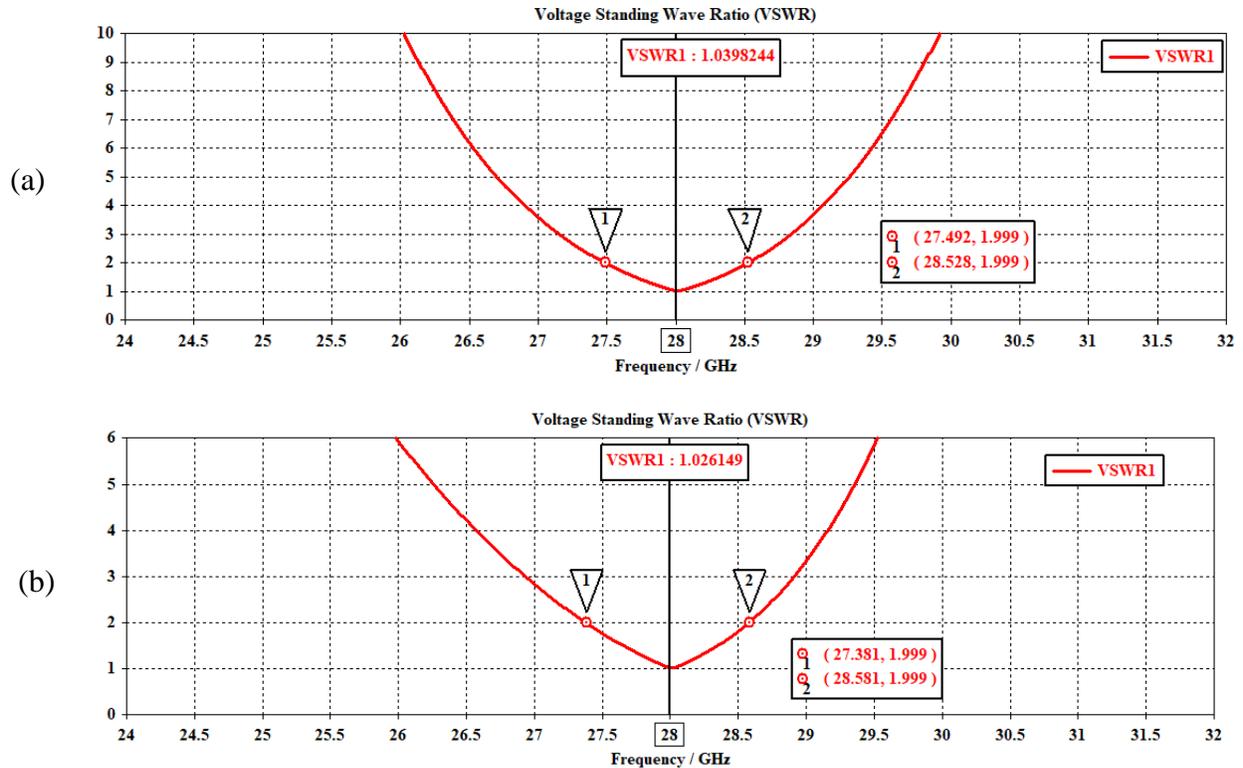

Figure 4.5. VSWR Plot of (a) Typical and (b) Semi-elliptical Slotted Single MPA.

Also, the patch width, the inset length, and the inset gap have been carefully tuned, and then the impedance mismatch between the feeder line of the microstrip and the patch edge becomes a matched point, i.e., the input power is passed to the patch with lower standing waves of voltage. Consequently, maximum power is transferred to the radiating patch. Compared to the design reported in [10], [19], [21], [23], [27], [33], [48], [49], the optimized MPA has achieved a minimum magnitude of VSWR.

Figure 4.6 shows the 3D radiation pattern of the proposed optimized MPA. As displayed in Figure 4.6, the MPA gain is 7.128dBi, and the achieved directivity of the antenna is 7.183dBi. As shown in Table 4.2, the gain of the proposed antenna outperforms the reported designs of [4], [6], [10], [19], [23], [24], [26], [48], [49]. But, it is low as compared with simulation results given in [20], [21], [25], [27], [33], [51], [52]. Whereas, the total efficiency of the proposed antenna structure is -0.05513dB (98.74%), which is higher than antennas cited in [10], [12], [23], [25-27], [33], [49], [51], [52]. Generally, in this study, the proposed single element rectangular MPA has attained better and improved results in terms of directivity, radiation efficiency, and gain.
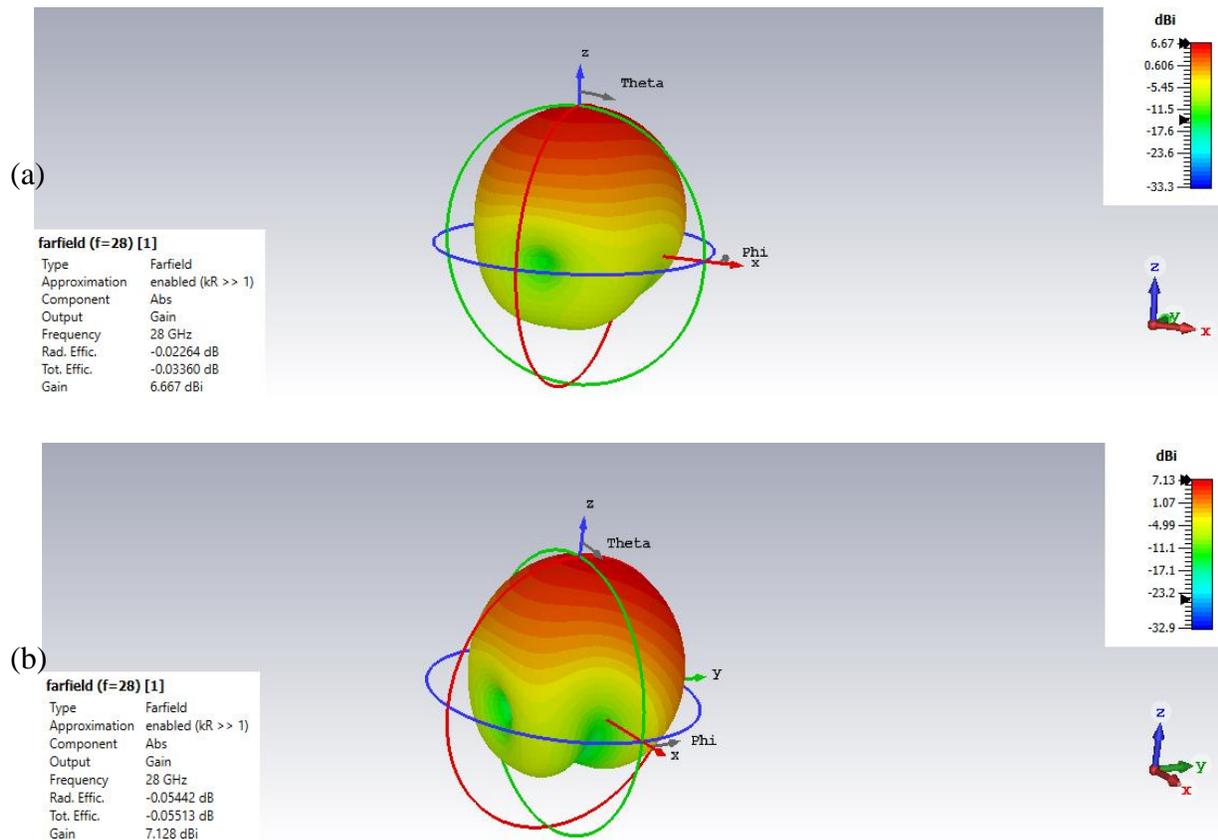

Figure 4.6. Radiation Pattern of Proposed (a) Typical and (b) Semi-elliptical Slotted Single MPA.

For the proposed semi-elliptical slotted MPA, the co-polarization farfield component which has the same polarization as the direction of electric field is given in Figure 4.7a. Also, its cross-polarization farfield component which is orthogonal to co-polarized component and main lobe direction is shown in Figure 4.7b. As it can be seen from the farfield plot, the cross-polarized component is minimal as compared to that of the desired polarization.


(a)   (b)
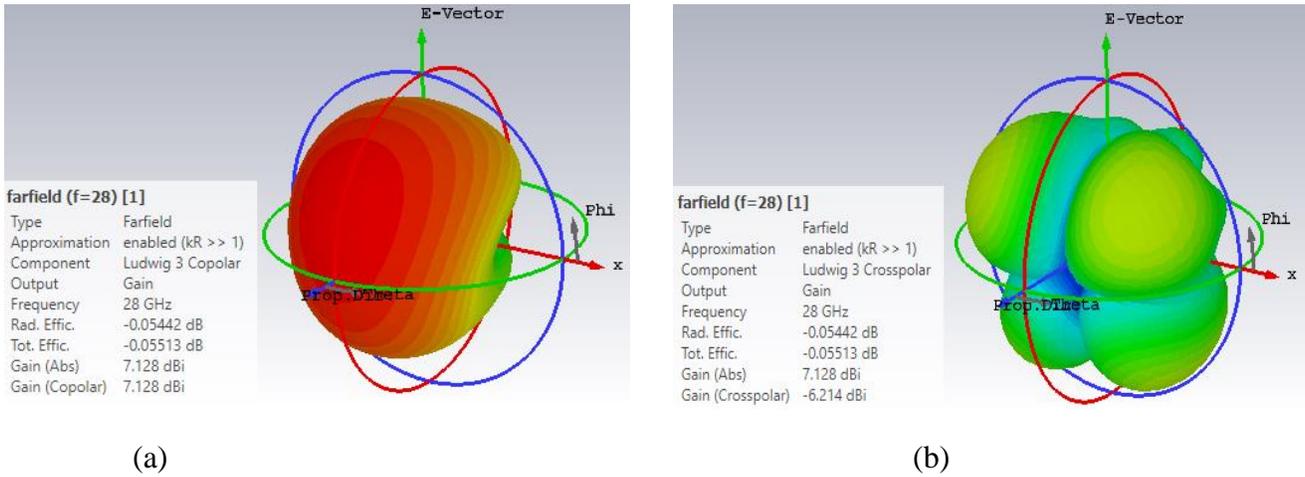
Figure 4.7. Co-polarization (a) and (b) Cross-polarization of Semi-elliptical Slotted Single MPA.

As revealed in Figure 4.8, the sidelobe level of the designed typical and modified single rectangular MPA are -13.7dB and -14.2dB, respectively. The achieved magnitude of the sidelobe level for each antenna is significantly minimized. Hence, the proposed antenna radiates highly towards the desired direction and less in the other directions.

(a)

Frequency = 28 GHz
Main lobe magnitude =   6.67 dBi
Main lobe direction =   17.0 deg.
Angular width (3 dB) = 106.5 deg.
Side lobe level = -13.7 dB

65
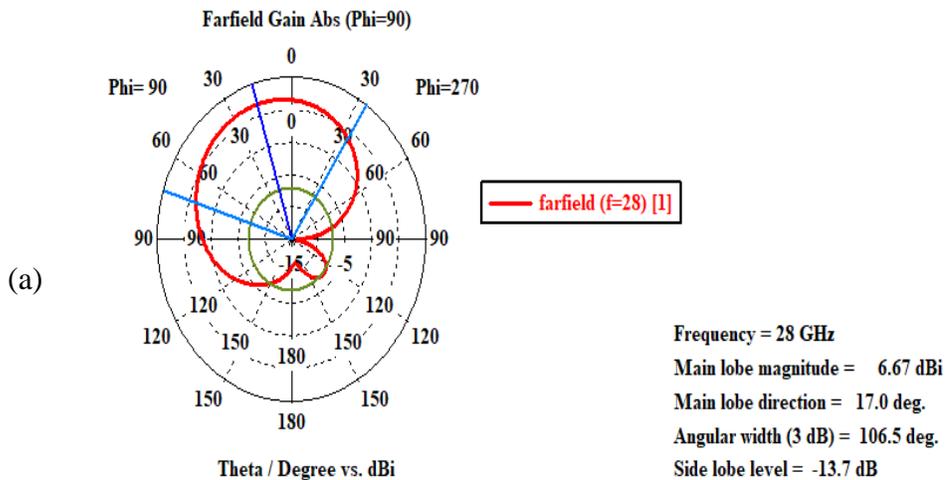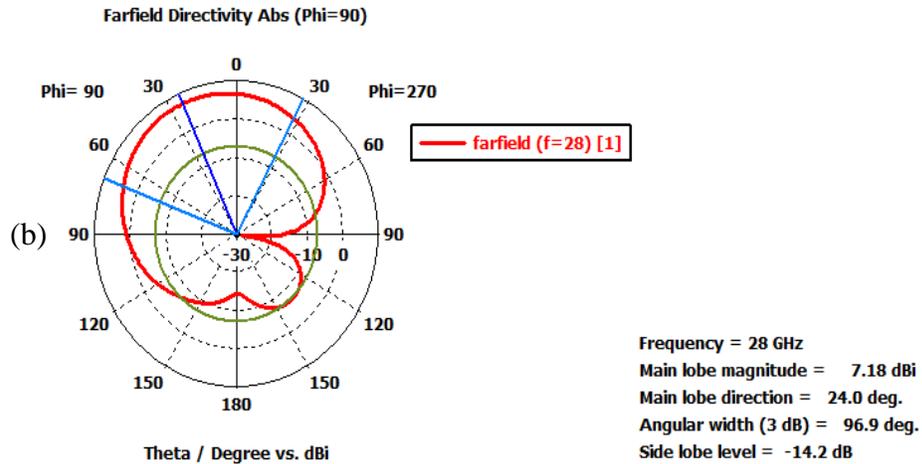
Figure 4.8. 2D Radiation Pattern of the (a) Typical and (b) Semi-elliptical Slotted Single MPA.

As shown in Figure 4.9, simultaneously introducing defect structure on patch and ground plane significantly alters the current distributions of both structures and then increases the radiation efficiency of the antenna. Besides, good impedance matching has been made in the middle of the edge of the patch and the microstrip transmission line. The dimensions of key design parameters have been tuned, which minimize the magnitude of the return loss, VSWR, and raise the radiation efficiency and bandwidth. In general, as it can be noticed from Table 4.2, the proposed modified single element MPA gives a highly competitive performance as compared to other single element MPA designs reported in the latest scientific studies.
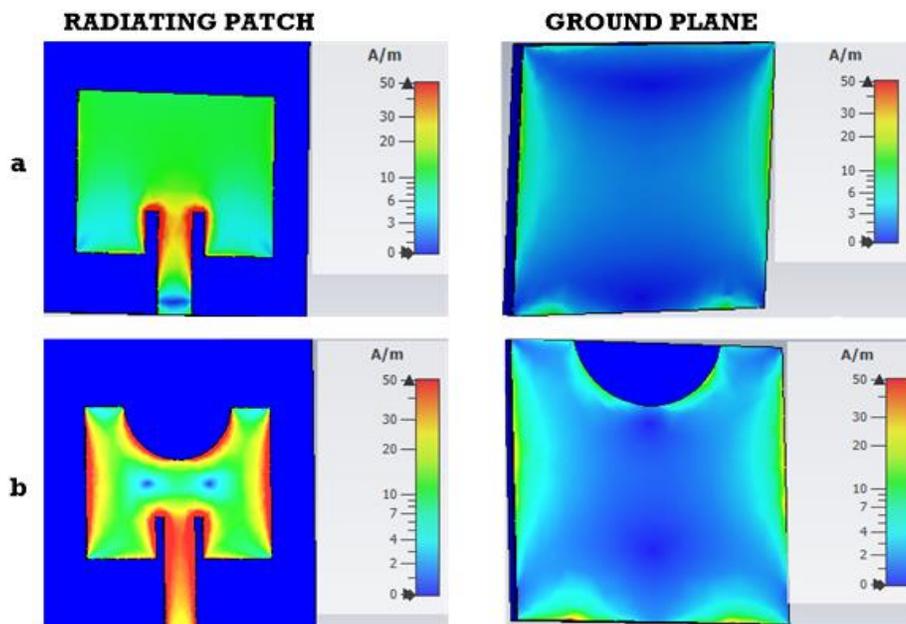

Figure 4.9. Current Distributions of (a) Typical and (b) Semi-elliptical Slotted Single MPA.

66

Table 4.2. Comparison of Reported Works and the Proposed Semi-elliptical Slotted Single MPA.

Ref.	S_{11} (dB)	BW (GHz)	G (dBi)	VSWR	η_{tot} (%)
[4]	-32	-	6.7	-	-
[6]	-22.51	5.57	3.6	-	-
[10]	-13.48	0.847	6.63	1.5376	70.18
[12]	-12	0.5	-	1.01	85.33
[19]	-14.15	0.8	6.06106	1.48784	-
[20]	-59.369	0.43	8.5	-	-
[21]	-34.05	0.582	8.00	1.75	-
[23]	-20.03	2.1	5.2	1.22	82.83
[24]	-48.25	4.07	5.61	-	-
[25]	-28.47	1.9	7.63	1.078	78.16
[26]	-39.37	2.46	6.37	1.022	86.73
[27]	-17.834	0.44	12.013	1.2994	92.655
[33]	-20.24	0.572	7.18	1.2156	94.95
[48]	-22.2	-	6.85	1.34	-
[49]	-27.7	0.463	6.72	1.22	75.87
[51]	-54.492	1.062	7.55	1.011	98
[52]	-38.86	1.046	7.587	1.023	98.214
This work (Modified)	**-37.784**	**1.132**	**7.128**	**1.026**	**98.74**

Where S_{11} denotes return loss, BW denotes bandwidth, G is gain, VSWR denotes voltage standing wave ratio, and η_{tot} denotes total efficiency.

4.2. Simulation Result and Discussions of Proposed Planar MPA Arrays

4.2.1. Planar 2x2 Rectangular MPA Array

The numerically calculated dimensions for a planar 2x2 rectangular MPA array have been explicitly presented in chapter three and tabulated in Table 3.2. The tuned physical dimensions of the structures, which have been used in the simulation process, are listed in Appendix two. The front and back view of the proposed 2x2 planar rectangular MPA array is exposed in Figure 4.10.

| FRONT VIEW | BACK VIEW |
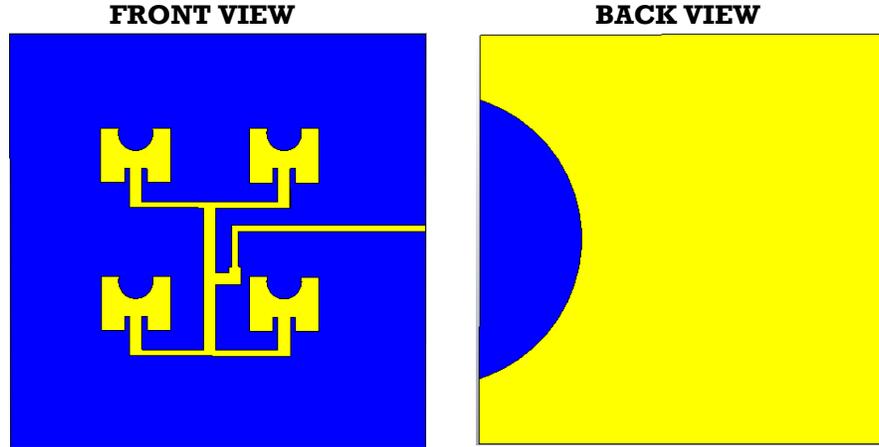
Figure 4.10. Front and Back View of the Proposed Planar 2x2 Rectangular MPA Array.

The plot of a return loss versus frequency of the proposed planar 2x2 rectangular MPA array is given in Figure 4.11. From the plot, it is easily inferred that between 27.386GHz and 28.716GHz, the return loss is less than -10dB, and at 28GHz, it is -43.321dB, which is significantly minimized as compared to the work demonstrated in [16], [19], [33]. As far as the magnitude of S_{11} is less than -10dB, the bandwidth of the antenna is easily obtained from the S_{11} plot. Thus, the -10dB bandwidth of the antenna is about 1.33GHz, which is profoundly wide as compared to the designs reported in [16], [19], [33].
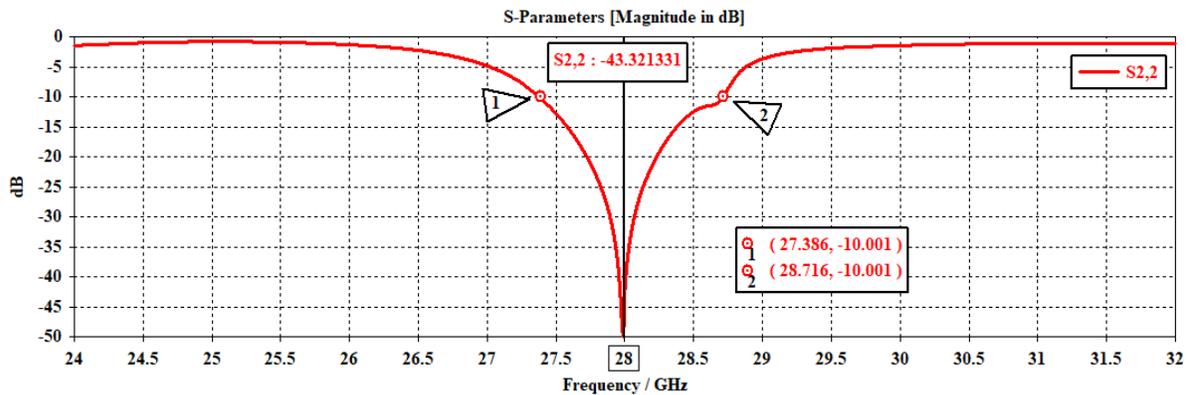

Figure 4.11. Return loss Plot of the Designed Planar 2x2 MPA Array.

On the other side, from Figure 4.12, between 27.386GHz and 28.716GHz, the magnitude of VSWR is less than two, and at 28GHz, it is 1.014. Moreover, to get maximum power transfer, the magnitude of the return loss and VSWR have to be minimum as much as possible. As compared to the work demonstrated in [16], [33], the proposed planar 2x2 rectangular MPA array shows a minimum magnitude of return loss and VSWR.

68

This minimum result is obtained because, in this work, good impedance matching has been made in the feeding networks, i.e., between the microstrip transmission line and feed point. Also, the arm of the 1:2 power divider and the edge of the patch have been seriously evaluated to bring them to a matched level by using inset-feed impedance matching technique, quarter-wave impedance transformer, and using optimized dimensions of physical antenna structures. Consequently, the minimum magnitude of return loss and VSWR has been achieved at the resonant frequency.
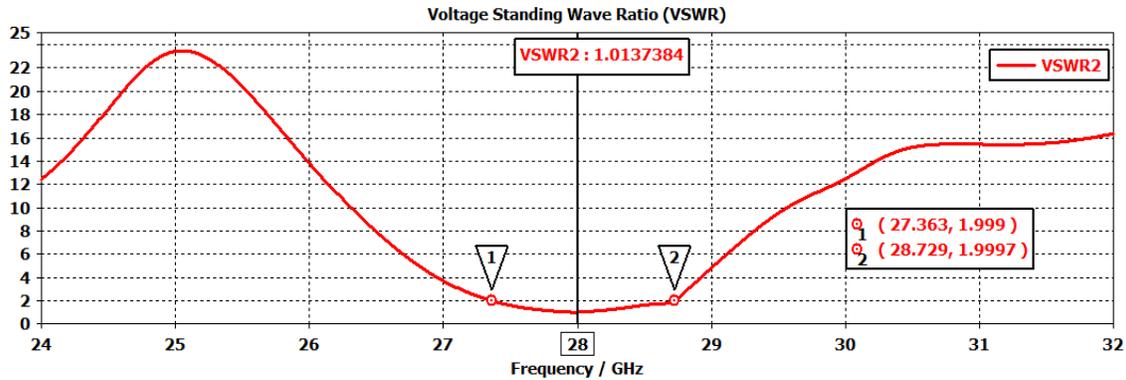

Figure 4.12. VSWR Plot of the Proposed Planar 2x2 MPA Array.

The 3D radiation pattern of the proposed planar 2x2 rectangular MPA array is indicated in Figure 4.13. Hence, from this graph, the achieved total efficiency of the antenna is -0.1310dB (97.03%). The proposed 2x2 MPA array directivity and gain are 12.81dBi and 13.24dBi, respectively. Similarly, from Figure 4.15, it can be observed that the mutual coupling between the elements in the array is -10.6dB, and a 3dB radiation pattern has occurred at 37.3 degrees.
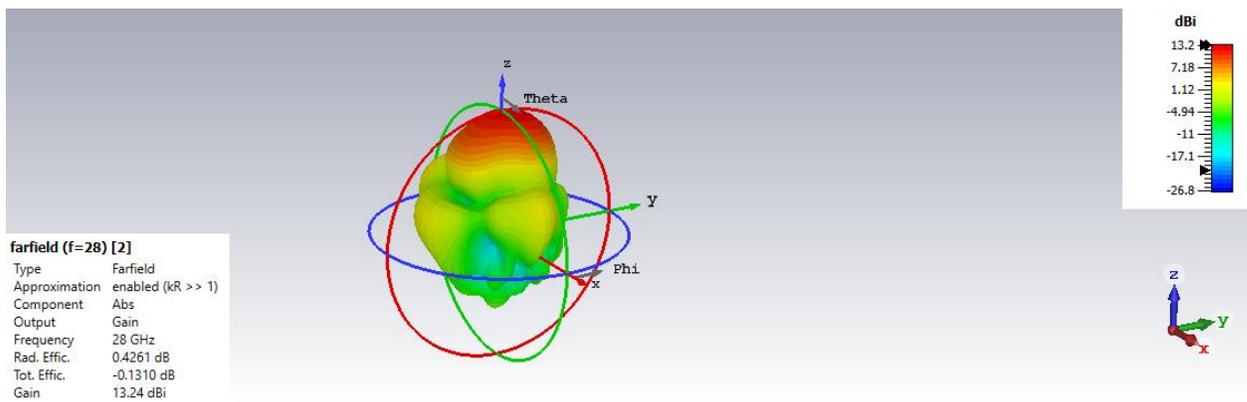

Figure 4.13. 3D Radiation Pattern of Planar 2x2 MPA Array.

The designed 2x2 MPA, has the co-polarization farfield along the excitation as shown in Figure 4.14a and the cross-polarization component is plotted in Figure 4.14b.

69

(a)   (b)
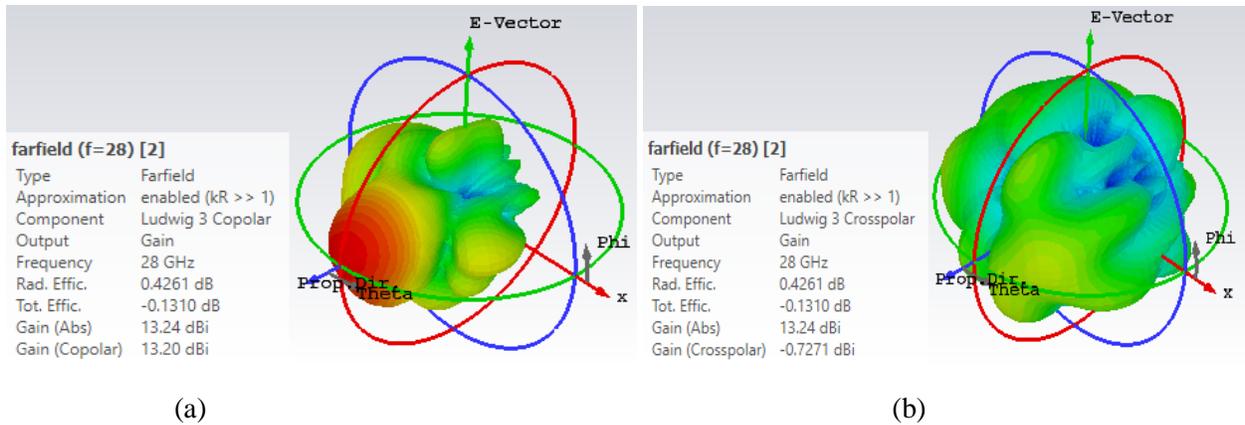
Figure 4.14. 3D Radiation Pattern Co-polarization (a) and (b) Cross-polarization of 2x2 MPA.
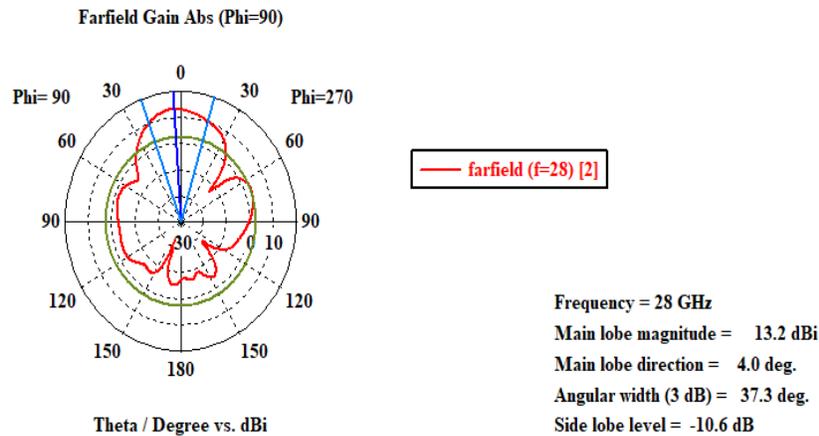

Figure 4.15. 2D Radiation Pattern of the Proposed Planar 2x2 MPA Array.

At working frequency, the performance comparison between the studied 2x2 MPA array and similar designs demonstrated in the literature are shown in Table 4.3. As it can be observed from the table, the achieved magnitude of the return loss of the proposed design is minimum, and the bandwidth is wide as compared to the designs mentioned in [16], [19], [33]. Similarly, the proposed design outperforms designs reported in [16], [33] in terms of radiation efficiency, VSWR, and gain. Generally, the design in this study provides better and improved performance as compared to the recently reported literature.

These significantly improved simulation results have been achieved because the defect structure is introduced on both radiating elements and ground plane structure, which greatly affects the current distributions of the structure to boost the radiation efficiency, as revealed in Figure 4.16. A proper impedance matching technique is made to minimize large impedance mismatch at the

70

edge of the patch, feed-point, and a microstrip feed line using the inset-feed impedance matching technique and also the physical dimensions of the structure have been tuned to improve the performance. As a result, power losses due to the impedance mismatch are minimized, which in turn boosts the antenna radiation efficiency and then its bandwidth. Also, inter-element spacing is carefully selected, which leads to radiation from all elements is added together constructively in the desired direction. Therefore, the proposed 2x2 MPA array can provide suitable performance with a very low profile, wide impedance bandwidth, and gain.
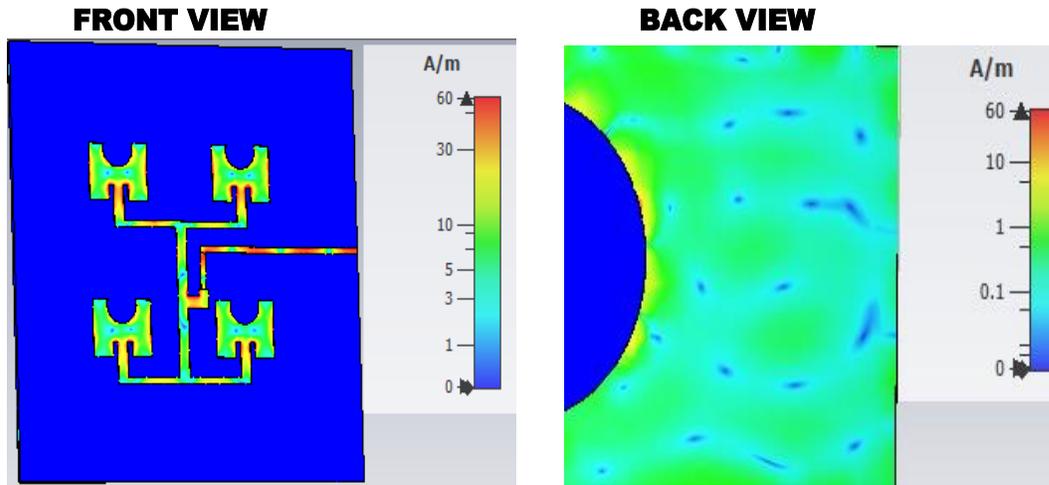

Figure 4.16. Current Distributions of 2x2 MPA Array.

Table 4.3. Comparison of Reported Works and the Proposed 2x2 MPA Array at 28GHz.

Ref.	S_{11} (dB)	BW (GHz)	G (dBi)	VSWR	η_{tot} (%)
[16]	-19.66	0.4	8.393	1.232	82.85
[19]	-20	0.95	-	-	-
[33]	-32.68	0.326	10.71	1.04752	89.79
This work	**-43.321**	**1.33**	**13.24**	**1.014**	**97.03**

Where S_{11} denotes return loss, BW denotes bandwidth, VSWR denotes voltage standing wave ratio, G is gain, and η_{tot} denotes total efficiency.

4.2.2. Planar 4x4 Rectangular MPA Array

The proposed 4x4 planar rectangular MPA array's front and back view are shown in Figure 4.17. The designed parameters of the proposed MPA array have been calculated in chapter three and tabulated in Table 3.3. But, all of the graphs used below discussion have been plotted using the design parameters listed in Appendix three.

FRONT VIEW   BACK VIEW
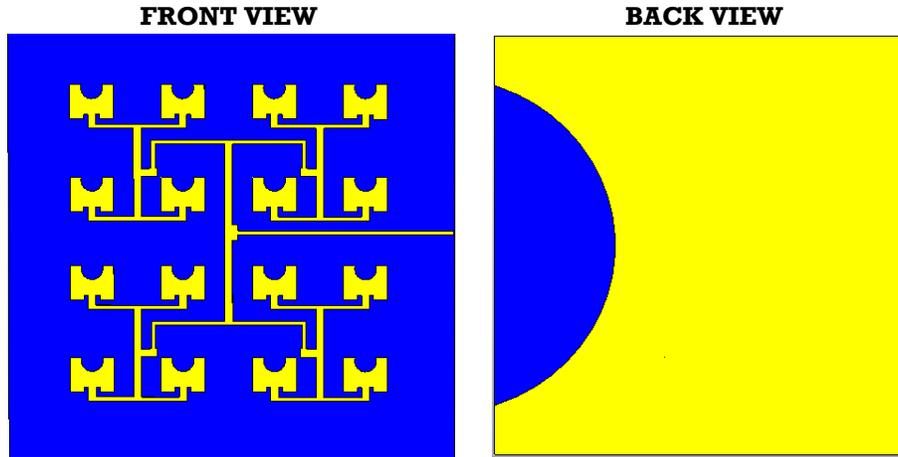
Figure 4.17. Front and Back View of the Proposed Planar 4x4 Rectangular MPA Array.

As explicitly shown in Figure 4.18, the return loss of the proposed 4x4 rectangular MPA array is less than -10dB between 27.271GHz and 28.732GHz. At the 28GHz, it is -40.665dB, and the achieved VSWR is minimum, which is 1.019, as shown in Figure 4.19. The -10dB impedance bandwidth of this antenna array is 1.461GHz, which is 131MHz wider than the bandwidth of the 2x2 rectangular MPA array proposed in the above section. The bandwidth has been improved since the defects on both patch structure and ground plane disturbs the distribution of the current, as indicated in Figure 4.23, which consequently enhances the overall radiation efficiency. Accordingly, the bandwidth of the antenna is improved, which is suitable for 5G applications.
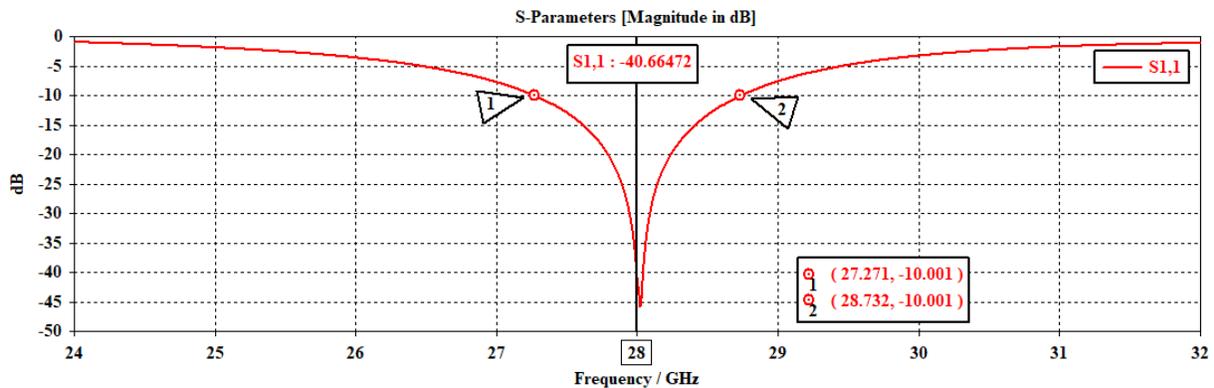

Figure 4.18. Return loss Plot of Proposed Planar 4x4 MPA Array.
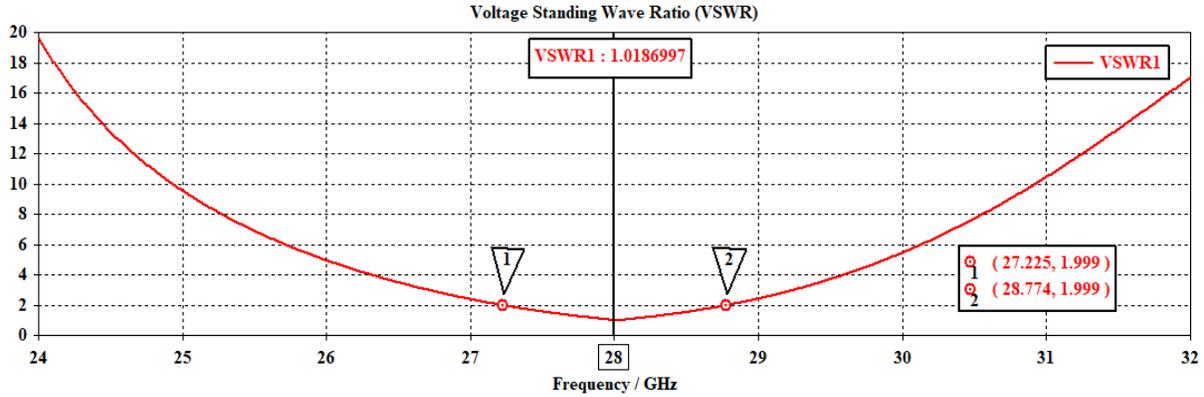
Figure 4.19. VSWR Plot of the Proposed Planar 4x4 MPA Array.

The 3D radiation pattern of the proposed 4x4 planar rectangular MPA array is revealed in Figure 4.20. Specifically, from the figure, it is perceived that the gain and total efficiency of the proposed array are 16.54dBi and -0.877dB (81.72%), respectively. Likewise, the achieved directivity of 4x4 MPA array is 16.38dBi. The directivity and gain of the modified single element in the above section are improved by 9.197dBi and 9.412dBi and that of 2x2 MPA array by 3.57dBi and 3.3dBi, respectively. The directivity and gain have been boosted since the number of the array elements have been increased to sixteen and the ground plane dimensions are properly tuned.
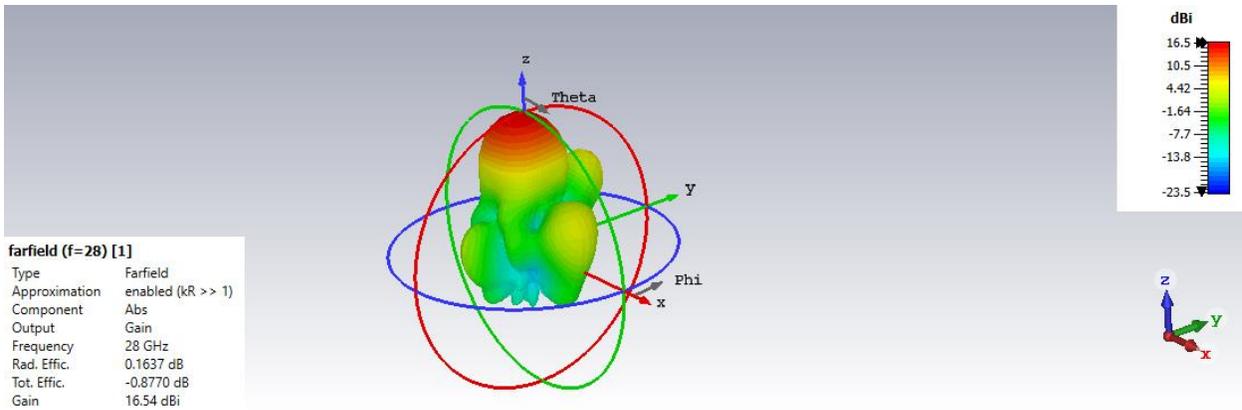

Figure 4.20. 3D Radiation Pattern of the Proposed Planar 4x4 MPA Array.

For the proposed planar 4x4 MPA, the co-polarization and cross-polarization farfield component are shown in Figure 4.21a and Figure 4.21b, respectively. As it can be seen from the farfield plot, the cross-polarized component is minimal as compared to that of the desired polarization.

(a)   (b)
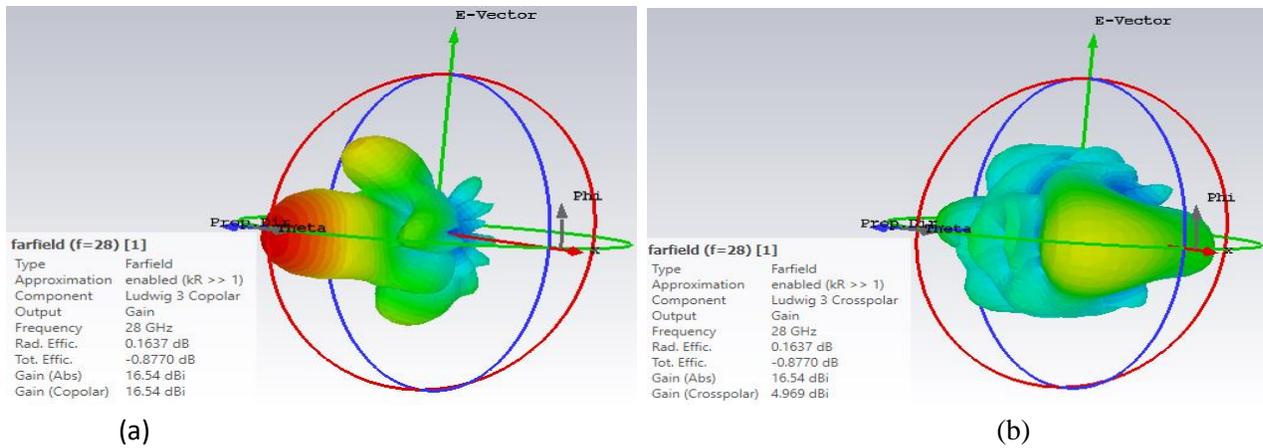
Figure 4.21. 3D Radiation Pattern Co-polarization (a) and (b) Cross-polarization of 4x4 MPA.

From Figure 4.15, the mutual coupling of a 2x2 rectangular MPA array is -10.6dB. Whereas the achieved mutual coupling of the 4x4 rectangular MPA array is -9.1dB and the 3dB radiation pattern has occurred at 25.2 degrees, as shown in Figure 4.22. Even though accurate design parameters have been considered, the effect of mutual coupling is increased with array elements. This is because the minimum mutual coupling from each of the quadrant planes is added together to increase the overall mutual coupling of the array. Still in both designs, the minimum magnitude has been achieved.
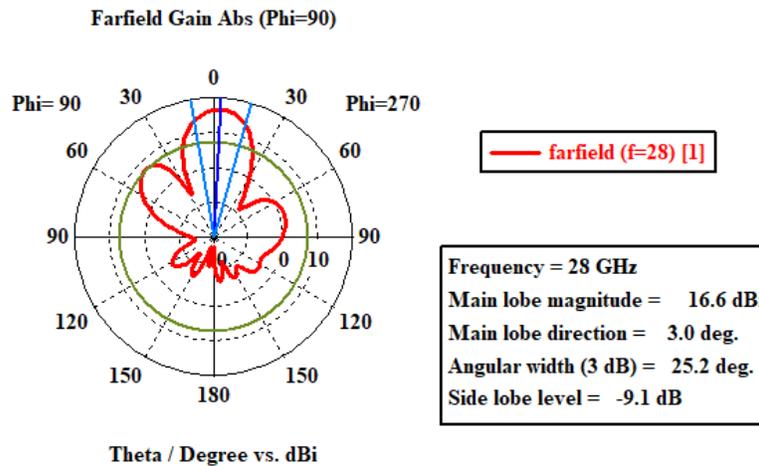

Figure 4.22. 2D Radiation Pattern of the Proposed Planar 4x4 MPA Array.

74
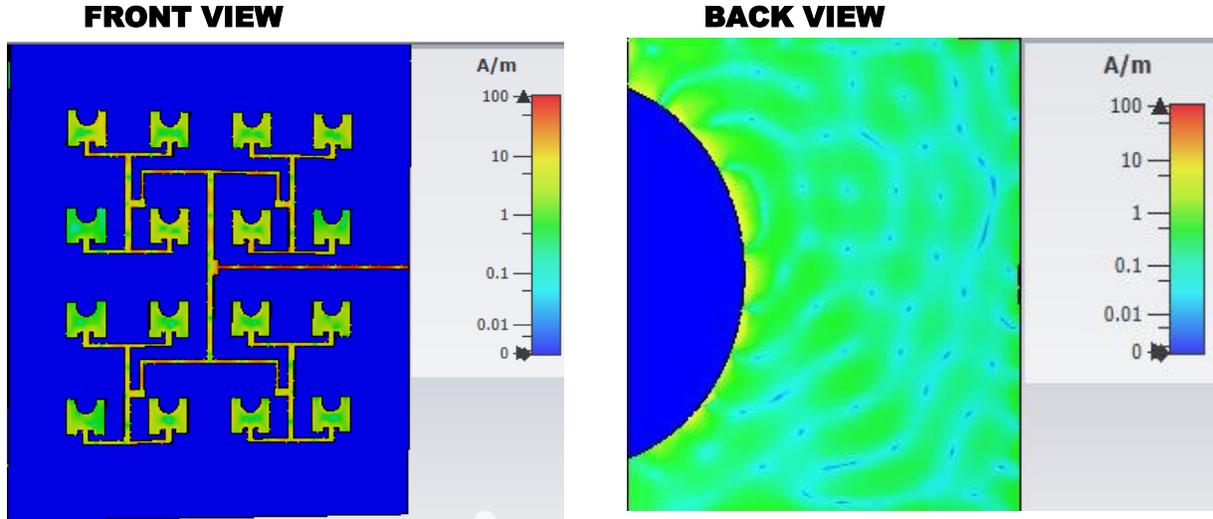
Figure 4.23. Planar 4x4 MPA Array Current Distributions.

Table 4.4 shows the performance comparison of the proposed 4x4 MPA array and other similar works reported in recent literature. From the table, it is evident that the large magnitude of the return loss of designs reported in [33], [34] has been minimized by the proposed design. This is because proper tuning of the physical dimensions of patch and ground plane structure is done in addition to shape modification of the given antenna. Likewise, wide and improved bandwidth have been obtained as compared to the design reported in [33]. However, the achieved bandwidth is narrow, as seen with the simulated result reported in [34]. Moreover, in terms of gain and VSWR, the proposed design outperforms the work demonstrated in [33], although its total efficiency is low. Hence, it can be concluded that the proposed 4x4 MPA array gives a highly competitive performance as compared to other identical MPA designs.

Table 4.4. Final Simulation Results of Existing and Proposed 4x4 MPA Array at 28GHz.

Ref.	S_{11} (dB)	BW (GHz)	G (dBi)	VSWR	η_{tot} (%)
[33]	-33.1499	0.332	15.17	1.0449	85.08
[34]	-13.48	4.91	16.48	-	-
This work	**-40.665**	**1.461**	**16.54**	**1.019**	**81.72**

Where S_{11} denotes return loss, G is gain, BW denotes bandwidth, VSWR denotes voltage standing wave ratio, and η_{tot} denotes total efficiency.

4.2.3. Planar 8x8 Rectangular MPA Array

Figure 4.24 illustrates the front and back view of the designed planar 8x8 MPA array. The numerically designed parameters of this antenna are calculated in chapter three and summarized in Table 3.4. The optimized design parameters that have been used for the simulations are listed in Appendix four.

FRONT VIEW **BACK VIEW**
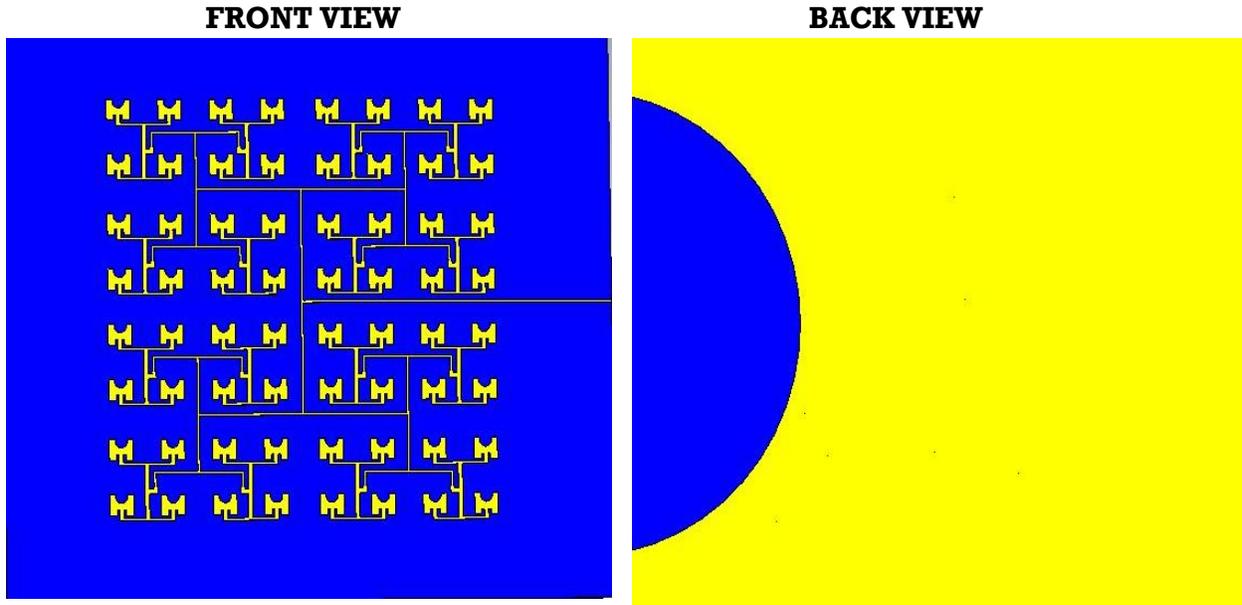
Figure 4.24. Front and Back View of the Proposed Planar 8x8 Rectangular MPA Array.

Figure 4.25 shows the S_{11} versus frequency, and Figure 4.26 expresses the VSWR plot of the designed 8x8 rectangular MPA array. From the plot, it can be depicted that between 27.215GHz and 28.157GHz, the return loss of this antenna is less than -10dB, and at the resonant frequency, it is -22.678dB with a VSWR of 1.159. The -10dB working bandwidth of this array antenna is 1.561GHz, which is 231MHz and 100MHz wider than the bandwidth of the 2x2 and 4x4 rectangular MPA arrays proposed in the above section.

The bandwidth has been improved because the defects on both patch and ground plane are integrated. As illustrated in Figure 4.30, the introduced defect disturbs the current flow in the antenna and thereby, the high impedance at the input is reduced. The fringing field of the antenna increased, and the impedance mismatch is minimized; thereby, the overall radiation efficiency is high, which in turn gives to improved bandwidth.
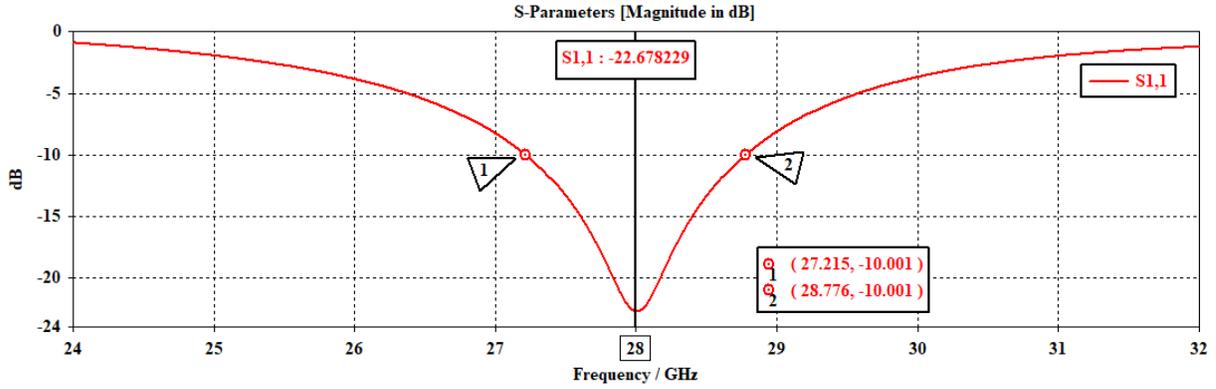
Figure 4.25. Return loss Plot of the Proposed Planar 8x8 MPA Array.
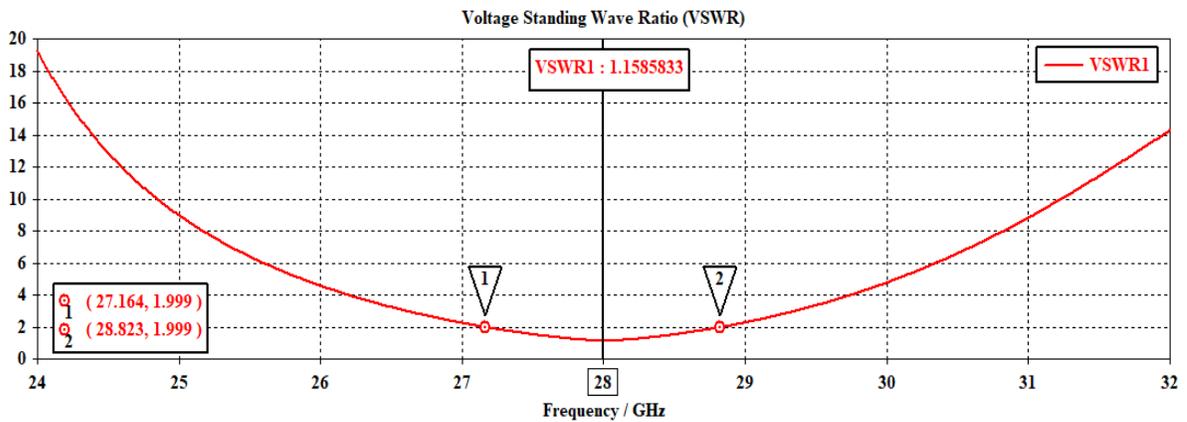
Figure 4.26. VSWR Plot of the Proposed Planar 8x8 MPA Array.

The 3D radiation pattern of the proposed planar 8x8 rectangular MPA array is depicted in Figure 4.27. From the figure, it can be seen that the achieved gain and total efficiency of the proposed MPA array are 21.45dBi and -1.616dB (69%), respectively. Similarly, the directivity of 8x8 MPA array is 19.6dBi. Therefore, from the obtained results, it can be said that the designed 8x8 MPA array improved the directivity and gain of the 2x2 MPA array by 6.79dBi and 8.21dBi. Similarly, the directivity and gain of the 4x4 MPA array have been improved by 3.22dBi and 4.91dBi, respectively.
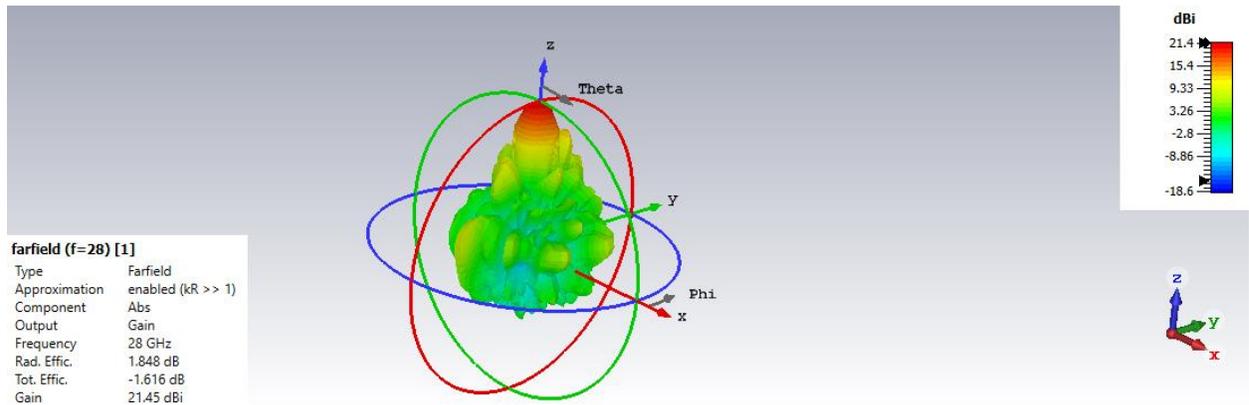
Figure 4.27. 3D Radiation Pattern of the Proposed Planar 8x8 MPA Array.

The co-polarization far field component of 8x8 MPA, which has the same polarization as the direction of electric field is given in Figure 4.28a. Also, its cross-polarization farfield component which is orthogonal to co-polarized component and main lobe direction is shown in Figure 4.28b. As it can be seen from the far field plot, the cross-polarized component is minimal as compared to that of the desired polarization.

(a)   (b)
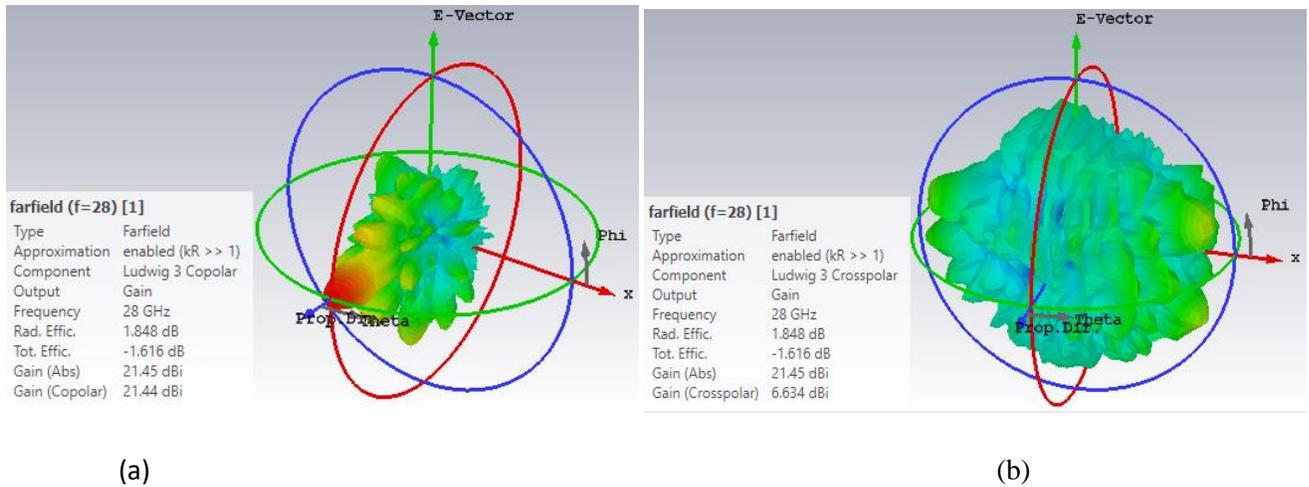
Figure 4.28. Radiation Pattern Co-polarization (a) and (b) Cross-polarization of 8x8 MPA Array.

As shown in Figure 4.22, the mutual coupling of the 4x4 MPA array is -9.1dB. However, the achieved mutual coupling of the proposed 8x8 planar rectangular MPA is -7.9dB, and the 3dB radiation pattern of this array has occurred at 12.3 degrees, as indicated in Figure 4.29.

Farfield Gain Abs (Phi=90)

|	
Frequency = 28 GHz	
Main lobe magnitude =	21.5 dBi
Main lobe direction =	1.0 deg.
Angular width (3 dB) =	12.3 deg.
Side lobe level =	-7.9 dB

Theta / Degree vs. dBi
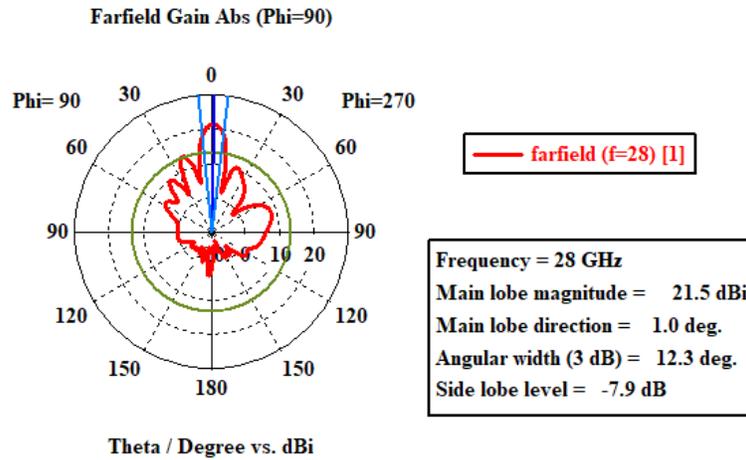
Figure 4.29. 2D Radiation Pattern of the Proposed Planar 8x8 MPA Array.

Therefore, significantly better directivity and gain are achieved because, in the design, proper tuning of the dimensions of the defect, the patch, and the ground plane has been properly made. Furthermore, the increased number of the MPA array elements to sixty-four largely improved the proposed antenna's gain and directivity.
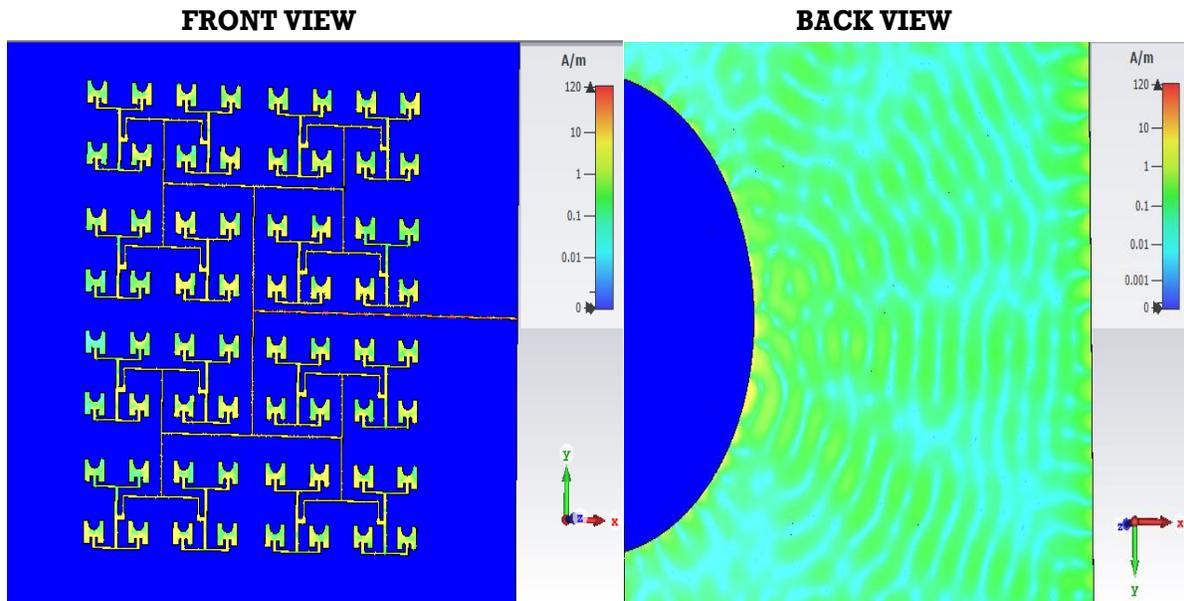
Figure 4.30. Current Distributions of 8x8 MPA Array.

The comparative analysis of the previously reported design and a planar 8x8 MPA array proposed in this work is tabulated in Table 4.5. The table signifies that the proposed design in this thesis work attained the improved return loss, bandwidth, gain, and VSWR as compared with simulation results described in [33]. However, achieved total efficiency is minimum. Therefore, the proposed

planar 8x8 MPA array in this study can be considered as an MPA array, which provides suitable performance for 5G mm-wave communication systems with significantly improved -10dB impedance bandwidth and radiation pattern gain.

Table 4.5. Simulated Results of Previous Reports and Proposed 8x8 MPA Array at 28GHz.

Ref.	S_{11} (dB)	BW (GHz)	G (dBi)	VSWR	η_{tot} (%)
[33]	-17.797	0.368	18.33	1.2977	74.23
This work	**-22.678**	**1.561**	**21.45**	**1.159**	**69**

Where S_{11} denotes return loss, BW denotes bandwidth, G is gain, VSWR denotes voltage standing wave ratio, and η_{tot} denotes total efficiency.

Chapter Five

Conclusion and Recommendations

5.1. Conclusion

In this thesis work, the performance of single element, planar 2x2, 4x4, and 8x8 MPA array with semi-elliptical slotted rectangular patch and ground plane have been analyzed to enhance their performance for 5G communication systems. All the single proposed element and planar rectangular MPA arrays are designed using Rogers RT 5580 substrate material with a thickness of 0.34490mm, a dielectric constant of 2.2, and a tangent loss of 0.0009.

Simulation results of this study reveal that the bandwidth, return loss, gain, and total efficiency of the proposed modified single element MPA are 1.132GHz (4.043%), -37.784dB, 7.128dBi, and -0.05513dB (98.74%), respectively. Likewise, the bandwidth, gain, and total efficiency of the examined planar 2x2 and 4x4 rectangular MPA arrays are 1.33GHz (4.75%), 13.24dBi, and -0.1310dB (97.03%) and 1.461GHz (5.218%), 16.54dBi, and -0.877dB (81.72%), respectively. Finally, the planar 8x8 MPA array attained the gain of 21.45dBi, the bandwidth of 1.561GHz (5.75%), and total efficiency of -1.616dB (69%).

To see whether the proposed rectangular MPA performance is improved or not, the entire studied single element and planar MPA arrays have been compared with similar designs reported in recent literature. Accordingly, as compared to designs reported in [10], [12], [21], [27], [33], and [49] the bandwidth of the proposed modified single MPA is widened by 285MHz, 632MHz, 550MHz, 692MHz, 560MHz, and 669MHz and return loss is minimized by -24.304dB, -25.784dB, -3.734dB, -19.95dB, -17.544dB, and 10.084dB, respectively. Likewise, the proposed antenna's gain has been boosted as compared with the simulation result of antenna presented in [4], [6], [10], [23], [24], and [26] by 0.428dBi, 3.528dBi, 0.498dBi, 1.928dBi, 1.518dBi, and 0.758dBi, respectively. Correspondingly, in terms of the bandwidth, the proposed planar 2x2 rectangular MPA array outperforms designs reported in [19], [16], and [33] and the bandwidth is increased by 380MHz, 930MHz, and 1.04GHz, respectively.

In the same way, better radiation efficiency is achieved, which improved the results cited in [16] and [33] by 14.18% and 7.24% and gain by 4.847dBi and 2.53dBi, respectively. The proposed 4x4 rectangular MPA array achieved bandwidth wider than the design reported in [33] by 1.129GHz. Its gain is increased by 1.37dBi and 0.06dBi as compared to the MPA array reported in [33] and

[34], respectively. Moreover, the proposed 8x8 MPA array attained wide bandwidth, which outperforms the design demonstrated in [33] by 1.193GHz and radiation pattern's gain by 3.12dBi.

Generally, in this research, the performance of rectangular MPA arrays has been substantially improved compared to other related works. The improved performance is achieved because of the introduced etched structure on both the radiating element and ground plane, which highly influences the current distribution of both structures. Also, the key physical dimensions of the antenna have been tuned to find where better performance has occurred. Consequently, the performance of the antenna is profoundly improved in terms of bandwidth, gain, and radiation efficiency.

In addition, good impedance matching has been made in the feeding network structures, and the dimensions are appropriately chosen. Therefore, the power losses occurred because of the large impedance mismatch, including the dramatically minimized return losses. As technology is getting advanced, the size of devices becomes very small. Regarding to this, in all of the proposed designs, the overall size of the MPA array has been critically considered. All of the designed MPA arrays provide high performance with a very compact size, which is suitable for the emerging 5G communication systems. In general, it can be concluded that by introducing semi-elliptical slot structure on radiating element and ground plane structures and also tuning the key design parameters simultaneously, the performance of the rectangular MPA arrays is greatly improved.

5.2. Recommendations

In this study, the performance of different planar rectangular MPA arrays has been meticulously enhanced for 5G communication systems. Still and all, the following points need further scientific research investigations.

- ❖ In this work, one-dimensional and two-dimensional various single band rectangular MPA arrays have been proposed. Despite, designing and analyzing multi-band planar rectangular MPA array performance for 5G base stations is left as future work.
- ❖ In this study, all the proposed MPA arrays have been validated using software simulation. However, manufacturing the hardware of all rectangular MPA arrays proposed in this study to check whether the achieved simulation results are attainable in real-life implementation is needed.

References

[1] E. Dahlman, G. Mildh, S. Parkvall, J. Peisa, J. Sachs, Y. Selen, and J. Skold, "5G wireless access: requirements and realization," Communications Magazine, IEEE, Vol. 52, No. 12, pp. 42 - 47, December 2014.

[2] X. Gu, D. Liu, C. Baks, O. Tageman, B. Sadhu, J. Hallin, L. Rexberg, A. Valdes-Garcia, "A multilayer organic package with 64 dual-polarized antennas for 28GHz 5G communication," In Proceedings of the IEEE International Microwave Symposium, pp. 1899 - 1901, June 2018.

[3] D. Mungur and S. Duraikannan, "Microstrip Patch Antenna at 28GHz for 5G Applications," Journal of Science Technology Engineering and Management Advanced Research and Innovation, Vol. 1, Issue 1, pp. 20 – 22, January 2018.

[4] W. Hussain, M. I. Khattak, M.A. Khattak, and M. Anab, "Multiband Microstrip Patch Antenna for 5G Wireless Communication," International Journal of Engineering Works, Vol. 7, Issue 1, pp.15 - 21, January 2020.

[5] A. Sohail, H. Khan, U. Khan, M. I. Khattak, N. Saleem, J. A. Nasir, "Design and Analysis of a Novel Patch Antenna Array for 5G and Millimeter-Wave Applications," 2019 2nd International Conference on Computing, Mathematics and Engineering Technologies (ICoMET), Sukkur, Pakistan, 30 - 31 January 2019.

[6] R. Przesmycki, M. Bugaj, and L. Nowosielski, "Broadband Microstrip Antenna for 5G Wireless Systems Operating at 28GHz", MDPI Proceedings Journals/electronics, Vol. 10, Issue 1, December 22, 2020.

[7] Y. Liu, et al., "Non-Orthogonal Multiple Access for 5G and Beyond," In Proceedings of the IEEE October 2017, pp. 1 - 33, 2017.

[8] B. G. Hakanoglu, O. Sen, and M. Turkmen, "A Square Microstrip Patch Antenna with Enhanced Return Loss through Defected Ground Plane for 5G Wireless Networks", 2nd URSI AT-RASC, Gran Canaria, 28 May - 1 June 2018.

[9] J. Zhang, X. Ge, Q. Li, M. Guizani, Y. Zhang, "5G Millimeter-Wave Antenna Array: Design and Challenges," IEEE Wireless Communication, pp. 106 - 112, 2017.

[10] O. Darboe, D. B. Onyango, and F. Manene, "A 28GHz Rectangular Microstrip Patch Antenna for 5G Applications," International Research Publication House, Journal of Engineering Research and Technology, Vol. 12, No. 6, pp. 854 - 857, 2019.

[11] E. Ershadi, A. Keshtkar, A. H. Abdelrahman, H. Xin, "Wideband high gain antenna sub-array for 5G Applications," Progress In Electromagnetics Research C, Vol. 78, pp. 33 - 46, 2017.

[12] A. Mohamed, E. Hassan, M. A. Misbah Omar, "Design and Analysis of Millimeter-Wave Microstrip Patch Antenna for 5G Applications", International Conference on Technical Sciences (ICTS2019), Tripoli - Libya, pp. 137 - 142, March 2019.

[13] S. Sridevi and K. Mahendran, "Design of Millimeter-Wave Microstrip Patch Antenna for MIMO Communication", International Research Journal of Engineering and Technology, Vol. 04, No. 10, pp. 1513 -1518, 2017.

[14] Dr. S. Shanthi, Dr. T. Jayasankar, P. J. Christydass, Dr. P. M. Venkatesh, "Wearable Textile Antenna for GPS Application," International Journal of Scientific and Technology Research, Vol. 8, No. 11, pp. 3788 - 3791, 2019.

[15] S. P. Jones, N. Gunavathi, "Codirectional CSRR inspired printed antenna for locomotive short-range radar", ICICI, 2017.

[16] S. Johari, M. A. Jalil, S. I. Ibrahim, M. N. Mohammad, and N. Hassan, "28GHz Microstrip Patch Antennas for Future 5G," Malaysian Journal of Engineering and Science Research, Vol. 2, No. 4, pp. 01 - 06, 2018.

[17] N. L. Vamsi, G. S. Sravanthi, K. Narmada, K. N. Kavya, G. Y. Swamy, and M. Durgarao, "A Microstrip Patch Antenna Design at 28GHz for 5G Mobile Phone Applications," International Journal of Electronics, Electrical and Computational System, Vol. 7, Issue 3, March 2018.

[18] C. A. Balanis, "Antenna Theory Analysis and Design," Third Edition. Hoboken, New Jersey: John Wiley and Sons, Inc., 2005.

[19] Dr. M. Kavitha, T. D. Kumar, Dr. A. Gayathri, V. Koushick, "28GHz Printed Antenna for 5G Communication with Improved Gain Using Array," International Journal of Scientific & Technology Research, Vol. 9, Issue 03, pp. 5127 - 5133, March 2020.

[20] P. Jeyakumar, Prof. P. Chitra, and Ms. G. Christina, "Design and Simulation of Directive High Gain Microstrip Array Antenna for 5G Cellular Communication," Asian Journal of Applied Science and Technology (AJAST), Vol. 2, Issue 2, pp. 301 - 313, 2018.

[21] N. V. Chaitanya, M. S. Poornima, P. L. Prahelika, R. Monika, and T. L. Rozy, "Inset Feed Compact Millimeter-Wave Microstrip Patch Antenna at 28GHz for Future 5G Applications,"

International Research Journal of Engineering and Technology (IRJET), Vol. 06, Issue 03, pp. 3137 – 3141, March 2019.

[22] W. A. Awan, A. Zaidi, and A. Baghdad, "Patch antenna with improved performance using DGS for 28GHz applications," IEEE Access, International Conference on Wireless Technologies, Embedded and Intelligent Systems, Fez, Morocco, 3 - 4 April 2019.

[23] V. Gupta, S. Vijay, P. Gupta, "A Novel Design of Compact 28GHz Printed Wideband Antenna for 5G Applications," International Journal of Innovative Technology and Exploring Engineering, Vol. 9, Issue 3, January 2020.

[24] Y. Ghazaoui, A. El Alami, M. ElGHzaoui, S. Das, D. Barad, and S. Mohapatra, "Millimeter-wave antenna with enhanced bandwidth for 5G wireless application," Journal of Instrumentation, January 2020.

[25] V. Karthikeyan, S. Vignesh, K. A. Reddy, G. B. Reddy, and R. S. Aparna, "A Millimeter-Wave Based Circular Slot Loaded Microstrip Patch Antenna for 5G Communication," International Conference on Frontiers in Materials and Smart System Technologies, 2019.

[26] A. F. kaeib, N. M. Shebani, and A. R. Zarek, "Design and Analysis of a Slotted Microstrip Antenna for 5G Communication Networks at 28GHz," 19th International Conference on Sciences and Techniques of Automatic control and computer engineering, March 24 - 26, 2019.

[27] S. A/L. Subramaniam, S. K. Selvaperumal, and V. Jayapal, "High Gain Compact Multi-Band Microstrip Patch Antenna for 5G Network," International Journal of Advanced Science and Technology, Vol. 29, No. 1, pp. 1390 - 1410, 2020.

[28] M. B. El_Mashade and E. A. Hegazy, "Design and Analysis of 28GHz Rectangular Microstrip antenna," WSEAS Transactions on Communications, Vol. 17, pp. 2224 - 2864, 2018.

[29] J. Maharjan and D. Choi, "Four-Element Microstrip Patch Array Antenna with Corporate-Series Feed Network for 5G Communication," International Journal of Antennas and Propagation, April 2020.

[30] D. Mungur and S. Duraikannan, "Design and Analysis of 28GHz Millimeter Wave Antenna Array for 5G Communication Systems," Journal of Science Technology Engineering and Management-Advanced Research & Innovation, Vol. 1, Issue 3, pp. 2581 - 4982, August 2018.

[31] H. Alwareth, M. Abu, and I. M. Ibrahim, "Design of a Broadband Microstrip Array Antenna for 5G Application," Journal of Telecommunication, Electronic and Computer Engineering, 2020.

[32] Md. F. Shah and A. D. Singh, "Design and Analysis of Microstrip Patch Antenna Arrays for Millimeter-Wave Wireless Communication," International Journal of Engineering and Advanced Technology, Vol. 9, Issue 3, February 2020.

[33] Mulugeta. T, "Comparative Performance Assessment of Different Rectangular Microstrip Patch Antenna Array Configurations at 28GHz for 5G Wireless Applications", Master's Thesis, Jimma University, Jimma Institute of Technology, Jimma, Ethiopia, 2020.

[34] K. Keum and J. Choi, "A 28GHz 4x4 U-Slot Patch Array Antenna for mm-wave Communication," International Symposium on Antennas and Propagation (ISAP2018), October 2018.

[35] M. Y. Mohamed, A. M. Dini, M. M. Soliman and A. Z. M. Imran, "Design of 2x2 Microstrip Patch Antenna Array at 28GHz for Millimeter Wave Communication," 2020 IEEE International Conference on Informatics, IoT, and Enabling Technologies (ICIoT), pp. 445-450, February 2020. DOI: 10.1109/ICIoT48696.2020.9089458.

[36] Efri Sandi, Rusmono, Aodah Diamah, and Karisma Vinda, "Ultra-wideband Microstrip Array Antenna for 5G Millimeter-wave Applications," Journal of Communications, Vol. 15, No. 2, pp. 198-204, February 2020.

[37] A. Siddik, M. Hossain, D. Haque, and O. Faruque, "Design and Radiation Characterization of Rectangular Microstrip Patch Antenna for Millimeter-wave Communication," American Journal of Engineering Research, Vol. 8, Issue 1, pp. 273 - 281, 2019.

[38] K. Suraj and M. N. Ammal, "Design and Development of Microstrip Patch Antenna at 2.4GHz for Wireless Applications," Indian Journal of Science and Technology, Vol. 11, No. 23, June 2018.

[39] P. Kokila, T. Saranya, and S. Vanitha, "Analysis and Design of Rectangular Microstrip Patch," Ever-science Publications, Journal of Network Communications and Emerging Technologies, Vol. 6, Issue 4, April 2016.

[40] Gary, A., Thiele, and Warren L. Stutzman, "Antenna Theory and Design," Third edition, John Wiley and Sons, Inc., 2013.

[41] S. Wanner, "Phased array system design," Retrospective Theses and Dissertations, 2008.

[42] A. Mehta, "Microstrip Antenna," International Journal of Scientific and Technology Research, Vol. 4, Issue 3, March 2015.

[43] N. H. Nor, M. H. Jamaluddin, M. R. Kamarudin, and M. Khalily, "Rectangular Dielectric Resonator Antenna Array for 28GHz application," Malaysia University of Technology, Progress on Electromagnetic Research C, Vol. 63, pp. 53 - 61, 2016.

[44] S. Gnanamurugan, B. Narmadha, A. Shamina, and M. Sindhu, "Gain and Directivity Enhancement of Rectangular Microstrip Patch Antenna," Asian Journal of Applied Science and Technology, Vol. 1, Issue 2, pp. 127 - 131, March 2017.

[45] C. Bergsrud, C.Freidig, M. Anderson, M. Clausing, T. Dito, and S. Noghanian, "Inset-Feed and Edge-Feed Patch Antennas With Rectifying Circuit".

[46] S. winder, "Analog and Digital Filter Design," Elsevier Science, Second Edition, 2002.

[47] A. Vesa, "The Radiation Pattern for Uniform Array Antennas," pp. 13 - 16, 2010.

[48] A. Sivabalan, S. Pavithra, R. Selvarani, and K. M. Vinitha, "Design of Microstrip Patch Antenna for 5G," International Journal of Control and Automation, Vol. 13, No. 2, pp. 546 - 552, 2020.

[49] M. Darsono and A. R. Wijaya, "Design and Simulation of a Rectangular Patch Microstrip Antenna for the Frequency of 28GHz in 5G Technology," International Conference on Innovation in Research, Conference Series 1469, 2020.

[50] S. Tyagi and G. Saini, "Antenna Array Design Using Hybrid Feed for High-Frequency Application," International Journal of Engineering and Advanced Technology (IJEAT), Vol. 8, Issue 6, August 2019.

[51] Kinde. A., Mulugeta T., "Broadband microstrip patch antenna at 28GHz for 5G wireless applications", International Journal of Electrical and Computer Engineering (IJECE), Vol. 11, No. 3, pp. 2238-2244, 2021.

[52] Mulugeta T., Kinde A., Hana L., and Ayane L., "Design and Analysis of a 28GHz Microstrip Patch Antenna for 5G Communication Systems", Vol. 08, Issue 02, pp. 881-886, Feburary 2021.

Appendixes

Appendix One: Initial Calculated and Tuned Physical Dimension of Typical and Modified Single MPA.

Design Parameters	Typical Single Element MPA		Modified Single Element MPA	
	Calculated Values (mm)	Tuned Values (mm)	Calculated Values (mm)	Tuned Values (mm)
PW	4.23519	4.7	4.23519	4.73
PL	3.40451	3.3398	3.40451	3.66
LMTL	1.80589	1.861	1.80589	1.67
WMTL	0.82137	0.821	0.82137	0.8
IL	0.89268	0.89268	0.89268	1
IW	0.02475	0.3	0.02475	0.2
GPW	6.30459	6.4	6.30459	7
GPL	5.47391	5.8	5.47391	7

Appendix Two: Initial Calculated and Tuned Physical Dimension of Planar 2x2 MPA Array.

Design Parameters	Calculated Values (mm)	Tuned Values (mm)
PW	4.23519	4.7
PL	3.40451	3.5
IL	0.89268	0.95
IW	0.02475	0.35
LMTL	1.80589	1.7
WMTL	0.82137	0.822
LPD	0.41069	0.42
WPD	10.40656	10.4
(GPW) $_{2 \times 2}$	15.88978	30
(GPL) $_{2 \times 2}$	17.84020	28
(LLMTL) $_{2 \times 2}$	0.41069	0.42
(WLMTL) $_{2 \times 2}$	7.24683	13.8
IS	5.35	5.3

Appendix Three: Initial Calculated and Tuned Physical Dimension of Planar 4x4 MPA Array.

Design Parameters	Calculated Values (mm)	Tuned Values (mm)
PW	4.23519	4.7
PL	3.40451	3.72
IL	0.89268	0.67
IW	0.02475	0.45
LMTL	1.80589	1.34
WMTL	0.82137	0.822
LPD	0.41069	0.42
WPD	10.40656	10.3
$(GPW)_{4x4}$	35.06016	48
$(GPL)_{4x4}$	31.73744	50
$(LLMTL)_{4x4}$	0.41069	0.42
$(WLMTL)_{4x4}$	17.32474	23.17
IS	5.35	5.32

Appendix Four: Initial Calculated and Tuned Physical Dimension of Planar 8x8 MPA Array.

Design Parameters	Calculated Values (mm)	Tuned Values (mm)
PW	4.23519	4.52
PL	3.40451	3.7009
IL	0.89268	0.95
IW	0.02475	0.35
LMTL	1.80589	1.28
WMTL	0.82137	0.822
LPD	0.41069	0.42
WPD	10.40656	10.21
$(GPW)_{8x8}$	73.40092	116
$(GPL)_{8x8}$	66.75547	100
$(LLMTL)_{8x8}$	0.410685	0.42
$(WLMTL)_{8x8}$	36.49512	59.06
IS	5.35	5.34